Okinawa Institute of Science and Technology
Graduate University

Thesis submitted for the degree
Doctor of Philosophy

Designing a Tractable Behavioral Paradigm for Investigating Olfactory Figure-ground Segregation

by
Aliya Mari Adefuin Purser

Supervisor: Izumi Fukunaga

September 2022

Declaration of Original and Sole Authorship

I, Aliya Mari Adefuin Purser, declare that this thesis entitled **"Designing a tractable behavioral paradigm for investigating olfactory figure-ground segregation"** and the data presented in it are original and my own work.

I confirm that:

- No part of this work has previously been submitted for a degree at this or any other university.
- References to the work of others have been clearly acknowledged. Quotations from the work of others have been clearly indicated and attributed to them.
- In cases where others have contributed to part of this work, such contribution has been clearly acknowledged and distinguished from my own work.
- None of this work has been previously published elsewhere, with the exception of the following (with authorization from co-authors obtained):

  Adefuin AM, S Lindeman, JK Reinert, and I Fukunaga. 2022. State-dependent representations of mixtures by the olfactory bulb. *Elife* 11.

Signature: 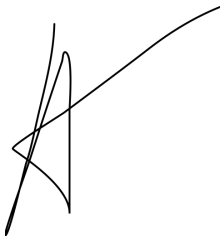

Date: September 2022

Abstract

Odors naturally exist as mixtures in the environment. Detecting relevant cues amidst other signals and noise, a task called figure-ground segregation, is important for survival. Understanding mechanisms that enable animals to solve such a challenging task requires a paradigm that recapitulates key features of the task, yet ideally should be simple enough that allows these mechanistic bases to be studied experimentally. In my PhD, I developed a behavioral paradigm using only binary mixtures as a model for olfactory figure-ground segregation in mice. Ethyl butyrate (EB) was assigned as target odor and ten other background odors with differing degrees of chemical similarity to EB were included as part of a Go/No-Go task. The fact that the mixtures comprised only two odors made the number of possible odor combinations limited, which therefore made the paradigm tractable and ensured that all combinations can be presented exhaustively per behavioral session. Despite its simplicity, I demonstrate that the experimental paradigm can still impose a degree of challenge for mice through the use of a highly similar background odor. This captures recent findings that the degree of overlap between odor-evoked neural representations underlies figure-ground segregation difficulty. Additionally, it was determined that mice performing the binary mixture task can easily generalize when presented with a novel odor, which suggests that demixing is likely involved. Finally, two example cases are presented as examples how the experimental paradigm can be applied to investigate possible neural mechanisms of olfactory figure-ground segregation. Overall, despite its simplicity, the experimental paradigm using only binary mixtures may be used to probe neural mechanisms of olfactory figure-ground segregation.

Acknowledgement

Thank you, first and foremost, to Prof. Izumi Fukunaga for giving me the opportunity to be a member of her lab and providing unrelenting guidance throughout the years I worked on my thesis. I am eternally indebted.

Additionally, many thanks to all my colleagues in Fukunaga Unit (Taha Soliman, Cary Zhang, Yu-Pei Huang, Xiaochen Fu, Adam Mago, Josefine Reuschenbach, and Sourjya Nath) for sharing their knowledge and expertise. Special thanks to our unit postdocs Janine Reinert for, amongst other things, providing me with surgically-prepared mice for my experiments and reviewing my manuscript; and to Sander Lindeman for teaching me how to perform surgeries and for always being open to consultations/discussion. I was given the opportunity to be a co-author of an article with Janine, Sander and Prof. Fukunaga. I am incredibly fortunate and honored to have the opportunity to work with them closely.

I am also thankful to Prof. Ichiro Maruyama and Prof. Tomoyuki Takahashi, who served as members of my OIST thesis committee. They reviewed my work and provided relevant insights to the project from its inception. Additionally, thank you to my thesis examiners, Prof. Jun Tani, Prof. Kevin Franks, Prof. Alexander Fleischmann and Prof. Venkatesh Murthy for lending their time to review my thesis proposal and dissertation.

There are also many staff at OIST who have helped me work seamlessly throughout the years. Thank you to the OIST Graduate School staff, the Engineering Department, Animal Resource Section, Imaging Section, Ganjuu Wellbeing Service, and our unit RUAs Ms. Saeko Hedo and Ms. Sayori Gordon.

On a personal note, I am incredibly grateful to my family (my parents, sister and in-laws), who cheered me on from a distance. Finally, I would like to say thank you to my husband, Lee, and to our daughter, Selah, for being my number one support system and biggest motivators.

List of abbreviations

Acet.	Acetophenone
ACUC	Animal Care and Use Committee
AON	Anterior olfactory nucleus
B6	C57BL/6
BA	Butyl acetate
BB	B. butyrate
Bl.	Blank
EB	Ethyl butyrate
EP	Ethyl propionate
EPL	External plexiform layer
ET	Ethyl tiglate
Eug.	Eugenol
FV	Final valve
GCL	Granule cell layer
GL	Glomerular layer
IA	Isopropyl acetate
IPL	Internal plexiform layer
LC	Locus coeruleus
LED	Light emitting diode
MA	Methyl anthranilate
MB	Methyl butyrate
Mbe	Methyl benzoate
MC	Mitral cell
MCL	Mitral cell layer
MCS	Maximum common substructure
MS	Methyl salicylate
MT	Methyl tiglate
MTC cell	Mitral and tufted cell
MV	Methyl valerate
OB	Olfactory bulb
ONL	Olfactory nerve layer
OSN	Olfactory sensory neuron
OSR	Olfactory receptor
OT	Olfactory tubercle
PCoA	Principal coordinate analysis
PCx	Piriform cortex
PG cell	Periglomerular cell
PID	Photoionization detector
Sal.	Salicylaldehyde
sSA cell	Superficial short axon cell
Van.	Vanillin
ΔRT	Change in reaction time

Contents

List of figures

GENERAL INTRODUCTION

Introduction to figure-ground segregation

Animals are presented with continuous streams of sensory information as they navigate their environments. To deal with this, their sensory systems have been developed to parse and detect relevant information. An important aspect of this is to segregate the signal of interest from the background, irrelevant signals. This task is known as figure-ground segregation (Lamme, 1995). This ability is crucial for hunting food, avoiding danger, mating - overall, to survive. For example, during mating season, frogs of different species congregate in the same area such as a pond in search of suitable mates. Male frogs loudly generate species-specific "advertisement" calls (Nityananda and Bee, 2011; Bee, 2015). The females then listen intently to detect the right mating call (i.e. the "figure") amidst the noisy background, resulting in a "cocktail party effect" (Cherry, 1953).

Some concepts gained from early studies of figure-ground segregation

In the visual system, research into figure-ground segregation dates back over a century. During the early 20th century, many psychological studies on this topic often occurred with respect to viewer's perceptions of forms in art (Kandel, 2012, 2016). This soon led to the emergence of the *Gestalt* (a German word for configuration) psychology, whose early proponents suggested that humans respond not to the disparate features of visual stimuli but rather to specific combinations or configurations of stimuli (Kandel, 2012; Wagemans et al., 2012). Key to understanding perceptions of objects is to relate the configural processing to representations of these building blocks (Vecera and O'reilly, 1998; Wagemans et al., 2012; Self et al., 2019). For example, the ambiguous figure by Rubin (1915) famously illustrates how border ownership determines figural assignment (Figure 1.1).

Figure 1. 1 Rubin face-vase illustration (1915)
Depending on border assignment, one may be able to perceive a goblet or two facial profiles on the ambiguous figure (Image from Rubin, 1915).

Neural correlates of border ownership have been observed in the visual cortex (Zhou et al., 2000; Roelfsema et al., 2002; Qiu and Von Der Heydt, 2005; Fang et al., 2009). In one study, Zhou et al. (2000) could show that firing rates of neuros in V1, V2, and V4 of macaque monkeys changed depending whether or not the edge belonged to either the figure or the background. Similar coding principles have been later observed in other sensory modalities (Zelano et al., 2011; Mesgarani and Chang, 2012; Kok et al., 2017).

Other known mechanisms of figure-ground segregation include feature extraction, modulation/contrast enhancement, predictive coding, attention and object recognition (Vecera and O'reilly, 1998; Rao and Ballard, 1999, Self et al., 2019). In addition, many other factors influence which stimulus is assigned as the target/figure including prior experience, attention, and intention (Wagemans et al., 2012; Wang et al., 2019).

Olfactory figure-ground segregation

My thesis work is on the olfactory figure-ground segregation - a task where a target odor is detected or recognized in the presence of a noisy background. This is because the sense of smell is a dominant modality in many organisms (Nielsen et al., 2015; Blazing and Franks, 2020), in particular in the mouse, which has become a widely used model system across laboratories.

Before I discuss the characteristics of the olfactory figure-ground segregation, it is first necessary to introduce the relevant nomenclature and concepts, including the architecture and coding principles of the early olfactory system in the mouse.

Organization of the early olfactory system

Transduction of olfactory stimuli begins in the nose. In the mouse, mature olfactory sensory neurons (OSNs) located in the nasal epithelium express a single olfactory receptor (OR) gene, which encodes an olfactory receptor (Buck and Axel, 1991). While there is a vast library of OR genes, it is still outnumbered by odor molecules in existence. To enable perception of the large repertoire of volatile odor molecules, the olfactory system uses combinatorial receptor coding (Malnic et al., 1999). A single odorant molecule can bind to different OR types and multiple molecules can bind to the same OR type. This is because each odorant molecule contains multiple chemical features and many odorant molecules can share the same chemical feature, respectively (Chess et al., 1994; Malnic et al., 1999; Serizawa et al., 2004).

The olfactory bulb (OB) is the first olfactory brain region where synaptic processing of odor information occurs. OSNs in the nasal epithelium are only coarsely organized in the nasal epithelium such that OSNs expressing different receptors can be intermingled with one another in different zones (Vassar et al., 1994). But a highly organized topographic arrangement is achieved, where the axons of OSNs expressing the same OR coalesce onto the same glomeruli in the OB. Here, they form synapses with the primary apical dendrites of the OB output cells, the mitral and tufted cells (MTCs) (Mombaerts et al., 1996). This forms a distinct spatial map of glomerular activity in the OB that helps confer odor identities (Uchida et al., 2000; Nagayama et al., 2014).

A vast network of inhibitory cells across its different layers is involved in modifying the spatial and temporal patterning of the MTCs (Land and Shepherd, 1974; Burton, 2017) – impacting the odor information transmitted to higher olfactory regions (Figure 1.2A). For example, inhibition in the OB shifts the timing of MTC activation and adds to the distinction between the two OB output cells (Fukunaga et al., 2012; Ackels et al., 2020). Additionally,

centrifugal inputs from downstream olfactory areas contribute to odor information processing in the OB.

In general, centrifugal input to the OB can be classified into two: those that come from areas that the OB directly projects to, and those that do not directly receive input from the OB.

The former includes the piriform cortex, anterior olfactory nucleus (AON), and tenia tacta; while the latter includes areas such as the locus coeruleus (LC), which project neuromodulatory fibers to the bulb (Matsutani and Yamamoto, 2008).

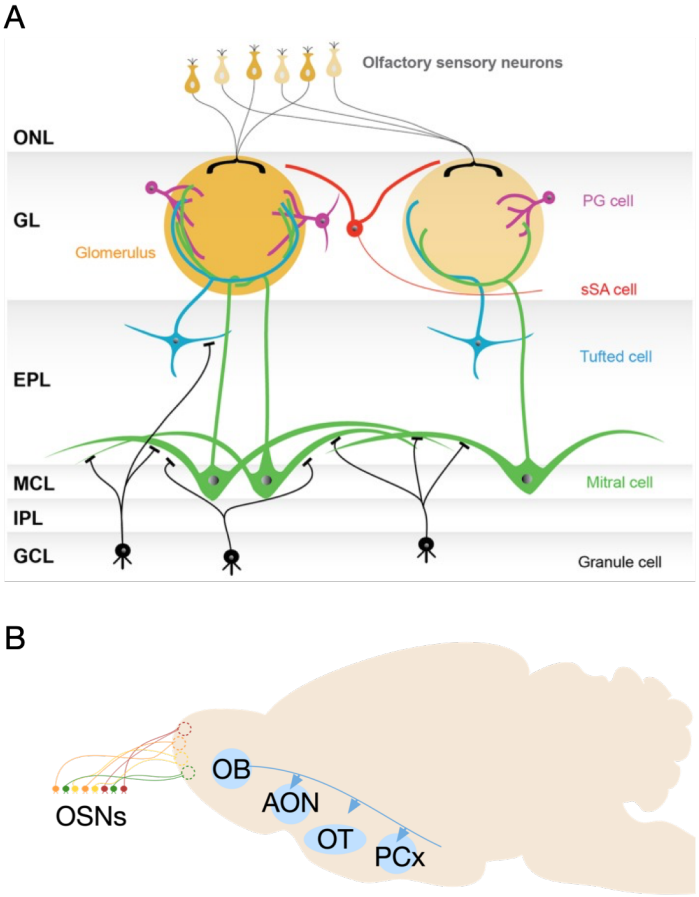

Figure 1. 2 Anatomical organization of the mouse olfactory system

A) Anatomical organization of neurons in the OB. (ONL: olfactory nerve layer; GL: glomerular layer, EPL: external plexiform layer, MCL: mitral cell layer, IPL: internal plexiform layer, GCL: granule cell layer, PG cell:, sSA cell (Image from Nagayama *et al*., 2014). B) Sagittal plane illustration of the mouse brain showing the main targets of the OB output cells in the early olfactory system (OB: olfactory bulb, AON: anterior olfactory nucleus, OT: olfactory tubercle, PCx: piriform cortex).

One distinct feature of the olfactory system is the OB output simultaneously project to different cortical regions –without passing the thalamus – rather than a hierarchy of subdivided cortical regions (Brann and Datta, 2020). Notably, the direct connection between the OB output cells and their downstream targets is unlike other sensory areas wherein feedforward sensory information initially goes through the thalamus before reaching the corresponding early sensory cortex (Courtiol and Wilson, 2015).

Combinatorial coding and evoked activity patterns

As introduced before, individual OB glomeruli receive input from OSNs expressing the same odor receptors (Ressler et al., 1994; Mombaerts et al., 1996). Thus, a given odor activates a distinct subset or pattern of OB glomeruli, which is the anatomical correlate of combinatorial coding mentioned above (Malnic et al., 1999). However, these odor-evoked glomerular representations may be thought of as starting points, since the olfactory system further refines these patterns. Exactly how this occurs may even change dynamically depending on the behavioral context, experience, state, etc. Indeed, pattern decorrelation is observed in the olfactory bulb and is behaviorally associated with ability to discriminate odorants (Gschwend et al., 2015). Refinement of odor information in the OB via processes such as pattern decorrelation is thought to reduce redundancy and improve the discriminability of activity patterns evoked by odors. As mentioned later, pattern decorrelation may be a mechanism that is relevant for olfactory figure-ground segregation (Gschwend et al., 2015; Otazu et al., 2015; Grabska-Barwińska et al., 2017).

Olfactory cortices

Brain regions that are targeted by the OB outputs are generally called olfactory cortices. Many regions that fall into this category, including the anterior olfactory nucleus (AON), piriform cortex (PCx), olfactory tubercle (OT) among others (Figure 1.2B). Of these, the piriform cortex is the largest. It is a three-layer allocortex, like the hippocampus, with many similarities in connectivity and the proposed functions, including in learning and memory (Blazing and Franks, 2020). Pyramidal neurons in the piriform cortex receive input from mitral and tufted cells from different glomeruli. The stereotyped anatomical segregation like the OB glomeruli is lost here: pattern of projection to the piriform cortex is random or at least does not have a clearly discernible topographic pattern (Stettler and Axel, 2009). This is thought to be important, as this means that piriform neurons are able to integrate features from different OB cells (Stettler and Axel, 2009). This convergence in the piriform cortex is thought to be the anatomical correlate of configural representations (Stettler and Axel, 2009; Howard and Gottfried, 2014). Random convergence, rather than a genetically determined pattern, may be advantageous where adaptive changes are involved.

Feedback loop

Another unique feature of early olfactory processing is the presence of dense cortical feedback to the primary sensory area (OB). For example, the AON ends glutamatergic feedback to the OB, particularly glomerular interneurons and granule cells but also mitral cells (Markopoulos et al., 2012). While the functional role of the AON is less understood, recent studies have shown that the AON is associated with olfactory place memory (Aqrabawi and Kim, 2020) and odor recognition and discrimination, especially involving the superficially located OB output, tufted cells (Chae et al., 2020). There is also dense feedback from the piriform cortex. While the pyramidal neurons that feed back to the OB may be unique types (Mazo et al., 2017), it is possible that some of the patterns that the piriform cortex "learns" may be projected back to the OB.

Having briefly introduced the anatomical regions and pathways of the mouse olfactory system, below, I discuss what is known about the olfactory figure-ground segregation.

Olfactory figure-ground segregation: Knowns and unknowns

As mentioned earlier, different odorants may evoke overlapping patterns of neural representations in the OB (Araneda et al., 2000; Johnson and Leon, 2008). The degree of pattern overlap of evoked neural representations in the early olfactory system forms the basis of how difficult it is to detect the presence of a target odor in an odor mixture (Rokni et al., 2014).

Activity patterns in the OB evoked by odors and underlying circuit mechanisms

Our understanding about the neural mechanisms of olfactory figure-ground segregation is still limited. For example, whether pattern decorrelation in the OB is a driving force or merely an outcome of olfactory figure-ground segregation is still uncertain (Grabska-Barwińska et al., 2017). Additionally, which olfactory features are preserved during pattern decorrelation of MTCs (Brann and Datta, 2020) and how the vast network of inhibitory neurons exactly partake in the process is not fully understood. Inhibition mediated by granule cells has been shown to increase pattern correlation, thereby affecting olfactory performance in mice (Gschwend et al., 2015), but there are still many unknowns in how other inhibitory cells spanning different layers of the OB may affect pattern decorrelation and olfactory figure-ground segregation. These neurons implement inter- and intraglomerular inhibition, as well as overall normalization of MT cell activity via different circuit motifs (Burton, 2017). These may contribute to the changes in the patterns of responses that could affect the ability of animals to perform such olfactory task.

Temporal patterns and odor encoding

Olfactory information is not only defined by spatial patterning but also timing of responses of different olfactory regions/cells. The primary OB output neurons themselves are delineated from one another based on their temporal response profiles (Fukunaga et al., 2012; Ackels et al., 2020)**.** Timing of responses are also crucial in processing odor information. Early responses in both the OB and piriform cortex are associated with conferring odor identity (Bolding and Franks, 2017; Wilson et al., 2017), and late responses indicate odor intensity (Bolding and Franks, 2017). Additionally, fine discrimination experiments show that animals improve accuracy when forced to sample odors longer, which has implications in the duration of integration and processing of odor information (Rinberg et al., 2006). Similar occurrence has been observed during figure-ground segregation in the visual system. Modulation/contrast enhancement in the early visual cortex, which is dependent on stimulus complexity, emerges a few milliseconds later than the initial feedforward input. This modulation is dependent on the figure-ground complexity (Koivisto et al., 2014; Groen et al., 2018). When it comes to olfactory figure-ground segregation, which epoch of mixture-evoked responses especially in the early olfactory areas important in solving the task is unknown.

Olfactory pathways relevant for figure-ground segregation

While some mechanisms relating to olfactory figure-ground segregation have been revealed in the olfactory bulb and piriform cortex, the role of other downstream olfactory is even more limited. For example, the anterior olfactory nucleus (AON) receives direct input from the olfactory bulb (primarily from tufted cells) and also sends feedback to the OB. The AON

also sends associative input to the piriform cortex (Igarashi et al., 2012). As it has been recently shown that it has a role in odor discrimination of binary mixtures (Chae et al., 2020), it would be worth further exploring the role of the AON in olfactory figure-ground segregation.

Overall, olfactory figure-ground segregation is an important task for the survival of animals. Mechanistically, there are still many aspects of olfactory figure-ground segregation that remains to be explored.

Role of experimental models in probing neural mechanisms

Many factors are taken into consideration when using guided behavioral experiment to probe neural functions. Associative learning has been a powerful approach not just to study the mechanisms of learning and memory, but to probe the nature of sensory representations in the brain. Classic examples are Pavlovian conditioning and operant conditioning, differing in whether or not the experimental animal initiates the task. Other factors taken into consideration are the choice of environment, animal model, and complexity, to name a few (Rescorla and Holland, 1982; Carandini and Churchland, 2013).

A crucial aspect to be mindful of the is the practical and ethical use of animal models, thus task complexity and experimental duration are critical. That is, being able to utilize and maximize the use of animal models to gather relevant data, suited to question at hand, without subjecting animals to prolonged used is crucial.

To explore this, designing a practical experimental paradigm is important. My goal in this thesis is to develop and explore the use of a simple and tractable experimental paradigm to probe mechanisms of olfactory figure-ground segregation. This would enable a more practical and time-sensitive approach in collecting behavioral data. To address this, my specific aims are as follows:

1. Design a simple experimental paradigm for probing figure-ground segregation (Result Chapter 1)
2. Address how mice are solving the figure-ground segregation paradigm (Result Chapter 2); and
3. Present use cases showing how the proposed behavioral paradigm can be used to probe the mechanisms of figure-ground segregation (Result Chapter 3).

Result Chapter 1: Design of a simplified olfactory figure-ground segregation paradigm that captures the essence of the task

Introduction

Olfactory perception is a complex process influenced by acquired and innate factors such as repertoire and sensory tuning of olfactory receptor (OR) genes in relation to the stimuli present, as well as learning or experience and behavioral contexts.

The ligand-receptor interaction is the primary driver of activity leading to olfactory percept. As mentioned already in Introduction, a single molecule is a ligand for many olfactory receptors (Malnic et al., 1999), leading to overlapping glomerular activity patterns when odors occur as mixtures. As an extreme example, Inagaki et al. (2020), report in their study that a monomolecular odor could have the capacity to activate up to 90% of the olfactory sensory neurons in the mouse olfactory epithelium (Inagaki et al., 2020). This implies the need for complex processing for when other – perhaps even just one – background odors are mixed in. To compensate, olfactory information from the mixture components is modulated or normalized at different levels of the olfactory circuitry (Reddy et al., 2018; Inagaki et al., 2020; Zak et al., 2020). These mixture interactions ultimately affect the perceptual qualities of mixtures, especially compared with their component odors in isolation.

Characteristic of mixture perception: synthesis and analysis

The combination of odors may either create novel perceptual qualities (synthetic/configural perception) or retain perceptual qualities of one or more component odors (analytical/elemental perception). Odor complexity and background identity are known to be strong determinants of whether or not mixtures are perceived configurally or elementally. In general, the more complex the mixture is, the more likely configural perception takes place (Livermore and Laing, 1998b; Lindqvist et al., 2012; Thomas-Danguin et al., 2014).

Furthermore, the number of odor components in a mixture impacts configural perception (Thomas-Danguin et al., 2014).For example, varying “olfactory white” (mixture with about 30 equal-intensity odorant components) mixtures smell alike to non-expert subjects, regardless of the exact composition of the mixture (Weiss et al., 2012). Note, however, each component odor could contribute different degree of "complexity" in a mixture, based on its own molecular structure. It has been suggested that larger molecules evoke a wider array of olfactory notes than simpler ones among human subjects (Kermen, 2011). Thus, binary mixtures, albeit the simplest, also could produce perceptual qualities different from their components (Jinks and Laing, 2001).

Use of binary mixtures to probe olfactory mixture perceptions

It has been shown, that binary mixtures could be perceived elementally or configurally depending on the perceptual qualities of the component odors (Wiltrout et al., 2003). This was exemplified in humans where certain perceptual descriptors for monomolecular odors were lost when these monomolecular odors are combined with others. Configural perception for binary odors was evident in rats when the mixture contains odors that individually were perceived as similar to each other (Kay et al., 2003). On the other hand, elemental perception was evident when the individual component odors were perceptually different from one another.

Further, a proposed computational model for binary mixtures comprised of highly similar odorants showed that overlapping glomerular responses are inhibited - generating a distinct code that induces configural perception (Linster and Cleland, 2004). Overall, properties of the component odors (odor identity/similarity, receptor binding, and perceptual qualities, etc.) as well the mixture as a whole (e.g. mixture size) impact how mixtures are spontaneously perceived. These same factors also play a role when animals have to perform specific olfactory tasks such as figure-ground segregation.

Features to capture in the new behavioral paradigm

A study by Rokni et al. (2014) elegantly captured the effects of mixture size, odor similarity, and more importantly pattern overlap - or masking - in such task (Rokni et al., 2014). They showed that the size of the mixture may only be relevant if the background components are similar to the target odor of interest. Although there was some decline in the ability to detect the target odor (specific tiglates) when increasing the number of background odors that are dissimilar to the target, the effect was not as impactful as when the number of similar background odorants increased. This demonstrated the relevance of the background odor similarity and size on the perceptual task. In essence, the greater the masking index, which relates to the similarity and size of the background odors, the more difficult the task is for the animals (Rokni et al., 2014).

As mentioned in the general introduction, insights on neural mechanisms are often revealed when configural percepts are studied in terms of component responses. However, to do so exhaustively using complex mixtures (with many component odors) can pose practical challenges. Thus, my goal for this chapter is to design a behavioral paradigm that balances the two essential aspects: To impose a degree of perceptual difficulty consistent with previous studies, while remaining tractable. I therefore chose to design an olfactory figure-ground segregation task using binary mixtures.

Methods

Animals

Behavioral experiments were approved by the OIST Animal Care and Use Committee (ACUC) prior to experimentation. Eight to twelve week-old male C57BL/6J (B6) mice were used in the study.

Olfactometry

Odors were presented using a custom-built olfactometer (Figure 2.2A) that allowed the presentation of 11 different odors, as well as non-odorized air/blank (“Bl.”). Briefly, during odor presentation, a controlled flow of air was passed through odor canisters containing saturated vapor and mixed with a diluting air, and finally presented to the mouse through a 5-way valve placed closed to the nose of the animal. Two separate manifolds with separate sets of odorants were used to generate binary mixtures. The first odor line (‘Group 1’)

contained the following odors: ethyl butyrate (W242705, Sigma-Aldrich, >98% purity), ethyl tiglate (T0247, TCI, >98%), methyl valerate (V0005, TCI , >99%), acetophenone (A0061, TCI, >98.5%), methyl anthranilate (A0500, TCI, >99%), butyl butyrate (B0757, TCI, >99%). The second odor line ('Group 2') contained the following: methyl butyrate (B0763, TCI, >99%), methyl salicylate (S0015, TCI, >99%), salicylaldehyde (S0004, TCI, >98%), methyl tiglate (T0248, TCI, >98%) and eugenol (A0232, TCI, >99%; Figure 2.1A). Non-odorized air (air that passed through blank canisters) was also presented randomly during the behavioral tasks. Odors were presented at 1-5% saturated vapor.

Behavioral training

Habituation: Prior to odor presentation experiments, head-fixed and water-restricted mice were acclimated in the setup for at least three days. Mice were provided with water (10 µl per droplet). Licks were recorded using an IR-beam sensor (Panasonic PM-F25) positioned in front of the mouth of the animal. Water droplets were given until mice were satiated for each habituation day. Habituation was conducted once per day and continued until mice learned to lick vigorously to receive water.

Pure odor discrimination

After habituation, mice were trained to perform pure odor discrimination. This comprised training to associate the target odor, ethyl butyrate, with reward (20 µl water), but to refrain from licking in response to presentations of other single odor presentations. Correct trials were where anticipatory licks (1-2.2s after final valve offset) were observed upon presentation of the target odor, but not other, odors. Odors were presented in a pseudo-random manner using a custom olfactometer. This continued until the mice showed at least 80% accuracy in performance for two consecutive sessions, mice were presented with binary mixtures, generated by combining odors from Group 1 and Group 2 and presenting them as one pulse.

Figure-ground segregation

After the habituation and pure odor discrimination training, the head-fixed mice went through the figure-ground segregation task using binary mixtures. To control the air flow independently, two odors used in the mixtures came from separate odor manifold of the olfactometer. Thus, in the experiment, the combination of odors from Group 1 and 2 (including blank) generated 42 possible mixtures.

Target switching

Mice began with training for multiple sessions of pure odor discrimination, where ethyl butyrate as the target odor was cued with blue LED, and methyl anthranilate as the alternative target odor was cued with green LED.

After several sessions of training the pure odor discrimination task with ethyl butyrate as the target, the light cue was changed to a green light and the target odor was changed to methyl anthranilate. When mice reached at least 80% accuracy for odor discrimination with this new target odor, they were then trained to switch between the two. The target odor was changed every 50 trials. I refer to these 50 trials as a "block" for convenience. When mice learned the switching component using pure odors, they were trained to perform switching on the figure-ground segregation task, switching between the two assigned target odors every 50 trials.

Analysis and data display

Custom MATLAB codes were used to analyze and visualize the data. Behavioral accuracy was calculated as the proportion of correct responses. A correct response was defined as one or more anticipatory licks on rewarded trial, and no anticipatory lick on unrewarded trial. Learning curves were calculated as performance in blocks of 50 trials.

Pairwise structural similarities of odors (maximum common substructure (MCS) Tanimoto coefficient) for each pair of odors were determined using the online service, ChemMine Tools (Backman et al., 2011). MATLAB function *cmdscale* was used to perform multidimensional scaling (principal coordinate analysis) for odor dissimilarities (1-Tanimoto Coefficient). Statistical analysis was done using MATLAB functions *ttest2* for two-sample t-test and *anova1* for analysis of variance (ANOVA).

Results

Structural and perceptual similarities of target and background odors

Because of the importance of odor choices in the design of the olfactory figure-ground task, I first selected a range of molecules that ranged in similarity to ethyl butyrate, the target odor. Chemical similarities are often evaluated either by using descriptors or structure matching. In my case, I obtained the pairwise similarities (Tanimoto coefficient) of the selected odors based on their maximum common substructure (MCS) using the online tool ChemMine Tools (Backman et al., 2011). For this analysis, a structure matching method using MCS represents the two-dimensional description, where the similarities of chemical structures of a pair of molecules as molecular graphs. It identifies the largest common subgraph shared by them. As such, it puts forth emphasis on the largest matching substructure, which is assumed to be relevant in the bioactivity of the molecules (Cao et al., 2008; Backman et al., 2011). This provides a simple and intuitive estimate of the odor similarity based on structure.

Among the non-target odors, methyl butyrate has the highest structural similarity to EB (MCS Tanimoto coefficient = 0.875). Other odors that are highly similar to EB include butyl butyrate, ethyl tiglate, methyl valerate and methyl tiglate. Some other odors are dissimilar to EB but share common substructures to one another (Figure 2.1). The neural similarity of these odors was confirmed separately through collaboration within the lab, by calculating the masking indices of odors relative to ethyl butyrate in a manner similar to Rokni et al., (2014). Here, the glomerular signals came from apical dendritic activities of mitral and tufted

cells (Adefuin et al., 2022). Overall, I selected a set of odors that have a variable degree of similarity to EB based on their structures.

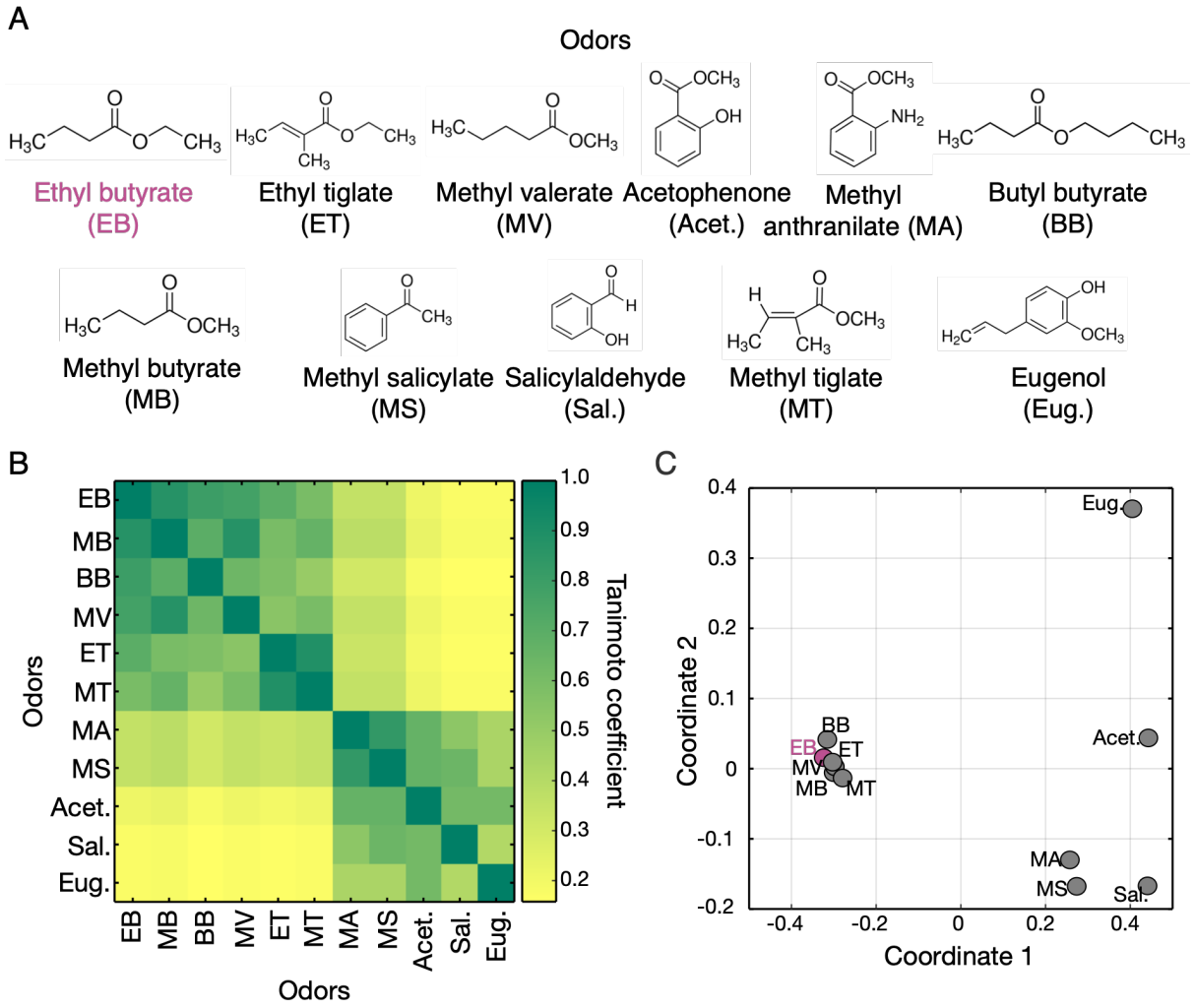

Figure 2. 1 Molecular structures of odors used.
A) Odors selected for the experiments and their respective structures. Ethyl butyrate (pink) is assigned as target odor. B) Pairwise structural similarities (Tanimoto coefficients) of the odors based on their maximum common substructure. C) Multi-dimensional scaling of the odors based on their dissimilarities (1-MCS tanimoto coefficient) shows how the odors were clustered. Ethyl butyrate in pink.

I then aimed to assess the perceived similarity relative to ethyl butyrate. This was done using a pure odor discrimination task (Fig 2.2B-D). This, as well as all subsequent behavioral tasks for the head-fixed mice is a Go/No-Go behavioral task.

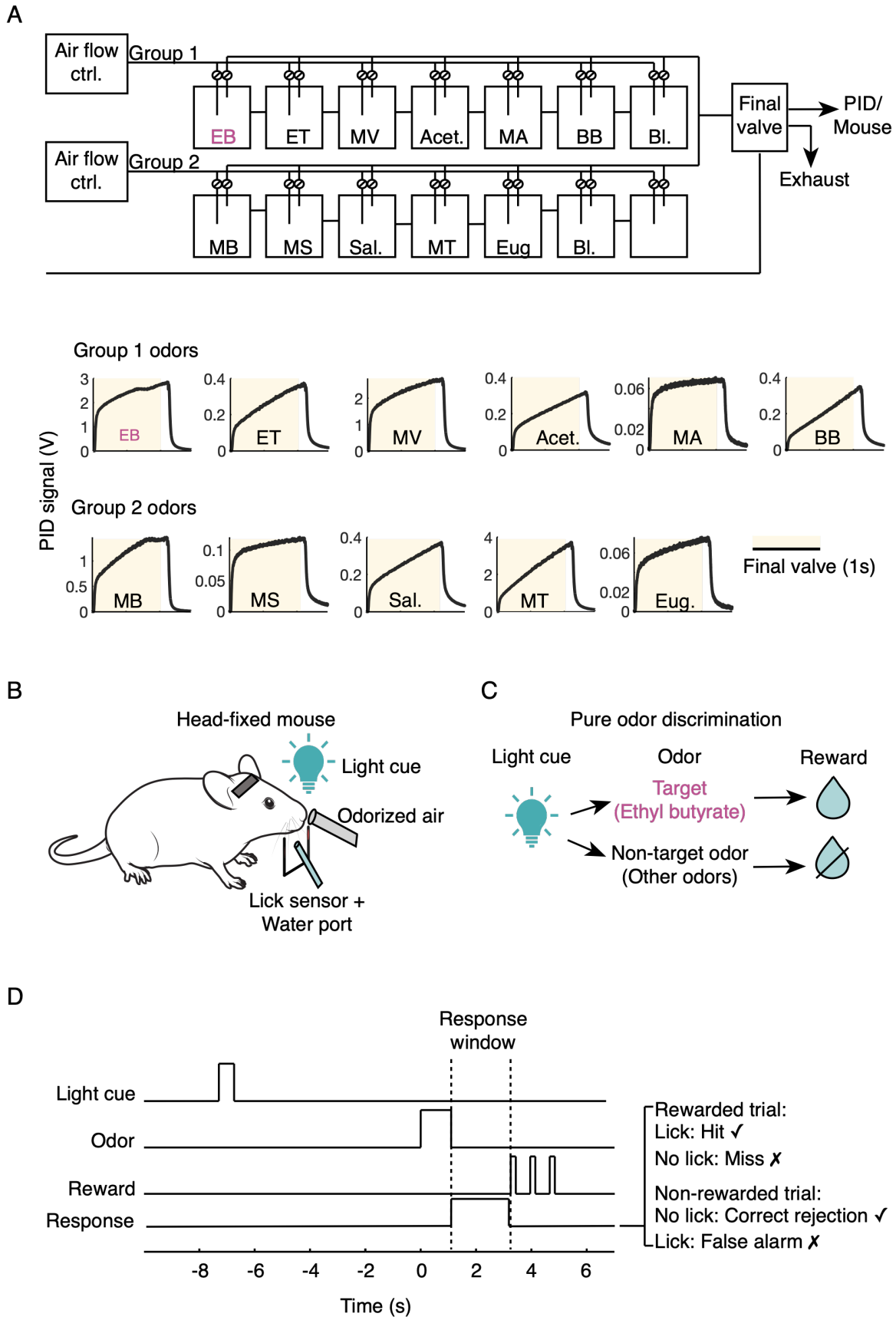

Figure 2. 2 Behavioral experiment for assessing perceptual similarity to target odor.
A) (Top) Layout of olfactometer used for presenting odors. Selected odors were separated into two groups. (Bottom) Example recordings using a photoionization detector (PID) to estimate the concentrations of the odors.

Shaded yellow region indicates the duration of the final valve (FV) opening (1s). B) Illustration for head-fixed mouse. Odorized air is presented in one nostril. A lick sensor, alongside a water port, is placed in front of the mouse. The beam of the lick sensor is broken whenever a mouse licks and the lick is recorded. C) Structure of pure odor discrimination task. D) Detailed trial structure. An LED cue indicates the beginning of each trial. In this task, a monomolecular odor is presented in each trial and water is given after the odor presented is the target odor (EB), while no water is given when other odors are presented. Example responses for rewarded and non-rewarded trial type are also shown. Correct responses are either hits (anticipatory licking on trial with target odor) or correct rejection (refraining from anticipatory licking on trial with non-target odor).

Over the course of the pure odor discrimination training, mice learned to lick after presentation of the target odor and to refrain from licking on non-target odors (Figure 2.3 A-C; mean anticipatory lick count on first vs. last day for S- and S+ trials: 1.1 ± 0.2 and 5.1 ± 1.5 ($p = 1.8e^{-04}$, t-test for equal means, t-score = -5.5) vs. 0.5 ± 0.1 and 15.4.± 4.5 ($p = 3.5e^{-07}$, t-test for equal means, t-score = -10.8), respectively (n= 12 mice). Overall, mice learned to perform the task with high accuracy, reaching 80% performance accuracy after about 150 trials (Figure 2.3D).

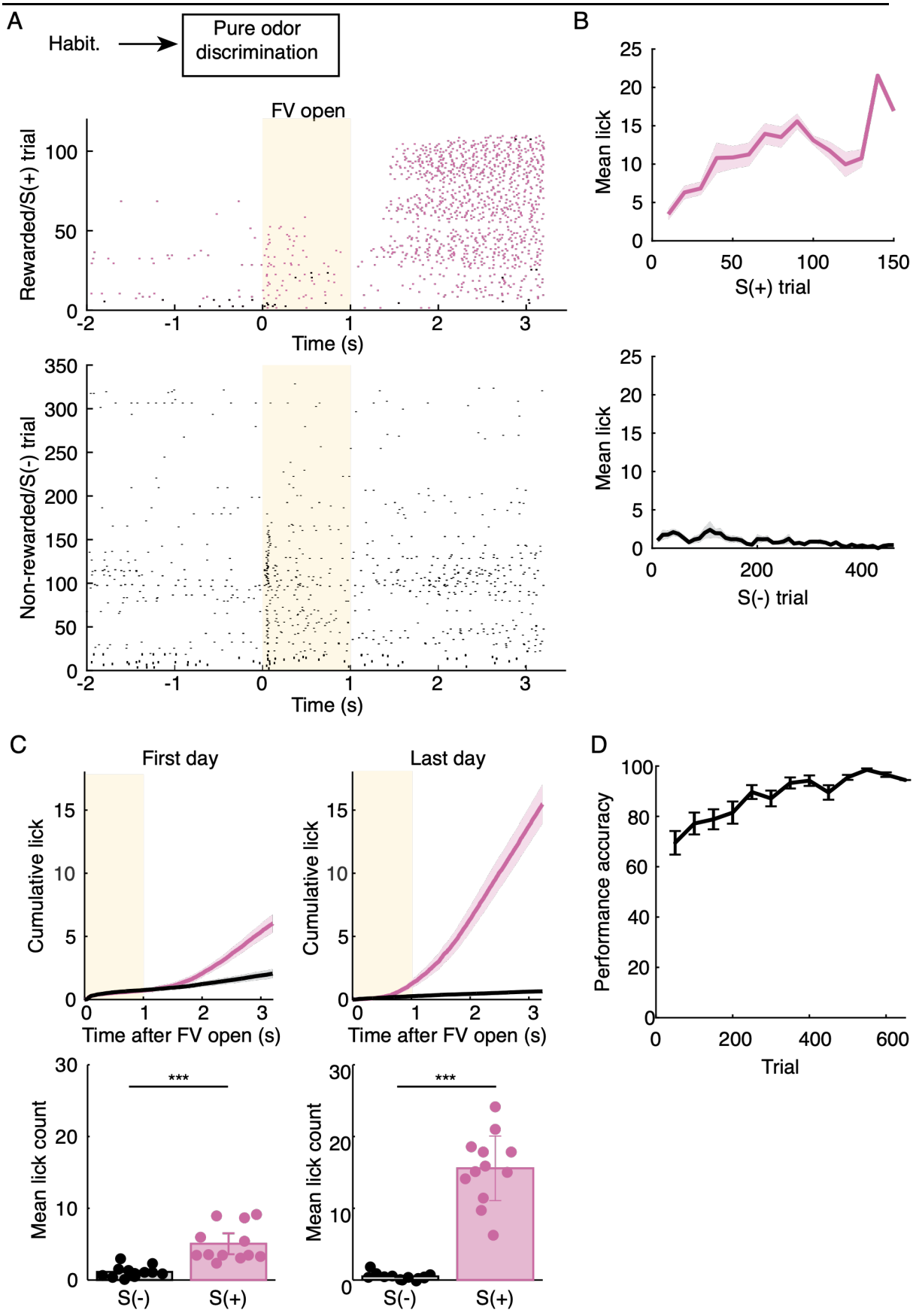

Figure 2. 3 Pure odor discrimination task reveals perceptual similarity between target and non-target odors.

A) Raster plots showing lick responses of an example mouse during multiple sessions of pure odor discrimination, separated by trial type (S+, top; S- bottom). Black ticks correspond to incorrect responses on both. Yellow indicates period for final valve opening. B) Average anticipatory lick count during multiple sessions of pure odor discrimination task (n=12 mice). Block of 10 trials. C) Average cumulative licks and average anticipatory lick count of mice during first (left) and final (right) day of training. Yellow indicates final valve opening. Paired t-test, *** denotes p<0.05, n=12 mice, circles equal individual mice. D) Average performance of mice during sessions of pure odor discrimination. Block of 50 trials, n=12 mice.

For non-target odors, mice performed worst during trials with methyl butyrate (Figure 2.4A, mean accuracy = 74.6 % ± 0.04). Thus, mice perceived methyl butyrate closest to the target odor, ethyl butyrate. Furthermore, performance accuracies of the mice declined with their MCS similarities to ethyl butyrate (Figure 2.4B, correlation coefficient r = -0.74, p-value = 0.015).

Overall, I demonstrate here the perceptual relationship between the target and selected non-target odors. Among the non-rewarded odors, those with high structural similarity with ethyl butyrate tend to be perceived similarly.

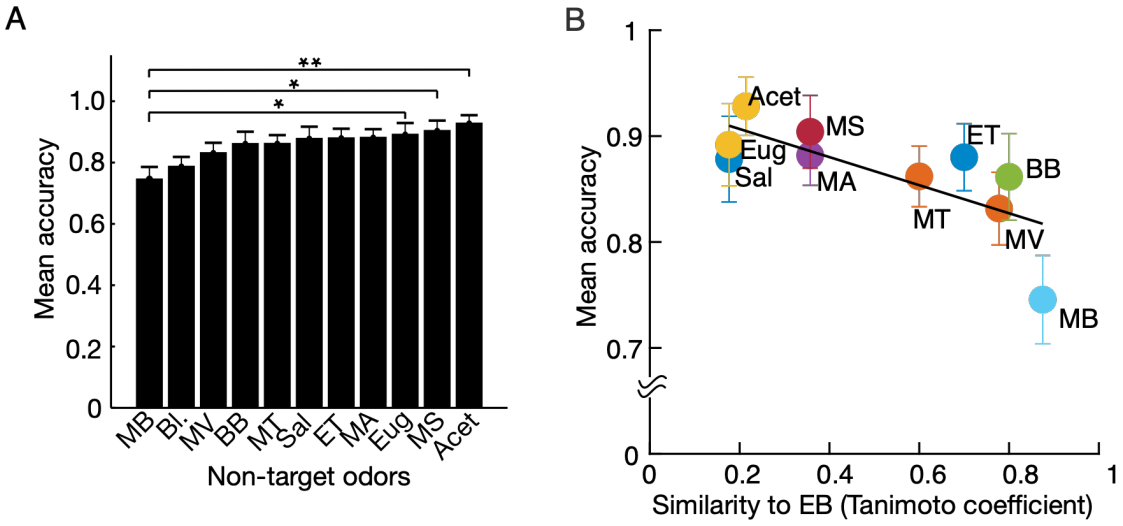

Figure 2. 4 Pure odor discrimination task reveals perceptual relationships between target and non-target odors.

A) Average accuracy in non-rewarded trials. One-way ANOVA showed significant differences between odorants (F(10, 121) = [2.7], p = 0.004). *Post-hoc* analysis using Tukey's HSD confirmed differences in mean correct responses, particularly on methyl butyrate training. * denotes p<0.05 and ** denotes p<0.01. Data are shown as mean±SEM. (n=12 mice). B) Relationship between accuracy mean±SEM in non-rewarded trials and similarity (Tanimoto coefficient) of each odor to ethyl butyrate (r = -0.74, p = 0.015).

Binary figure-ground segregation

Having learned how mice perceived each selected odor, I then tested how well mice could report the presence of the target odor (EB) when presented in a binary mixture. Here, I used the same sets of odorants, assigned them into two groups, then combined them together to form binary mixtures. The structure of the task is similar to pure odor discrimination, except any mixture with ethyl butyrate in it was associated with water (Figure 2.5).

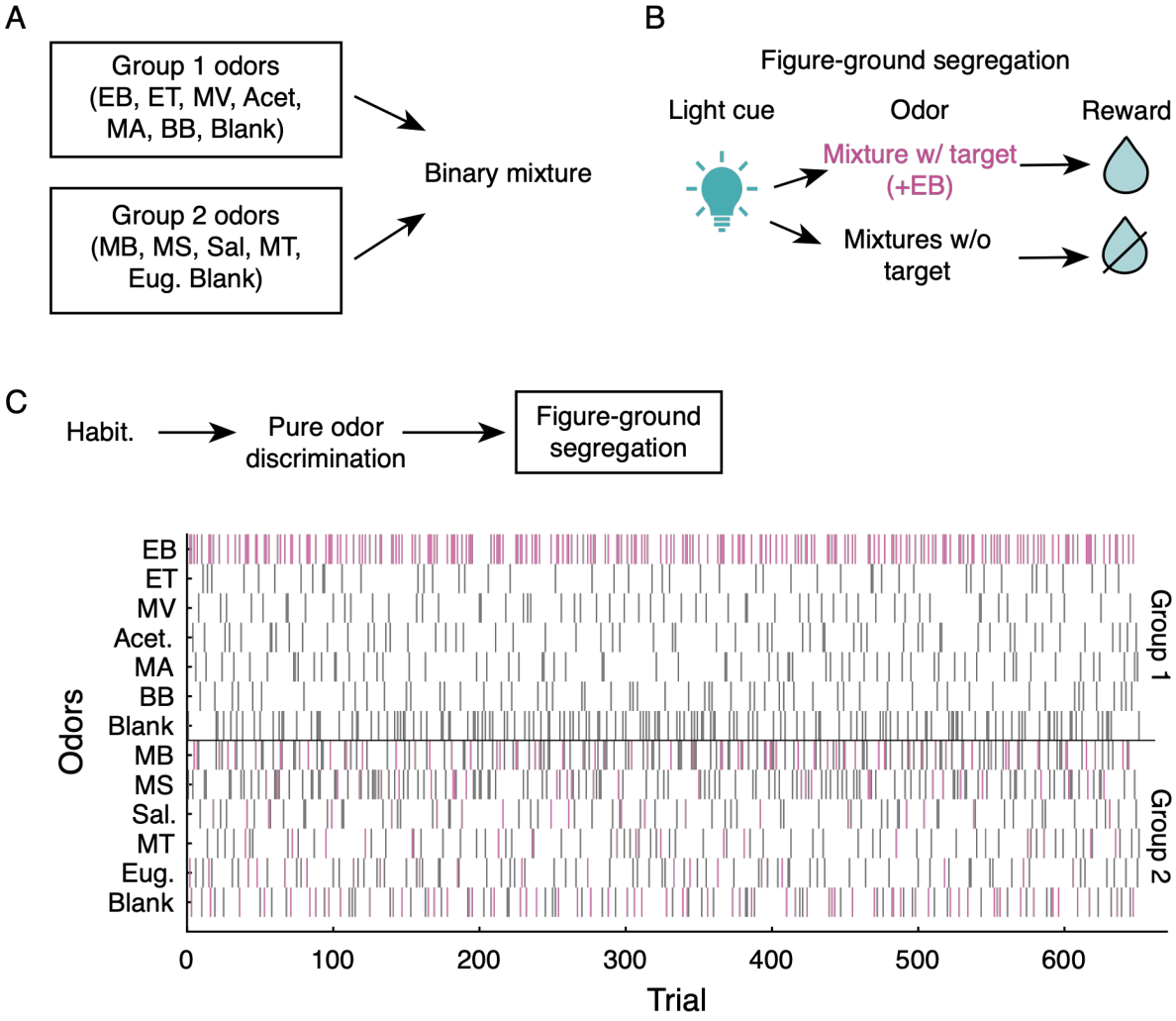

Figure 2. 5 Experimental structure for binary figure-ground segregation
A) Odors were grouped into two to generate binary mixtures, with ethyl butyrate in one group and methyl butyrate on the other. A binary mixture is made of an odor from each group. No mixture contained two odors from the same group. B) Structure of figure-ground segregation task. An LED cue indicates the beginning of each trial. In this task, a binary mixture presented in each trial and water is given after the mixture presented contains the target odor, ethyl butyrate. C) Example odor combinations used during figure-ground segregation. (Top) Prior to performing figure-ground segregation, mice were habituated and trained in pure odor discrimination. (Bottom) Odors are combined and presented in a semi-random manner. Ticks indicate odors presented in each trial. Pink ticks are trials with ethyl butyrate.

Once the mice acquired the pure odor discrimination task, as shown previously, the mice were subjected to figure-ground segregation tasks. They performed with high accuracy from the onset, with mean accuracy 0.8 from the first mixture session (Figure 2.6A).

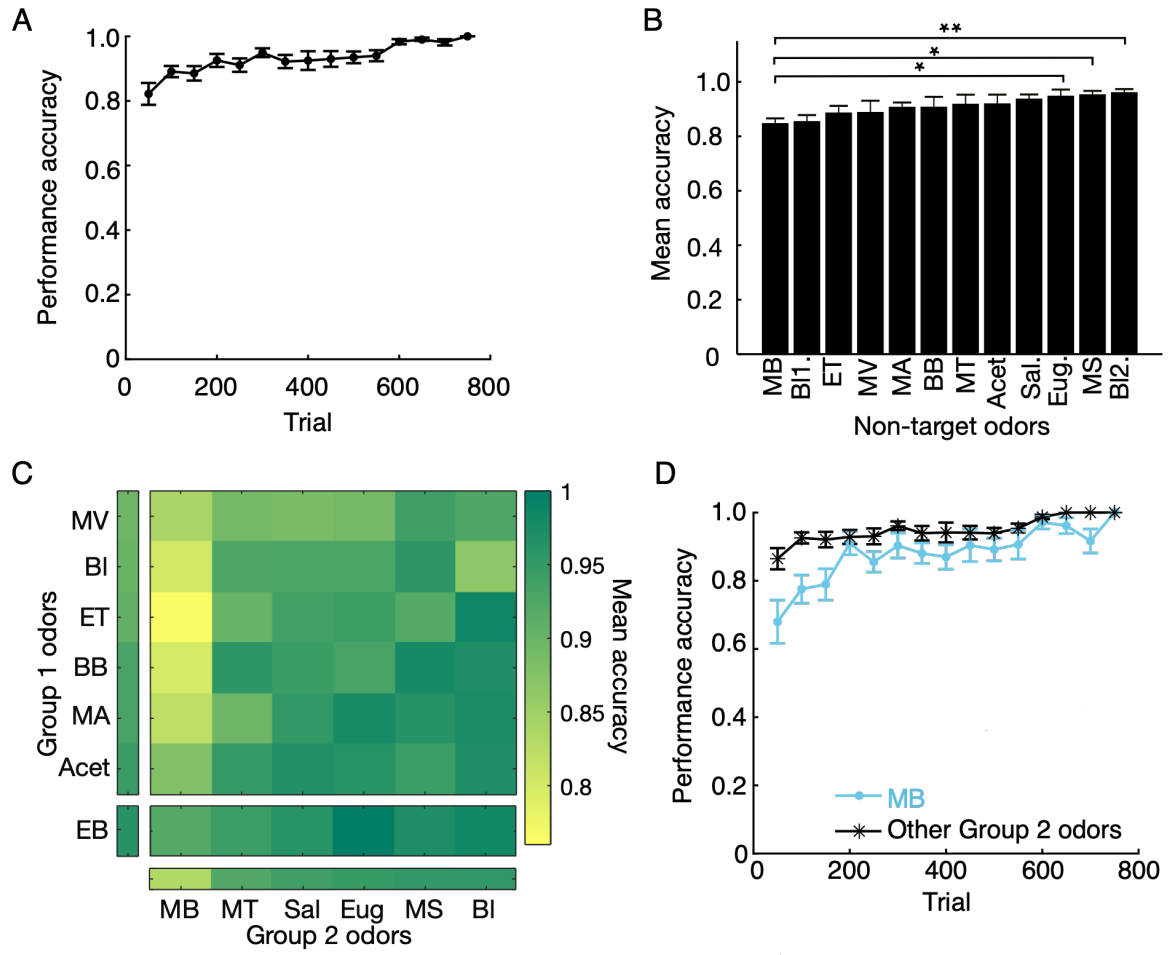

Figure 2. 6 Using similar background odor in binary mixtures recapitulates properties of olfactory figure-ground segregation

A) Average performance of mice during sessions of figure-ground segregation. B) Average response of mice to non-target odors. One-way ANOVA showed significant differences among mean accuracies for the odorants ($F(11, 121) = [3.3]$, $p = 6.4e^{04}$). *Post-hoc* analysis using Tukey's HSD confirmed differences in mean correct responses, particularly on methyl butyrate training. * denotes $p<0.05$ and ** denotes $p<0.01$. C) Average responses of mice for each odor combination. D) Average performance of mice, specifically on methyl butyrate (blue) and other group 2 odors (black), during figure-ground segregation. Each point is an average accuracy in a block of 50 trials. Data are shown as mean±SEM. (n=11 mice).

I then looked at their specific performances on the non-target odors (Figure 2.6B-D). Consistent with the earlier observation, mice again performed worst on trials containing methyl butyrate (mean accuracy = 0.85). Regardless of the presence of ethyl butyrate, animals tended to lick when methyl butyrate was present (Figure 2.6C). The mice needed more trials to improve, when compared to any other background (group 2) odor (Figure 2.6D; mean accuracy on first bin: 0.68 ± 0.06 (MB) vs. 0.86 ± 0.03 (other group 2 odors), p= 0.02, t-test for equal means, t-score = 2.6). Eventually, the mice were able to accurately discriminate against MB-containing odors. This demonstrates that despite the simplicity of using binary mixtures could, an appropriate choice of the background odor can pose suitable level of difficulty.

Tractability of binary mixture experimental paradigm

One aspect of the task design that was important was the tractability - the ability to compose all combinations of odors and single, component odors within the timeframe of an experiment. As described earlier (Figure 2.5A), because there were two independent air streams, with 6 and 7 odors respectively, this olfactometer generated 42 possible mixture combinations. Moreover, given that the experimental paradigm was designed with certain odors having different chances (e.g. rewarded trials had a third of a chance occurring during a session), I quantified the frequency of each odor combination to ensure all of them were indeed present in an average training session (Fig 2.7). It is not a uniform distribution, since rewarded trials occurred on 33% of the trials, making ethyl butyrate appear most frequently. Overall, the two-component mixtures make the experiment tractable in terms of number of odor combinations.

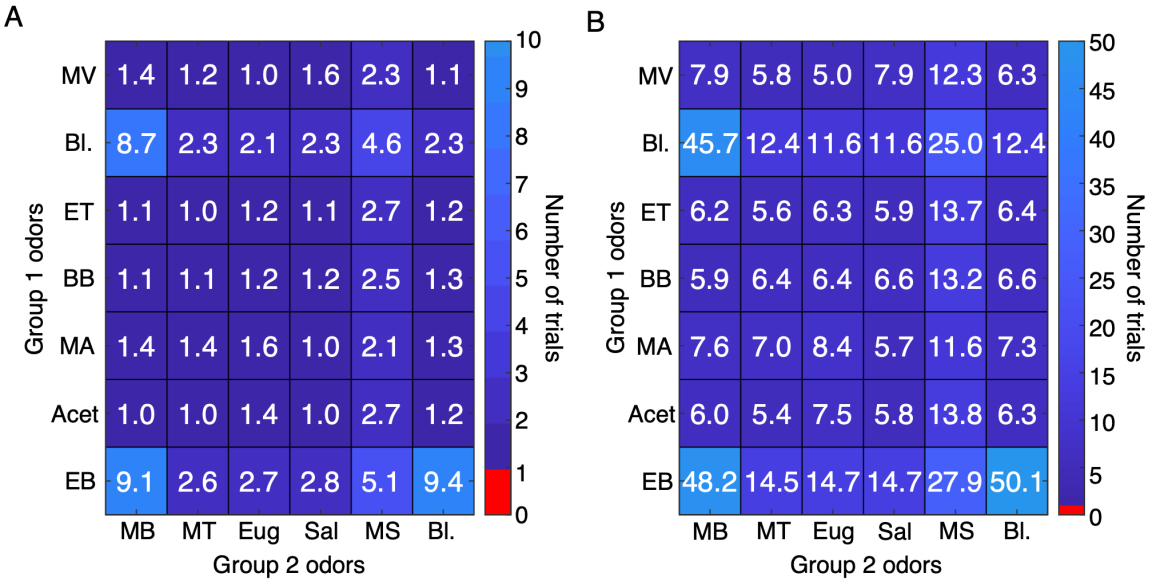

Figure 2. 7 Tractability of the experimental paradigm
A) Average number of trials for each mixture combination per experimental day or session. B) Average total number of trials for each mixture combination per mouse.

Target switching paradigm to induce attention shifts

Having determined that binary mixtures could be used as a model for figure-ground segregation I sought to extend the behavioral experiment even further. The main goal here was to switch the target odor rapidly using the same odor panels. In particular, by choosing the target odors that are structurally different from each other, a successful paradigm may enable different kinds of decision boundaries to be analyzed.

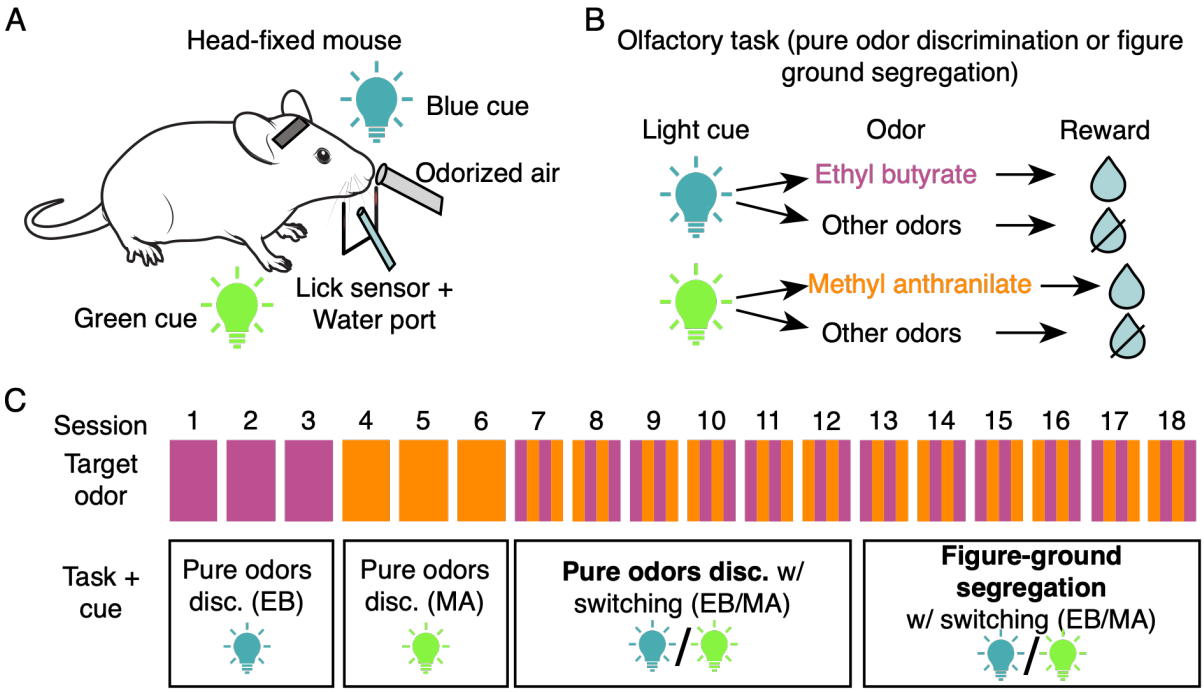

Figure 2. 8 Structure for task switching experiment.
A) Illustration for head-fixed mouse. Blue and green LEDs were placed on opposite sides of the mouse. B) Two odors, ethyl butyrate and methyl anthranilate, were alternately assigned as the rewarded odors along with different contextual cues for both olfactory tasks. C) A typical experimental flow for target odor training and switching during pure odor discrimination and figure-ground segregation. The number of trials and days for each type of experiment type varied, depending on the performance of each mouse.

Pure odor discrimination training with target switching

Mice were initially trained to perform pure odor discrimination. Separately, two odors were chosen as reward-associated odor, with two different contextual cues: blue LED flashes for ethyl butyrate and green LED flashes for methyl anthranilate (Figure 2.8). The two odors were chosen because of their dissimilarity with one another (MCS Tanimoto coefficient = 0.3571).

After three days of training, performance reached an accuracy of 90% when ethyl butyrate was assigned as the target odor. After this, a new target odor (methyl anthranilate) was assigned – with the previous target odor (EB) no longer associated with any reward. Mice eventually improved on this target as well, reaching at least 90% accuracy after 300 trials (Figure 2.9A).

Predictably, most errors occurred on trials when the previously rewarded odor was presented as a non-target (i.e., methyl anthranilate trials when ethyl butyrate is the assigned rewarded odor, and vice versa). The improvement takes form in the decrease in lick counts for the odor that was the target odor in the previous block. This trend is even clearer when counting the number of licks produced in response to the relevant odors (fig 2.9B). Generally, mice showed significant improvement within each block of 50 trials, as there is a clear difference between how mice responded to an odor as target versus non-target (Figure 2.9A & C).

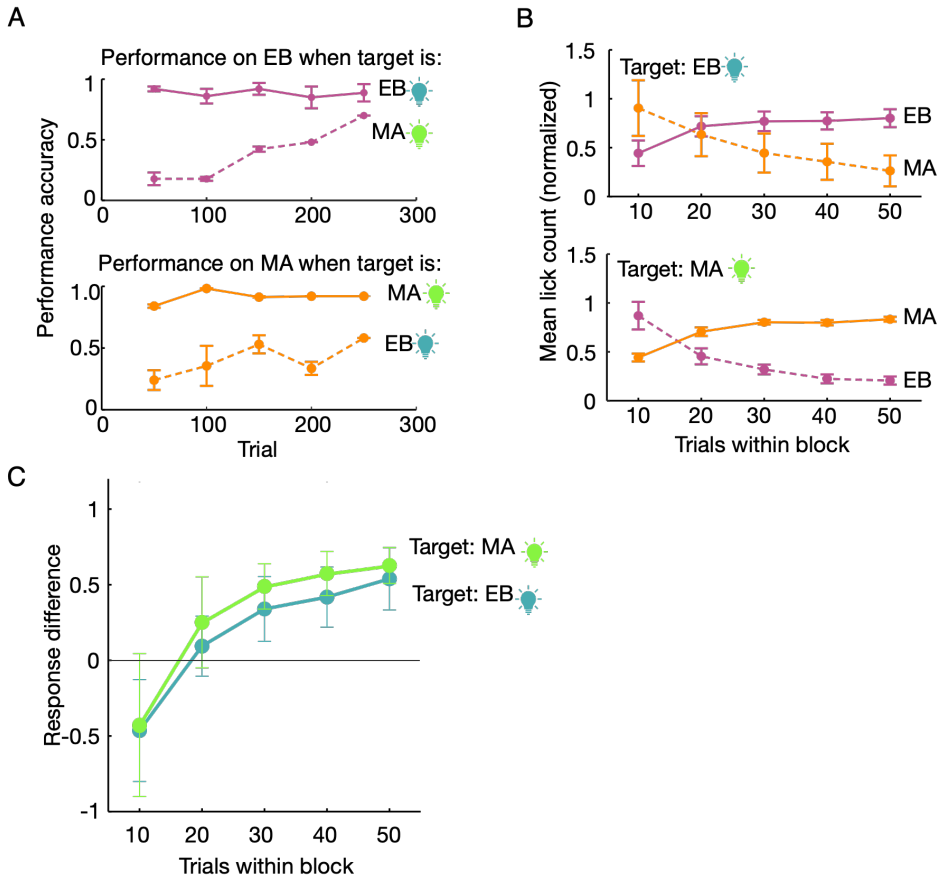

Figure 2. 9 Behavioral performance during switching when mice where presented with monomolecular odors.
A) Behavioral performance during switching when mice were presented with monomolecular odors. Mean correct responses for ethyl butyrate (EB, top) and methyl anthranilate (MA, bottom) as target (solid line) and as non- target (dashed line) odors during target switching. LED colors indicate target odors (blue = EB, light green = MA). B) Mean number of licks (normalized) of mice on ethyl butyrate (pink) and methyl anthranilate (orange) within the 50 trial block. Top shows when EB is the target odor, while bottom shows when MA is the target odor. C) Response difference indicates difference in the mean licking between EB and MA. Data are shown as mean±SEM (N= 3 mice).

Interestingly, when the target odors switched, the error types changed, too. The mice performed worst on methyl butyrate when the assigned target odor was ethyl butyrate. When the target odor assigned was methyl anthranilate, mice performed worst on trials with vanillin and non-odorized air (Figure 2.10B and C).

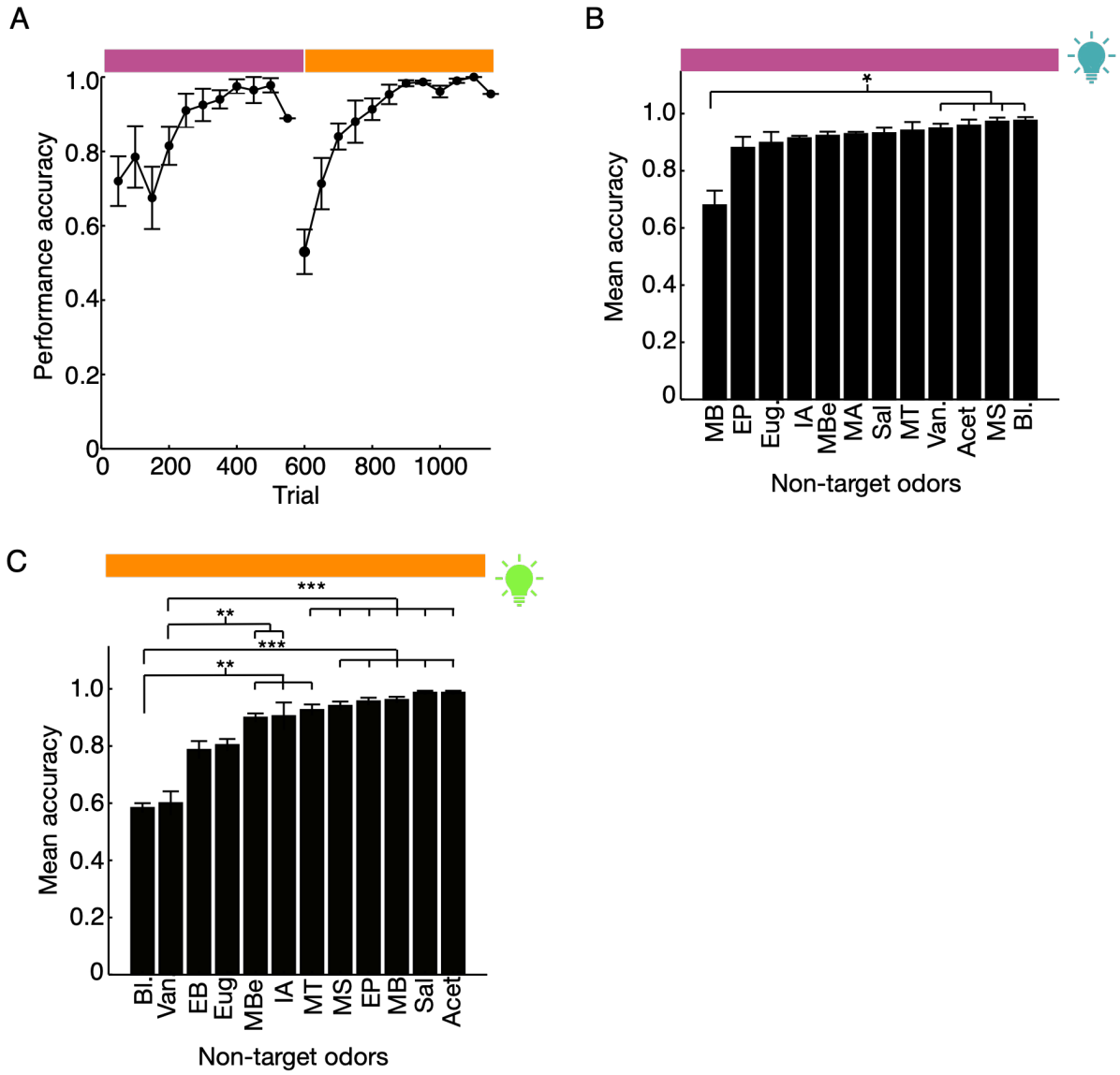

Figure 2. 10 Odor-specific analysis of behavioral performance during pure odor discrimination with different targets.
A) Behavioral performance during pure odor discrimination with two odors (ethyl butyrate, pink; and methyl anthranilate, orange) were assigned as the target odor, separately. B) Average response of mice to non-target odors when ethyl butyrate was the target odor. One-way ANOVA showed significant differences among mean accuracies for the odorants ($F(11,24) = [2.3]$, $p = 5.2e^{-06}$]). Post-hoc analysis using Tukey HSD confirmed differences in mean correct responses, particularly on methyl butyrate training. * denotes $p<0.05$. C) Similar to B but with methyl anthranilate as the target odor. One-way ANOVA showed significant differences among mean accuracies for the odorants ($F(11,24) = [8.8]$, $p = 0.04$). Post-hoc analysis using Tukey HSD confirmed differences in mean correct responses, particularly on methyl butyrate training. ** denotes $p<0.01$ and *** denotes $p<0.001$. Data are shown as mean±SEM (N = 3 mice).

Switching performance with figure-ground segregation

After reaching high accuracy on the pure odor switching paradigm, mice were tasked with identifying the target odors in a figure ground paradigm. Here, mice correctly identified ethyl butyrate and methyl anthranilate correctly as target odors 40-80% of the time (Figure 2.11A). While having already learned the switching context from the previous sessions (switching during pure odor discrimination), many of the errors here were produced when refraining to

lick to non-target odor that was the target odor in the previous block. The errors may not relate to the difficulty with which the mice detected the target odor in the presence of background odors. Generally, after training with single-odor discrimination, mice were able to perform figure-ground segregation with two-odor mixtures well from the beginning (as shown in Figure 2.6).

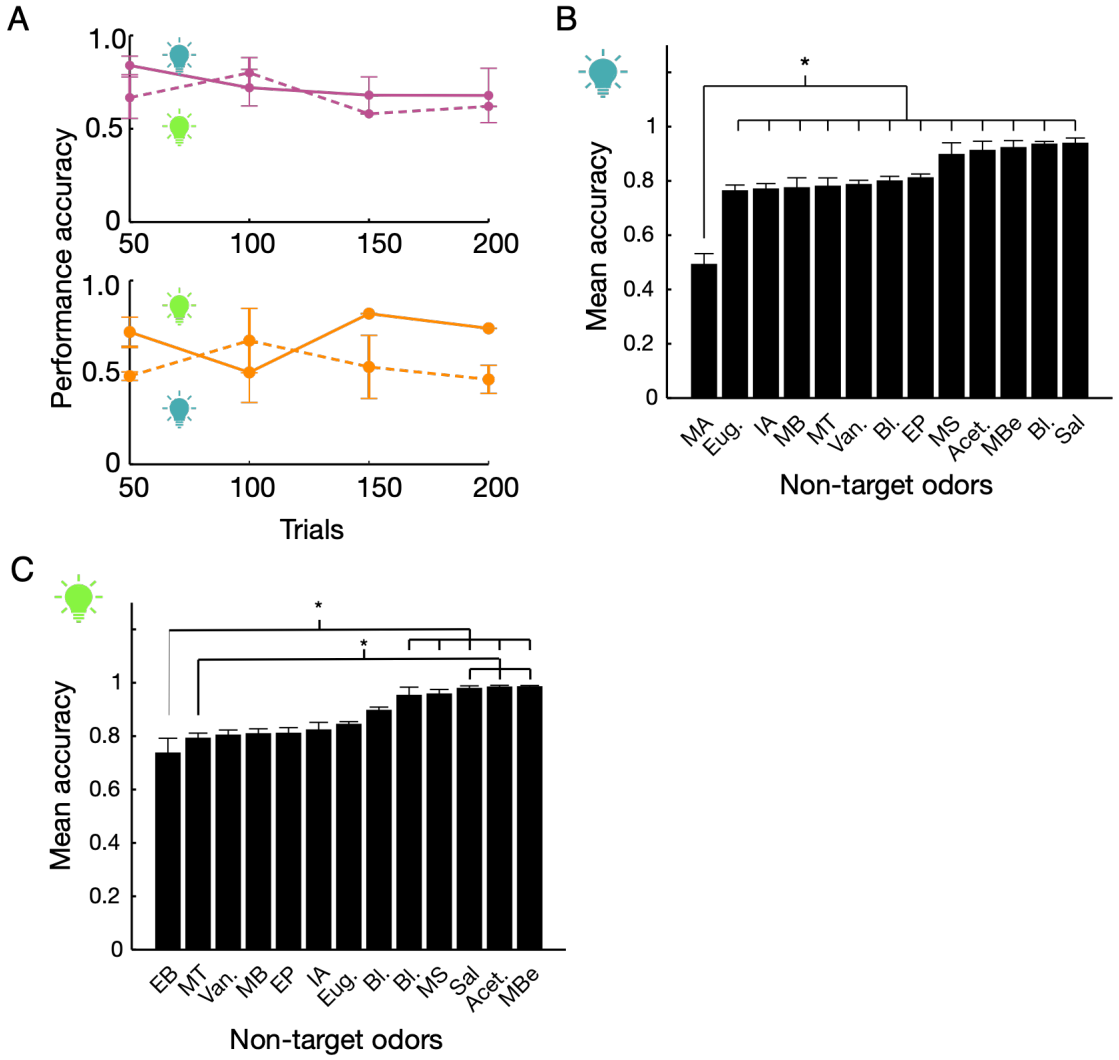

Figure 2. 11 Behavioral performance during switching when mice were presented with binary mixtures.

A) Mean correct responses for ethyl butyrate (top) and methyl anthranilate (bottom) as target (solid line) and as non-target (dashed line) odors for task switching during figure-ground segregation. B) Average response of mice to non-target odors on trials wherein ethyl butyrate is the assigned target odor One-way ANOVA showed significant differences between odorants ($F(12, 39) = [13.9]$, $p = 1.4e^{-10}]$). Post-hoc analysis using Tukey's HSD confirmed differences in mean correct responses, particularly on methyl butyrate training. * denotes $p<0.05$. C) Similar to B but with methyl anthranilate as the assigned target odor. odor One-way ANOVA showed significant differences between odorants ($F(12, 26) = [5.86$, $p = 8.24e^{-05}]$). Post-hoc analysis using Tukey's HSD confirmed differences in mean correct responses, particularly on methyl butyrate training. * denotes $p < 0.05$. Data are shown as mean±SEM (N = 3 mice).

When ethyl butyrate was the assigned target odor, mice performed poorly on methyl butyrate trials (mean accuracy = 0.77), albeit not the worst. Instead, mice performed worst on methyl anthranilate trials (mean accuracy = 0.49) (Fig 2.11B). Alternately, when methyl anthranilate was the assigned target odor, mice performed worst on ethyl butyrate trials (mean accuracy = 0.74; Figure 2.11 C).

Overall, the errors in the switching task for figure-ground segregation may reflect a target-specific difficulty, which may have a component of shifting attention between the two assigned target odors during switching.

Discussion

In this chapter, my main goal was to explore whether binary mixtures can be used in a relatively simple paradigm for figure-ground segregation. Here, the mice were trained to detect a target odor (ethyl butyrate) and were tasked to perform binary figure-ground segregation.

Using the pure discrimination task, I identified that methyl butyrate is perceptually similar to EB, which is most structurally similar to EB within my odor set according to the structural analysis. As a result, the errors in the mixture detection task mostly came from methyl butyrate trials. This pattern of errors is consistent with what we know about odor structure and evoked pattern overlap in the OB (Rokni et al., 2014).

Another important consideration was that the mice were not overtrained just on methyl butyrate but were presented with rest of the non-target odors, which helps reduce stimulus predictability and affect performance accuracy (Zariwala et al., 2013).

Looking specifically at the learning curve of mice on the trials with the background odors shows that mice performed poorly on MB trials initially but did improve later on (Figure 2.6D). What this shows is that despite the simplicity of the mixture composition, detecting and reporting the presence of the target odor may not be that readily obvious or attainable. Thus, the task assigned to the mice actually requires engaging in figure-ground segregation.

A potential argument against binary mixtures versus more complex ones is that the easiness of the former. There is no denying that more complex mixtures can be more difficult. Such would require more processing to demix the odors, and perhaps more potential for probing its mechanism. However, binary odors can still evoke configural percepts, which should require demixing for one odor to be detected. Further, the use of larger and more complex mixtures require longer training time (Rokni et al., 2014), which could be at the expense of the water-restricted animals. The simplicity of our experiment while still being able to probe the limits of figure-ground segregation makes for a more practical model for figure-ground segregation. Mechanistic insights that can be revealed with it may be applicable in more complex mixtures, akin to what animals may encounter in natural environments.

Having determined that binary mixtures could still be used to exhibit known features of figure-ground segregation, I extended the behavioral experiments to determine how mice

performed figure-ground segregation when having to switch between two assigned target odors.

While the mixture task performance demonstrated that the use of a background odor similar to the target (like methyl butyrate to ethyl butyrate) makes the figure-ground segregation task difficult despite the simplicity of the mixture composition, results for the switching experiment showed a different kind of difficulty. Most errors were on odors that were assigned prior as the target odor, and the mice were slow to switch. This slow speed of switching may pose some problems with physiological experiments. Further improvement and optimization regarding this switching experiment therefore need to be conducted. As such, I halted pursuing this experiment.

Overall, my behavioral experiment using binary mixtures was still able to capture relevant features, including psychophysical limits, of figure-ground segregation. By making use of a background odor that shares structural and perceptual similarity to the target odor – potentially maximizing its masking or evoked pattern overlap compared with the other background odors – we can stretch the potential of binary mixtures and use it as a model for figure-ground segregation task.

Result Chapter 2: Prior exposure to component odors and its effect on the behavioral strategy

Introduction

In the result chapter 1, I designed the olfactory figure-ground segregation using binary mixtures. Here, I aim to determine analyze further a possible behavioral strategy the mice may be using i.e., whether or not the mice subject to this behavioral paradigm demix mixtures when reporting the presence of an odor in a mixture or discriminating mixtures without separating the target odor from the background. My approach is to assess how prior knowledge of the component odors impacts the performance of mice in the task, especially when a novel odor is introduced.

Background

The computational process involved in detecting a specific object in a mixture is said to involve 'demixing'. This is a process where mixture of signals is segmented or decomposed into its components. Recognizing the presence of the target odor among the decomposed odors through pattern recognition may be a relevant computation for olfactory figure-ground segregation (Penker et al., 2020).

Whether demixing occurs in olfactory figure-ground segregation remains unclear. Recent olfactory studies offer differing insights. In a generative model for olfactory figure-ground segregation, demixing of odors involves predicting the probability distribution of the odor components present in the mixture through iterative interactions (Grabska-Barwińska et al., 2017). Alternately, it has been shown that mice can generalize with smaller mixtures but struggle with larger, more complex ones (Mathis et al., 2016).

The strategy used by the nervous system to solve the figure-ground segregation may depend on sensory experiences. Studies from other sensory modalities have shown that having a prior knowledge about the target pattern helps in figure-ground segregation. For example, humans who find that a highly familiar voice such as the voice of their spouses' (Johnsrude et al., 2013) or native language (Cooke et al., 2008) could help overcome the cocktail party effect.

Prior knowledge or experience is important as it may consolidate the circuitry for recognizing the template pattern. For example, learning reward-association of visual stimuli produces notable representations of the relevant stimuli in the primary visual cortex (V1) (Poort et al., 2015). In humans, predictive signals produced before stimulus presentation may be similar to stimulus-evoked representations (Kok et al., 2017). Additionally, prior sensory experience may provide top-down information that interacts with bottom up input to help with figure-ground segmentation. For example, in guided speech segregation, human subjects with advanced knowledge of target speech stream exhibited enhanced neuronal responses to the target (Wang et al., 2019).

Thus, in this thesis, my goal is to assess if knowledge of individual odors beforehand may affect how mice respond to mixtures. I assess how two groups of mice (with vs. without prior experience learning the monomolecular odors) acquire the binary mixture task, and further, how they generalize when exposed to a novel monomolecular odor. I hypothesize that mice with prior experience to monomolecular odors demix odors and, because they may be better at decomposing components, outperform in generalizing to the novel mixture.

Methods

Animals

Behavioral experiments were approved by the OIST Animal Care and Use Committee (ACUC) prior to experimentation. Eight to twelve weeks old male mice were used in the study.

Olfactometry

The same set of odors as in chapter 1 were presented during these experiments. Additionally, for the generalization experiment, butyl acetate (BA; Sigma 287725) was added in the olfactometer set up.

Behavioral training

The structure of the behavioral experiment is similar to chapter 1.

In this chapter, there were two groups of animals. The non-exposed group (non-exposed group) did not undergo "pure odor discrimination training". Instead, for this group (Figure 2.1E), they were immediately presented with binary mixtures and tasked to report the presence of EB in them. The other group (pre-exposed group) followed our behavioral paradigm for figure-ground segregation: mice underwent pure-odor training before being presented with binary mixtures to accomplish the same goal. For convention, in this chapter, experiments with mixtures were simply referred to as mixture training rather than figure-ground segregation.

Generalization with novel background odor

The structure of the generalization task is similar to the figure-ground segregation task already introduced, except that a novel odor (butyl acetate, BA) is added into the set of odorants. The generalization experiment was conducted when mice have had an overall performance of about 80% in the mixture training task.

Data analysis

Custom MATLAB codes were used to analyze and visualize the data as before. MATLAB function *boxplot* was used to illustrate box-and-whisker plot of the data with the horizontal line inside the box indicating the median and the whiskers and the upper and lower extremes showing the 25th and 75th percentile, respectively. Circle indicates an outlier.

Results

In this chapter, I wished to determine whether the mice utilizing my behavioral paradigm demix odors based on its behavioral performance and how prior knowledge relates to this. As stated before, my general hypothesis for this chapter is that mice that utilize prior exposure to single odors demix odorants in order to determine the presence of the target in binary mixtures. Further, I hypothesize that this aids generally in performing the olfactory figure-ground segregation task.

To this end, I trained two cohorts of animals to report the presence of ethyl butyrate in mixtures. One group comprised mice that went through pure odor discrimination i.e., they were pre-exposed and trained with all individual odor component before the binary mixture training ("pre-exposed group"). The other group ("non-exposed group") underwent the binary mixture training without prior exposure or training with monomolecular odors (Figure 3.1).

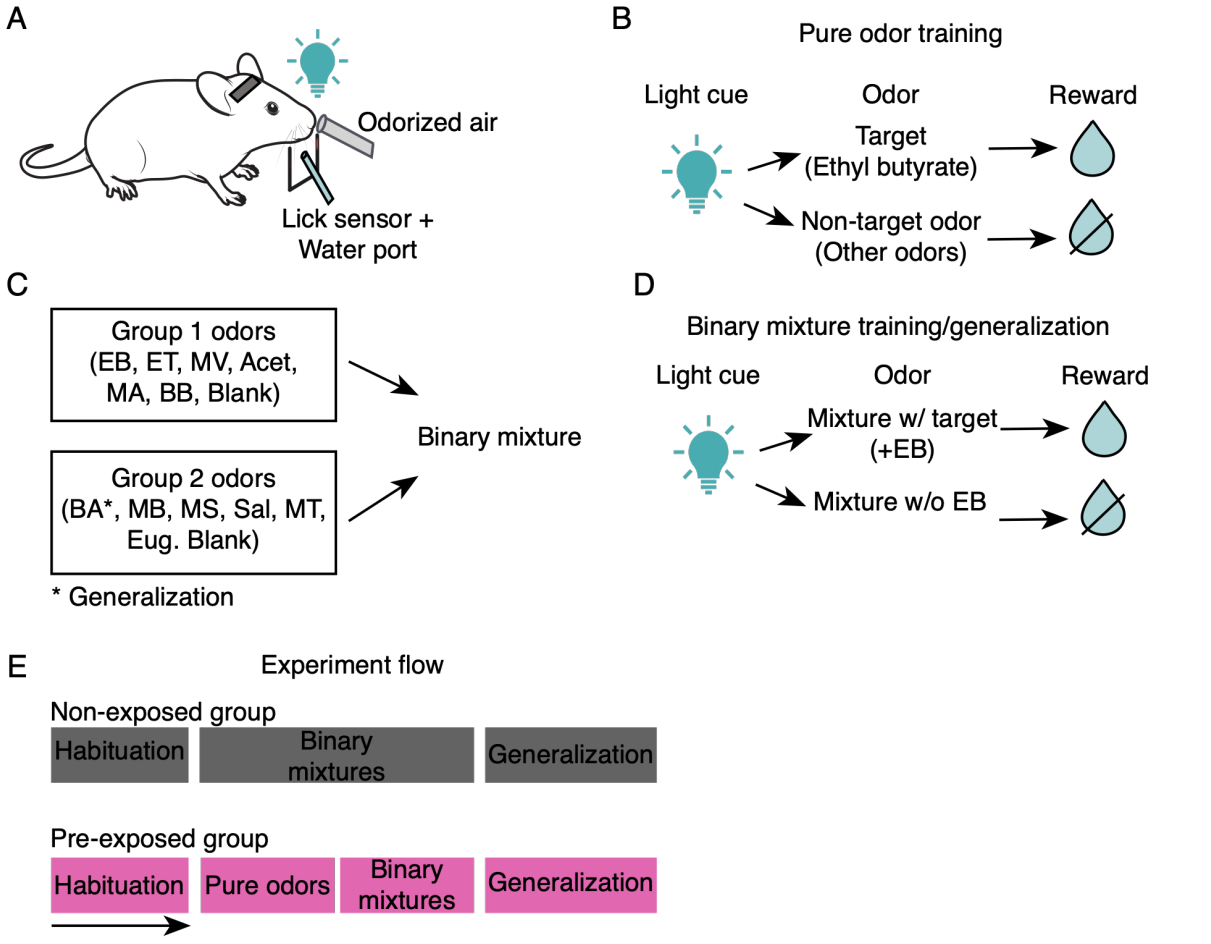

Figure 3. 1 Behavioral experiment for assessing whether mice demix odors when detecting a target odor in binary mixtures.
A) Illustration of experimental setup using a head-fixed mouse. Odorized air is presented in one nostril. A lick sensor, alongside a water port, is placed in front of the mouse. The beam of the lick sensor is broken whenever a mouse licks. B) Structure of pure odor discrimination task. C) Odor combinations for the binary mixture task. D) Structure of the binary mixture (and generalization) task. E) Flow of experiments for the two group of mice. The non-exposed group (grey) immediately underwent the binary mixture training after habituation. On the other hand, the pre-exposed group (pink) first underwent reward association training with all pure odors first before proceeding

to binary mixture training. Both performed one day of generalization experiment, which is similar to the binary training except for the addition of the novel odor, butyl acetate (BA).

With these two groups of mice, I specifically aimed to do the following: 1) first, compare the rate of mixture task acquisition for the two groups during the initial training phase; 2) determine if their ability to generalize and detect the target odor upon the introduction of a novel odor is influenced by prior exposure.

Overall, the pre-exposed group (in pink, Figure 3.2) began to perform a pure odor training task of up to 350 trials, then performed the binary mixture task, all in all totaled 600 trials. On the other hand, the non-exposed group (in grey) performed the binary mixture task all throughout, which totaled up to 650 trials (Figure 3.2B).

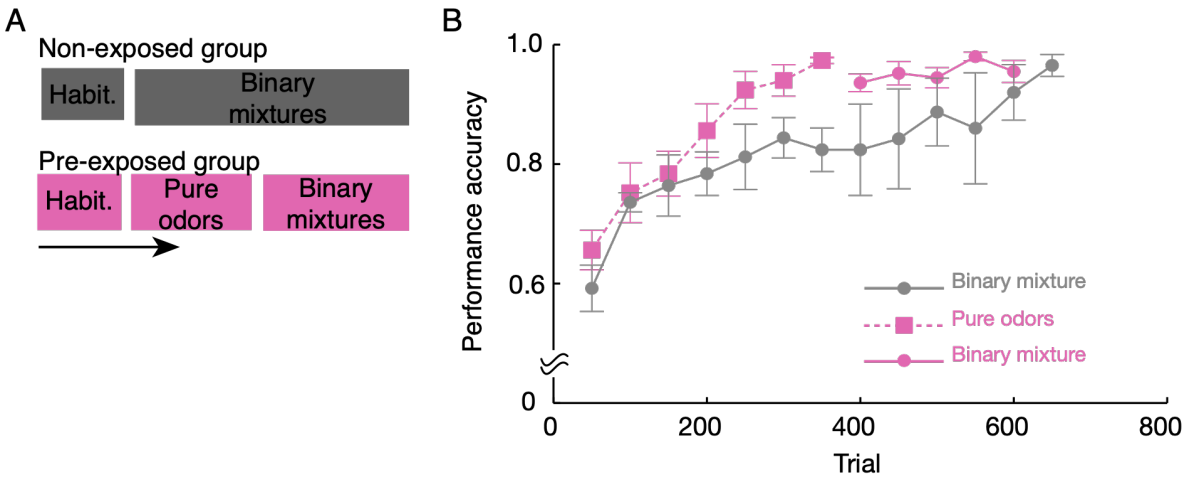

Figure 3. 2 Overall performance of mice during binary mixture training
A) Experimental flow for the two groups. The non-exposed group performed the binary mixture task after habituation, whereas the pre-exposed group a pure-odor discrimination task before doing the same binary mixture task as the other group. B) Response accuracy of the non-exposed group (grey) and pre-exposed group (pink) throughout multiple sessions of odor training. Block of 50 trials. Data are shown as mean±SEM. (n=5 mice per group).

To eliminate the possibility that the two cohorts experienced different amount of reinforcement, I analyzed the probability of rewarded trial occurrence (Figure 3.3). This is important given that expectancy of the rewarded signal is known to impact learning rate and accuracy in animals (Zariwala et al., 2013). I compared the overall chance of rewarded and non-rewarded trials per experimental session (Figure 3.3B-C). There was no difference in the probability of rewarded (mean probability: 0.3342 (non-exposed) vs. 0.3345 (pre-exposed), p-value =0.95, t-test, t-score = 0.06) and non-rewarded (mean probability: 0.6655 (non-exposed) vs. 0.6658 (pre-exposed), p = 0.95, t-test, t-score = 0.06) trials for the two groups (Figure 2.3C).

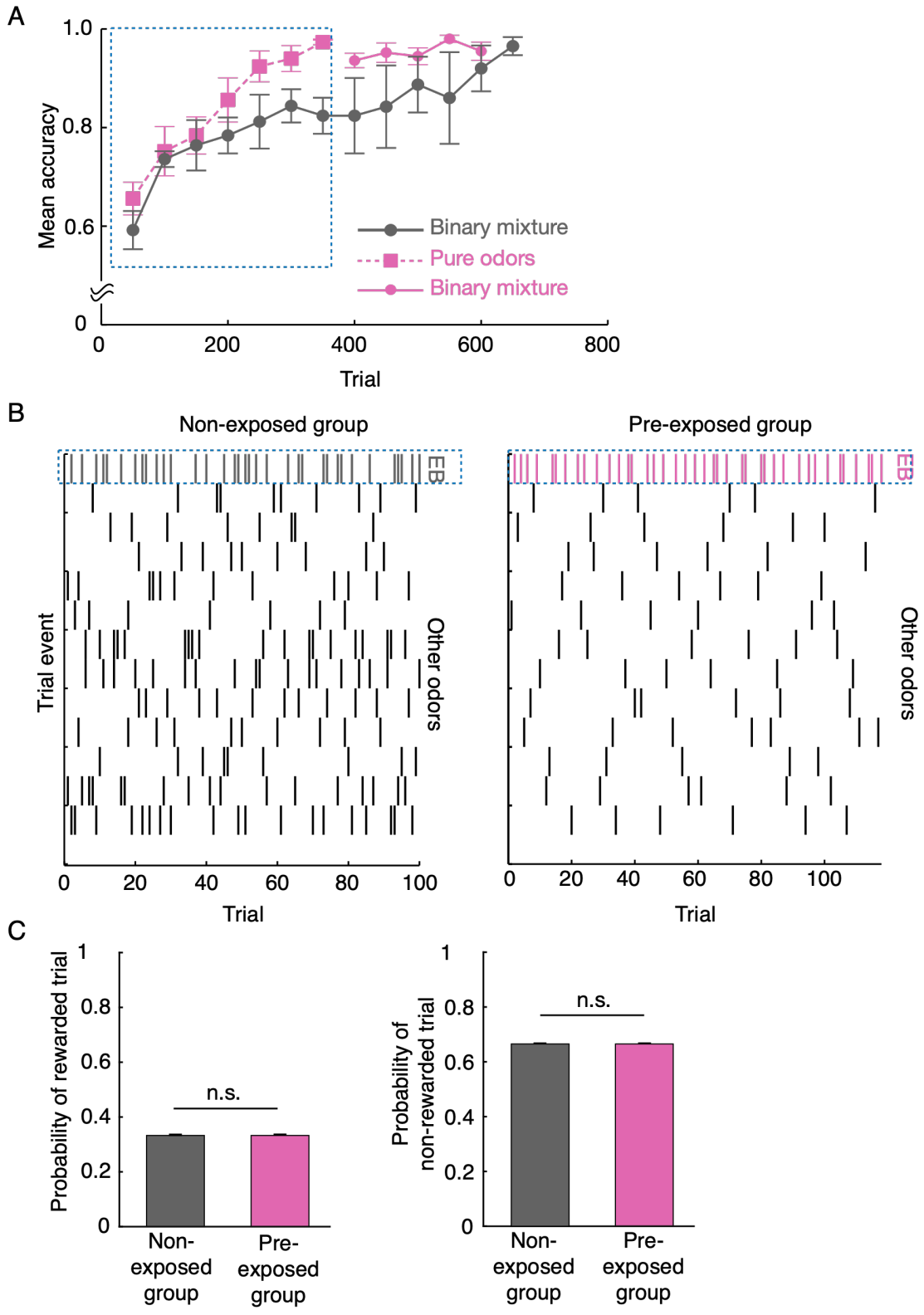

Figure 3. 3 Difference in responses of the two groups during the learning phase of the task
A) Learning curve with blue box showing the initial training phase of the experiments. Mice in the non-exposed group performed binary mixture training, while mice in the pre-exposed group performed pure odor training during the same period. B) Example session for one pair of animals showing the instances of individual odors for the non-exposed group (left) and the pre-exposed group (right). EB trials are highlighted on top of each. C) Overall chances of rewarded and non-rewarded trials throughout multiple training sessions. Statistical test by two-sample t-test, n.s. denotes not significant. N=5 mice per group.

Detailed analysis of task acquisition

I next analyzed how mice responded to the presence of each odor component, as error types could reveal insights on the strategy used. Note that this is a comparison of initial phase of training i.e., acquisition of pure odor discrimination for the pre-exposed group, and mixture detection for the non-exposed group. An analysis of mixture detection performance for the pre-exposed group is given later.

Since most of the errors for Go/No-Go paradigms occur on unrewarded trials, I focused on these trial types. I found a curious lack of odor-specific error that is common to pre-exposed group. Methyl butyrate still ranked worst on the non-exposed group, this was not statistically significant from any of the other odors (Figure 3.4B left; one-way ANOVA, $F(9,40) = [1.3]$, $p = 0.25$). On the other hand, the pre-exposed group showed preferential difficulty towards methyl butyrate trials (one-way ANOVA, $F(9,40) = [3.3]$, $p = 0.0044$; Figure 3.4B right). The non-specific false alarms in the non-exposed may suggest that the difficulty was less related to the similarity of the background to the target odor.

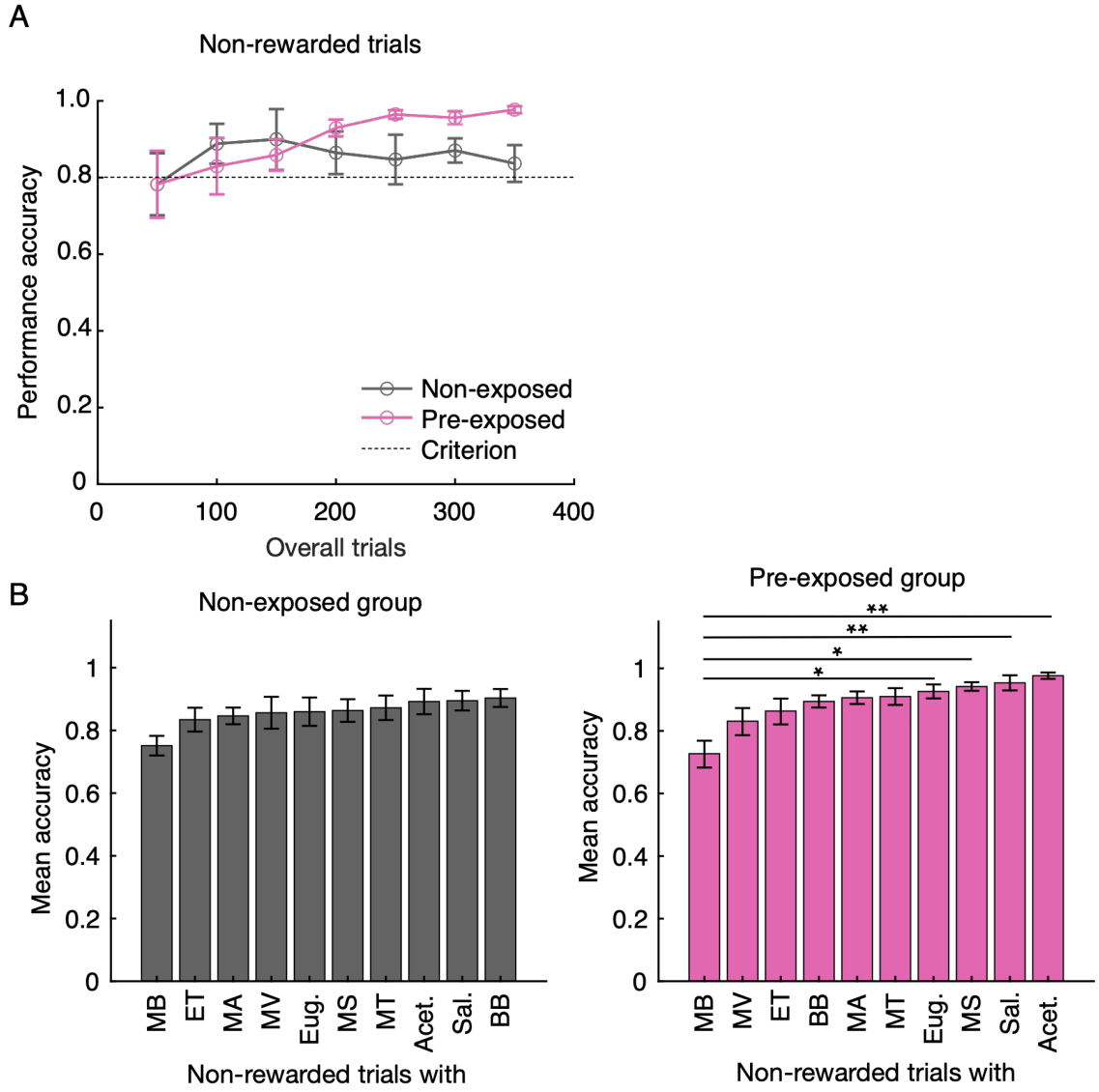

Figure 3. 4 Prior knowledge of component odors results in odor-specific errors
A) Overall performance of mice on non-rewarded trials only. B) Average performance of mice on non-rewarded trials containing specific component odors. (Left) Non-exposed group: One-way ANOVA showed no significant differences among odors. (Right) Pre-exposed group. One-way ANOVA showed significant differences among mean accuracies for the odorants. Post-hoc analysis using Tukey HSD confirmed differences in mean correct responses, particularly on methyl butyrate training. * denotes $p<0.05$ and ** denotes $p<0.01$. Data are shown as mean±SEM. (n=5 mice per group).

Additionally, to compare the behavioral performance of the two groups, I looked at how they specifically performed on rewarded trials. Having not learned stimulus-reward association yet, mice initially performed poorly on ethyl butyrate trials accurately (mean accuracy on first bin: 21.25 ± 7.29% (non-exposed group) vs. 41.25 ± 14.87% (pre-exposed group); 16 rewarded trials per bin). Both groups did reach comparably high accuracy by the end (Figure 3.5A).

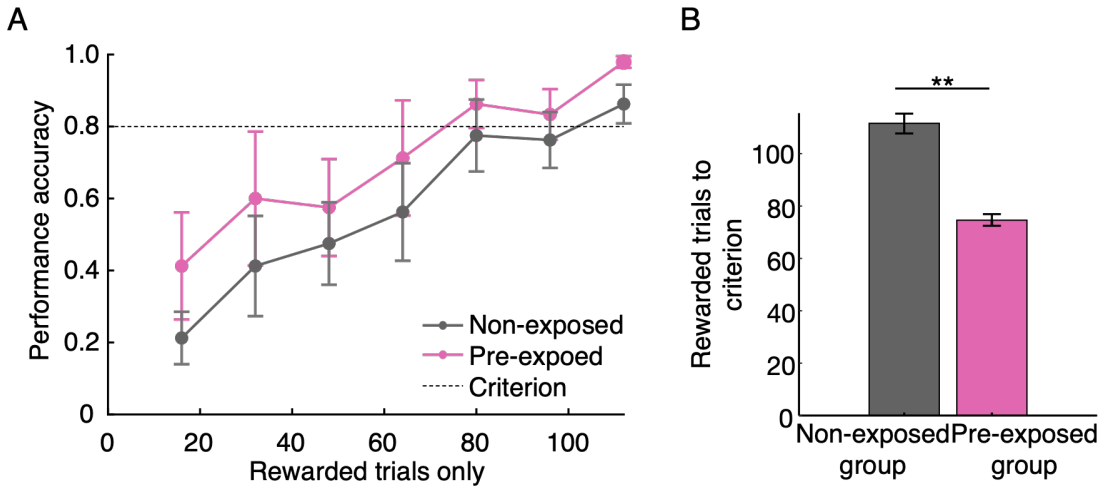

Figure 3. 5. Prior knowledge of component odors aids in correctly responding to rewarded trials
A) A) Overall performance of mice on rewarded trials only. B) Comparison of rewarded trials to criterion between the two groups. Two-sample t-test, ** denotes $p < 0.01$. Data are shown as mean±SEM. (n=5 mice per group).

I determined how many rewarded trials mice took to reach a criterion of 80% response accuracy (Figure 3.5B). I found that it took non-exposed group of mice longer to meet the response criterion compared with the non-exposed group (mean number of rewarded trials to criterion: 111.6 ± 3.9 (non-exposed group) vs. 74.6 ± 2.3 (pre-exposed group); paired t-test, p-value =0.0064, t-test for equal means, t-score = -3.66).

Overall, my results showed that there is a difference in how the two groups of mice learned. Prior exposure made the errors on non-rewarded odors more specific, and in the rewarded trials, overall, enabled mice to form odor-reward association. However, the data I analyzed for the pre-exposed group came from the acquisition of pure-odor discrimination. I next present an analysis of mixture detection performance.

Prior knowledge of odors improves performance on binary mixtures

Here, I address the question: how does prior knowledge affect how mice report presence of the target odor in mixtures?

I repeated the from the above section, to analyze how the pre-exposed animals perform on non-rewarded and rewarded trials. As both groups of mice had already learned the task contingency, I considered the pre-exposed group as the one with prior knowledge given it was initially trained to the monomolecular odors alone. Whereas the other group was presented with binary mixtures, and therefore six different combinations of odors that contain ethyl butyrate. I then compared this with the corresponding trials for the non-exposed group (Figure 3.6A). This allowed me to determine how having clear and exact knowledge of the target identity and the rest of the known background odors aids in detecting the odor of interest.

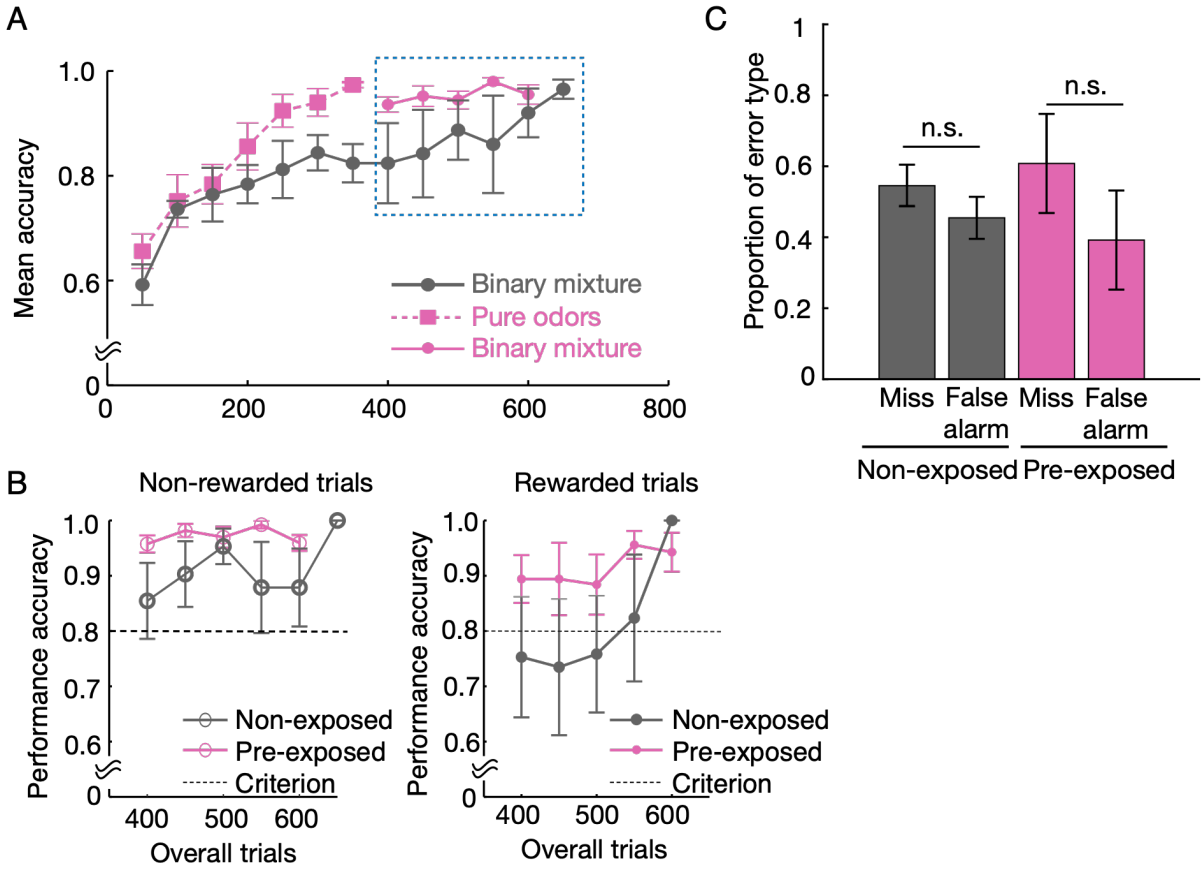

Figure 3. 6 Behavioral performance of mice during binary mixture training.
A) Overall performance of mice, blue box indicates the binary mixture training by both the non-exposed and pre-exposed group. Bin = 50 trials. B) Mean accuracy on rewarded and non-rewarded trials during the binary mixture task. C) Proportion of error type for non-exposed and pre-exposed group. Two sample t-test, $p > 0.05$, n.s denotes not significant. Data are shown as mean±SEM. (n=5 mice per group).

By this stage, overall, pre-exposed group of mice performed with high accuracy; and had a tendency to have a response accuracy slightly higher than the non-exposed group (mean accuracy on first bin: 82.4±3.65% (non-exposed group) vs. 93.6±1.47% (pre-exposed group); Figure 3.6A). However, in both rewarded and non-rewarded trials, the pre-exposed group of mice tended to perform slightly better than the non-exposed, despite the non-exposed group essentially performing the same task as they were before (Figure 3.6B). Non-exposed group had a tendency to make more misses rather than false alarms, that is, there was a tendency for them miss licking on the non-rewarded odors more frequently (Figure 3.6C).

To delve further, I repeated the analysis broken down by the specific odorant components (Figure 3.7). I hypothesized that prior knowledge of the odorants would lead to more stimulus-specific errors if mice were to make mistake – especially if they were demixing. I analyzed 1) responses of mice on non-rewarded trials with the presence of a specific odor component, then, 2) responses of mice to all possible combinations of odorants.

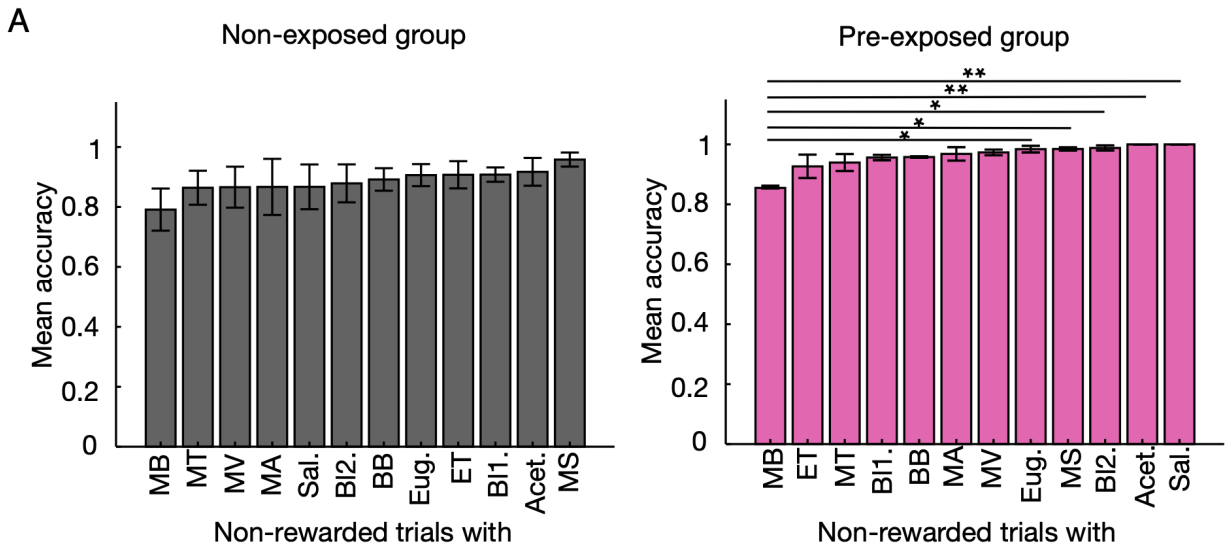

Figure 3. 7 Mice with differing learning histories responded differently to non-rewarded trials.
A) Mean response accuracies of non-exposed (left, grey) and pre-exposed group (right, pink) on non-rewarded odors containing specific component odors. Non-exposed group: One way ANOVA showed no significant difference. Pre-exposed group: One-way ANOVA showed significant differences between odorants. *Post-hoc* analysis using Tukey's HSD confirmed differences in mean correct responses, particularly on methyl butyrate training. * denotes $p<0.05$ and ** denotes $p<0.01$. Data are shown as mean±SEM. (n=5 mice per group).

I found that, for the pre-exposed group, the presence of methyl butyrate in non-rewarded mixtures particularly imposed difficulty for mice (one-way ANOVA, ($F(11, 24) = [3.03]$, $p = 0.01$; Figure 3.7 right). On the other hand, as before, while the non-exposed group also had a tendency to perform poorly on non-rewarded trials with methyl butyrate, this was overall indiscriminate from the rest of the odors (one-way ANOVA, $F(11, 48) = [0.42]$, p-value = 0.93; Figure 3.7 left).

The above, odor-specific analysis is informative, but still somewhat blind to the exact combination of odor (with which odor is the odor of interest was presented in a mixture). Taking advantage of the simple design, I analyzed how mice responded to all possible odor combinations (Figure 3.8).

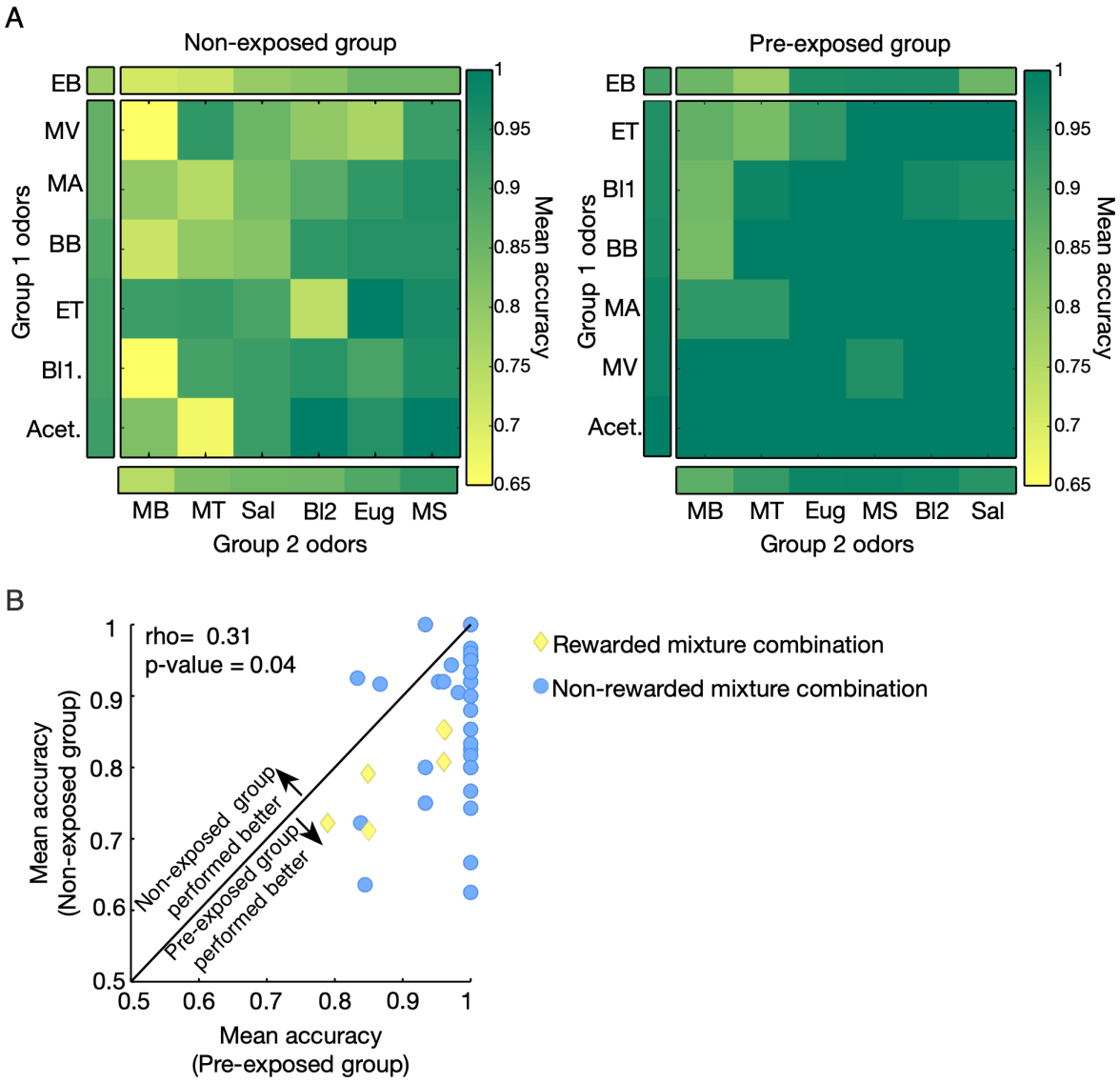

Figure 3. 8 Mice with prior knowledge of odors performed better on various mixture combinations

A) Response accuracies of non-exposed (left) and pre-exposed (right) group of mice to all possible mixture combinations. Data are shown as mean±SEM. (n=5 mice per group). B) Scatter plot showing relationship of A. Spearman rank correlation coefficient (rho) = 0.31, p-value = 0.04.

I summarized the response accuracies of the mice for each possible mixture combination and compared how the two groups responded to each. There were 42 mixture combinations possible, including six that were rewarded. The range of "yellow hue" (poorer performance) is wider in the non-exposed group than the pre-exposed group (Figure 3.8A). For most odor combinations, the pre-exposed group performed better than the non-exposed one (39 out of 42 mixture combinations fell under the unity line; Figure 3.8B). Additionally, there was little association in how the two groups of mice responded to each odor combination (Spearman rank correlation coefficient (rho) = 0.31, p-value = 0.04).

Overall, these results suggest that the two groups of mice learned and performed differently to solve the same binary mixture task. Additionally, these results indicate that prior knowledge of the odors enable mice to perform better in the binary mixture training.

Mice with prior knowledge of odors may be demixing to detect the target odorant

To further analyze how a prior exposure to pure odors influence the performance of olfactory figure-ground segregation, the same cohorts of mice were tasked to perform a generalization experiment (Figure 3.9A). In this case, apart from the known odors, mice were presented with mixtures containing butyl acetate, which both groups were naïve to. Butyl acetate is an ester with a fruity aroma that has some structural similarity to ethyl butyrate (MCS Tanimoto coefficient = 0.78), Figure 3.9B).

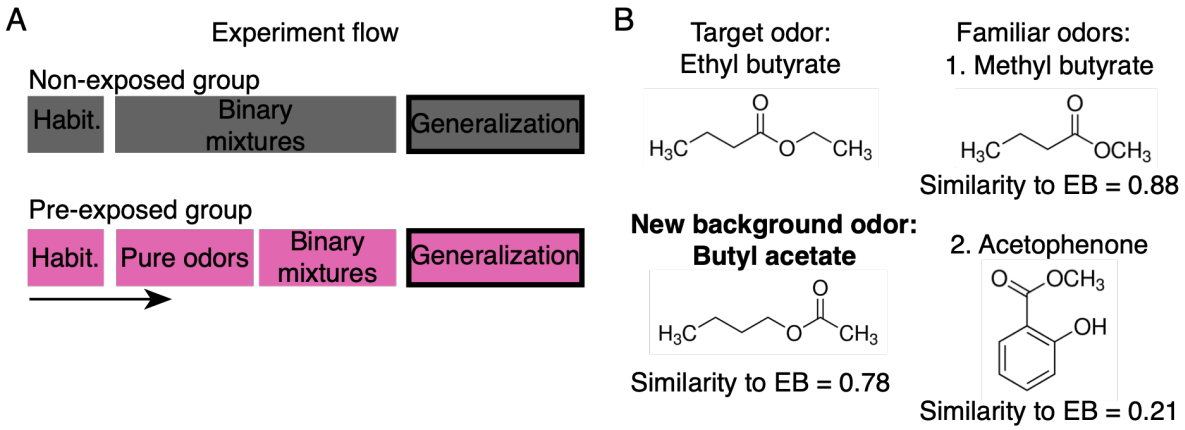

Figure 3. 9 Experimental scheme for generalization experiment.
A) Following the binary mixture training, the two groups of mice performed the generalization experiment for one day or session. The task was similar to the binary mixture training except a novel odor (butyl acetate) was introduced as another background odorant. B) Chemical structure of the novel background odor, butyl acetate, compared with the target and some familiar background odorants. Methyl butyrate still had the highest structural similarity to the target odor.

With its slight similarity to EB, I tested how mice behaved when butyl acetate was introduced as a novel background odor. I hypothesized that, if mice employ a demixing based on the knowledge of component odors, then mice will perform on the novel mixture combinations better.

Both groups of mice performed one day of generalization experiment, which involved at least 100 trials. Overall, both performed above 80% mean accuracy during the generalization session (Figure 3.10). This suggests that the addition of the novel odor did not drastically affect the overall performance of both.

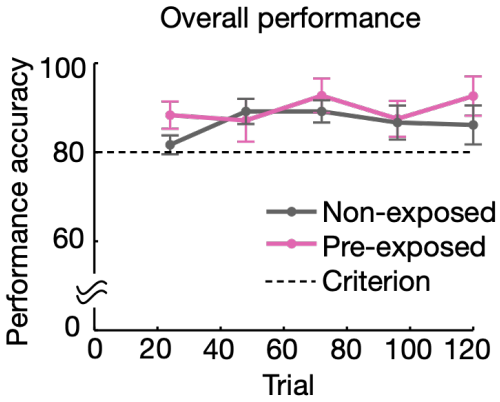

Figure 3. 10 Overall accuracy for the generalization session with a novel background odor
Overall performance of both groups of mice was not drastically affected by the addition the of novel background odor. Pink denotes pre-exposed group while grey denotes non-exposed group. N = 5 mice per group.

Since the overall performance analysis includes all odor combinations that the mice had already learned, I focused my analysis on trials with the novel background odor, butyl acetate. Overall, the pre-exposed group consistently had an average performance above the non-exposed group and performed above 80% criterion unlike the non-exposed group (Figure 3.11A). I further looked specifically at responses of mice to butyl acetate when combined with ethyl butyrate ("rewarded novel mixture") and other background odors ("non-rewarded novel mixtures").

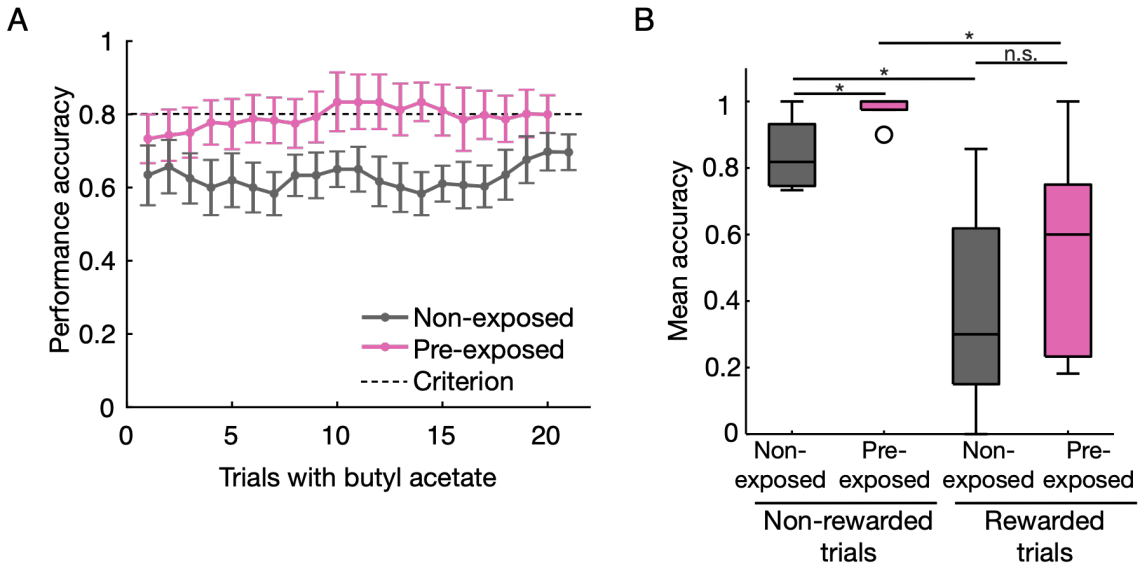

Figure 3. 11 Prior knowledge of component odors may facilitate performance in the presence of a novel background odor
A. Performance of non-exposed (grey) and pre-exposed (pink) groups of mice specifically on mixtures with butyl acetate. Data presented as moving average of 12. Horizontal line corresponds to 80% criterion. B) Boxchart showing the mean accuracies of the non-exposed (grey) and pre-exposed (pink) group of mice for rewarded and non-rewarded trials with butyl acetate. Two-sample t-test showed significant differences in some pairs, * denotes $p < 0.05$, n.s. denotes not significant. (n=5 mice per group).

Both groups of mice did not differ in their response to rewarded butyl acetate trials, that is, in combination with ethyl butyrate (mean performance accuracy on rewarded butyl acetate trials: 0.38 (non-exposed group) vs. 0.55 (pre-exposed group), p-value = 0.47, t-test for equal means, t-score = -0.77.) But the two groups significantly differed in responses to non-rewarded butyl acetate trials. The pre-exposed group made correct rejections of the non-rewarded trials with butyl acetate unlike the non-exposed group (mean performance accuracy on butyl acetate trials: 0.83 (non-exposed group) vs. 0.98 (pre-exposed group); p-value = 0.03, t-test for equal means, t-score -2.57; Figure 3.11B).

Discussion

In this chapter, I sought to understand how mice, following our behavioral model for figure-ground segregation, may solve the task. I looked at the role of prior knowledge of odor components, and to see if I could reveal an evidence of demixing.

I found that prior knowledge of mixture constituents (through pure-odor discrimination training) helped mice perform better in reporting the presence of the target odor, ethyl butyrate, during the binary mixture task (Figure 3.6). The result here adds to the body of knowledge regarding the role of prior experience in perception of mixtures, which is evident across different sensory modalities. The role of prior knowledge on the behavioral response during olfactory figure-ground segregation, specifically, is limited to a few studies. In one, prior repeated exposure to a component of a known configural binary mixture affected the reaction of rabbit neonates to that mixture (Sinding et al., 2011).

As mentioned earlier, mixture complexity may be a factor that determines how the brain makes computational decisions; and that this is related to the degree of input overlap that drives non-linearity (Mathis et al., 2016). Since my use of binary mixtures may not be nearly as complex as using a 14-component mixture (Mathis et al., 2016), the generalizability of my observation may be limited. In the future, this study may be extended to novel odors with different degrees of overlap with the target, or mixture complexity. In addition, further studies relating physiological responses and observed behavior may enable clearer interpretation of the result.

Conclusion

In this chapter, I delved deeper in understanding how mice using our model for binary figure-ground segregation perform the task. My results give hints that these mice may be demixing – i.e. decomposing the mixture representation into its component and finding the signal of interest. Further, I highlight the relevance of prior knowledge of constituent odors in facilitating demixing strategy.

Result Chapter 3: Use cases for the binary mixture paradigm

Introduction

A simple and tractable experimental paradigm may be a practical approach to probing mechanisms of figure-ground segregation. In this chapter, I aim to demonstrate this using two example cases below.

Case I: Using the experimental paradigm to probe mixture encoding in the OB during awake state

In this example, I worked in collaboration with members of Sensory and Behavioral Neuroscience Unit to analyze the state-dependent mixture representations in the olfactory bulb. This study, reported in Adefuin et al., (2022), used on my behavioral paradigm described earlier. In addition, I modified the "original" paradigm, in particular, by changing the reward contingencies, to enable different levels of behavioral engagement in naive and awake mice.

Motivation

Animals naturally encounter odors in the form of mixtures in the environment. Many past studies have explored how odor information from mixtures are encoded, which have revealed that evoked neural responses to mixtures are not equal to the sum of the individual component responses in the OB (Kurahashi et al., 1994; Duchamp-Viret et al., 2003; Oka et al., 2004; Cruz and Lowe, 2013; Reddy et al., 2018; Singh et al., 2019). A dominant outcome is a suppression, or sublinear summation. Non-linear summation is an outcome of different interactions and normalizing mechanisms. This interaction may lead to some loss of olfactory information, which could then negatively impact the perceptual discriminability component odors by animals (Laing and Francis, 1989; Kurahashi et al., 1994; Livermore and Laing, 1998a; Stevenson and Wilson, 2007)**,** although it may also prevent saturation at the early stage of olfactory processing (Reddy et al 2018b).

Most of the past studies reporting sublinear mixture summation have been conducted under anesthesia, specifically ketamine/xylazine, which alters network activity. For example, odor-evoked activity of OB output cells is enhanced during anesthetized state, compared with awake state, which is in part due to dampened inhibition and top-down modulation (Rinberg, 2006; Kato et al., 2012; Blauvelt et al., 2013). It is therefore important to make a distinction when drawing physiological conclusions given the effects of anesthesia. With that, it remained to be explored how mixtures are represented in awake animals, especially when performing a task like figure-ground segregation; and whether how representations are summed helps in the task.

To address this, Sander Lindeman, Janine Reinert, Izumi Fukunaga, and I paired my behavioral paradigm described in chapter 1, with additional modifications in reward contingency in some cases, with two-photon calcium imaging to record responses of mitral and tufted cells (MTCs) (Adefuin et al., 2022). My contribution was to train the mice on three variants of the task (original paradigm, random reward association, and complete dissociation of odor and reward).

Findings

We found that mixture responses tend to sum more linearly in the soma of MTCs in the awake, trained mice performing figure-ground segregation compared with the anesthetized group. The main explanation for this is due to diminished responses in these mice, keeping responses to the linear, not saturating, range. We further tested mixture responses in naïve mice that were awake but either task-engaged or disengaged. We observed the same result. Overall, this showed that linear summation is prevalent across different awake conditions. However, a more careful analysis of this data showed a decoupling between the linearity of mixture summation, and information relevant for mixture discrimination. That is, saturation effect is in general detrimental to the mixture task accuracy, as assed by a decoder performance, but only to a certain degree. Pattern decorrelation may overcome the detrimental effects of saturation.

Overall, we found that how binary mixtures are represented in the olfactory bulb depends on the state of mice. The ubiquity of linear summation across awake states indicates a state-dependence, while linearity in summation does not strictly correlate with capability to solve figure-ground segregation. Thus, my design enable an extension of our knowledge regarding the relevance of pattern decorrelation in the analytical abilities of animals (Wiechert et al., 2010; Gschwend et al., 2015). My earlier behavioral characterization allowed us to focus our analysis on EB, MB and EB-MB combinations, and how learning improves mixture representations in the olfactory bulb. It should be noted that the simpler and easier task allowed mice to be trained efficiently, which had practical advantages. This is also crucial given the possibility of craniotomy closure by wound healing (Koletar et al., 2019), which reduces optical clarity and therefore limits the number of two-photon imaging sessions.

Case II: Using the tractable experimental paradigm to explore a relevant temporal window in the OB during figure-ground segregation

Motivation: temporal patterning in olfactory encoding

Temporal patterning in the olfactory bulb is mediated by inhalation and intrinsic dynamics within the olfactory system. Many studies have revealed the timing of activity of different cells in the OB, especially in relation to inhalation (Shusterman et al., 2011; Fukunaga et al., 2012, 2014; Ackels et al., 2020). Understanding temporal response patterns of cells in the olfactory system is an important factor in further understanding of how odor information is represented and processed. For example, the two OB output cells exhibit different response latencies relative to inhalation onset, with the mitral cell having a wider onset unlike tufted cells that respond later (Fukunaga et al., 2012; Ackels et al., 2020). The temporal relationship of these cells and their different downstream target may be important in differentiating their specific functions in odor processing. Overall, the temporal patterns in the olfactory system is a crucial factor that contributes to odor information, which ultimately drives behavioral responses.

Despite this, how the timing of olfactory processing relates to performing olfactory figure-ground segregation is not fully understood. Determining this may be a way to reveal

mechanisms that underlie this task. Previous studies have revealed that sufficient information for solving a task like odor discrimination is contained within a single sniff (Uchida and Mainen, 2003). In more difficult cases of this, forcing mice to sample longer improves decision accuracy (Rinberg et al., 2006). This demonstrates a close relationship between processing time and the difficulty or the nature of a task.

Optogenetic probing of behaviorally relevant temporal windows

It has been previously estimated that enough information to identify odors has been relayed in the OSNs by as short as 100 ms after inhalation (Wilson et al., 2017). This was done by optogenetic activations of OMP-expressing cells in the nasal epithelium after odor inhalation, thereby masking the odor-evoked activity. By presenting this masking optogenetics stimulus at different latencies relative to inhalation, this study narrowed down the relevant temporal window to sub-sniff range, at least for relaying information in the OSNs.

Here, what I aim apply a similar method to reveal the time window during which the olfactory information is being processed in the binary olfactory figure-ground segregation. For example, it is possible that the relevant time window depends on the odors present in the mixture. For example, a susceptibility to optogenetic perturbation during a late time window may indicate an interaction between the local circuitry and the centrifugal inputs it receives (Matsutani and Yamamoto, 2008; Fletcher and Chen, 2010; Grabska-Barwińska et al., 2017). Refining olfactory information through a process like pattern decorrelation is important in minimizing redundancy and noise to preserve more informative information. This has been shown to be associated with improved behavioral response of animals to odors (Wiechert et al., 2010; Friedrich and Wiechert, 2014; Gschwend et al., 2015; Adefuin et al., 2022). Given this, I aim to explore whether there is a temporal window in which the OB is most relevant during figure-ground segregation. I aim to find a causal relationship between this possible temporal window and the behavioral response of mice when this temporal window is perturbed.

Methods

Animals

A transgenic mouse line, Vgat-cre::Ai32, which is a cross between a Vgat-IRES-Cre (Vong et al., 2011) and Ai32(RCL-Chr2(H134R)/EYFP) mice (Madisen et al., 2012) was used. The mouse heterozygous expresses channelrhodopsin2 (Chr2) in inhibitory Vgat+ cells. Light stimulation activates these Chr2-expressing inhibitory cells, which then inhibit the mitral and tufted cells (Fukunaga et al., 2014). All mice used were males.

Surgery

Surgeries were done by Dr. Izumi Fukunaga and Dr. Janine Reinert on 10 to 12-week old isoflurane-anesthetized mice. A fiber optic cannula (Thorlabs CFMC54L02) or a laser diode

(Thorlabs L450P1600MM) was implanted on top of the exposed olfactory bulb and fixed using

dental cement. Additionally, a custom metal head place was attached onto the parietal bone of the mice using histoacryl (B. Braun) and dental cement. For three consecutive days, mice were injected subcutaneously with carprofen (5 mg/kg body weight). Mice were then allowed to recover for 2 weeks before behavioral experiments were initiated.

Initial training of mice to go/no-go task

Head-fixed mice implanted with a pair of fiber optic canula or laser diode were trained similarly to the behavioral paradigm in Chapters 1 and 2. Briefly, mice were initially trained to perform a Go/No-Go behavioral task with ethyl butyrate assigned as the target odor, while other pure odors were the non-rewarded (S-) odors. After mice were proficient in the task (reaching at least 80% accuracy for two consecutive days), they proceeded to perform figure-ground segregation of binary mixtures using the same set of odorants and same target odor.

Optogenetics

Once mice were proficient in the figure-ground segregation task, they performed the same task but with light stimulation at random trials. A T-cube driver^{TM} LED driver (Thorlabs LEDD1B) send current to the light sources. The light source connected to the driver was connected to a fiber patch cable (Thorlabs M126L01), which was then connected onto the fiber optic cannula implant either through a mating sleeve (Thorlabs ADAL1) or interconnect (ADAF2). For mice with an LED implant, the LED driver was connected through a wire attached to the diode laser socket (Thorlabs S7060R) that can be attached to the pins of the laser diode during optogenetics experimentation.

During the optogenetics experiment, the onset of reward, in this case, was conditional to the timing and vigor of anticipatory licks. Licking earlier caused the reward to arrive earlier. A behavioral window of up to 3.2 seconds was provided. During trials with light stimulation, failure to generate anticipatory licks within the allotted temporal window was not rewarded with water. Data was recorded using a data acquisition interface (CED 1401) and Spike 2 software.

Analysis

Data analysis and figures were generated using MATLAB (R2021b). Performance of mice were analyzed similarly as previous chapters. Change in reaction time for a light stimulation trial was calculated as the difference between the reaction time during light trial (3rd lick response relative to odor onset) minus the mean reaction time during the control/non-light stimulation trials (3rd lick response relative to odor onset).

Results

Part I: Preliminary experiments confirming the effects of light stimulation

In contrast to previous works that used optogenetic stimulation of OSNs to mask activity in the OB, I wanted to silence the output of the olfactory bulb. The approach I turned to is a bulk optogenetic activation of GABAergic neurons in the OB, which leads to a robust inhibition of MTCs (Fukunaga et al., 2014).

To validate this approach for a behavioral experiment, which requires a substantial proportion of OB output to be silenced, inhibition of OB output cells upon light stimulation in the Vgat-cre::Ai32 mouse was characterized by Prof. Izumi Fukunaga. This was achieved by juxtacellular recordings from the MTCs in the OB of anesthetized mice. Light was presented from the brain surface through a fiber optic cannula (Figure 4.1).

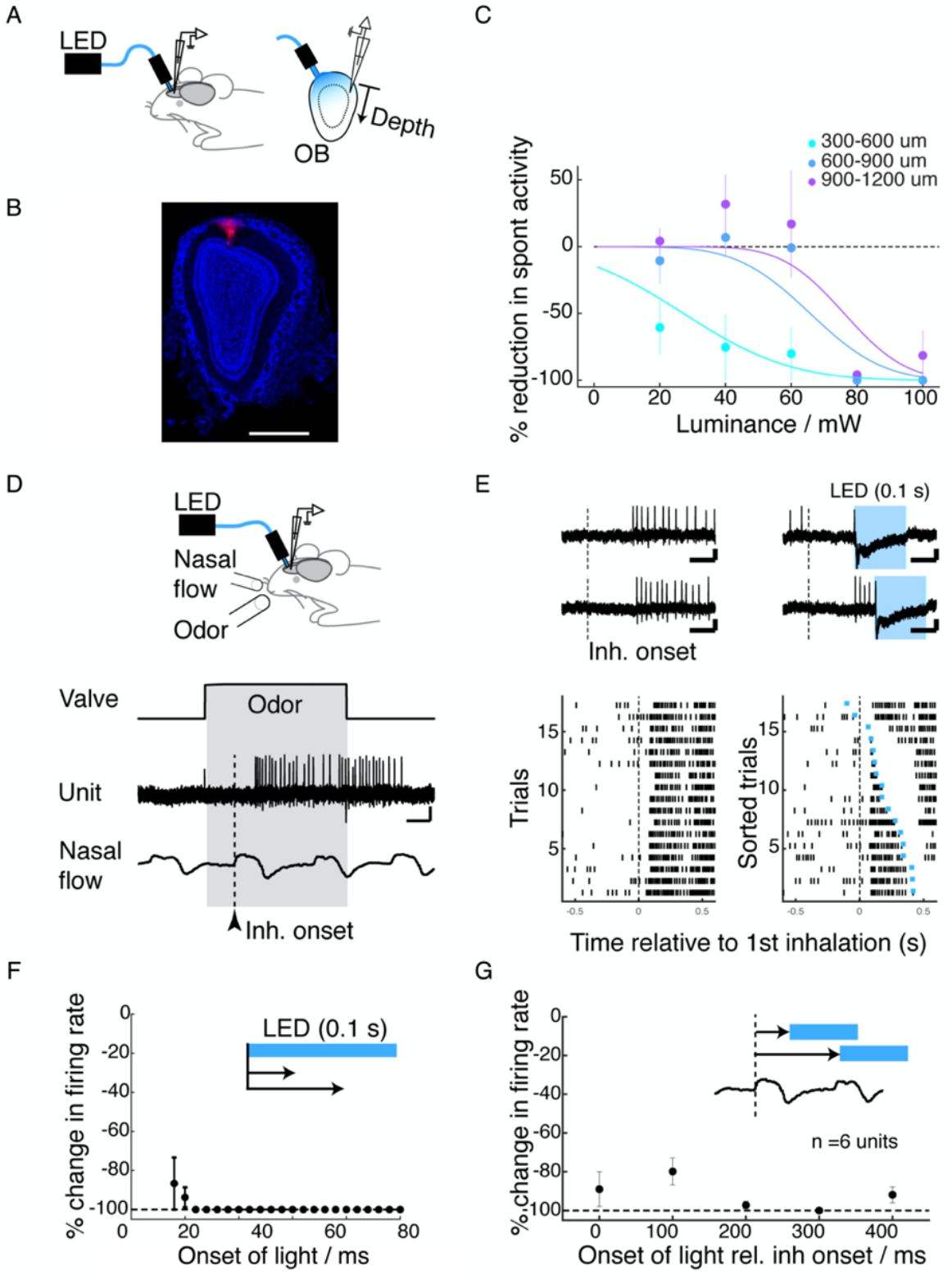

Figure 4. 1 Confirmation of OB output cell inhibition by electrophysiology
A) Schematic diagram showing head-fixed Vgat-cre::Ai32 mouse for extracellular recording in the OB, with fiber optic cannula placed over the OB, and connected to a light source via a patch cable for optogenetics. Mice were anesthetized with ketamine and xylazine (100 $mg.kg^{-1}$/20 $mg.kg^{-1}$ intraperitoneally). B) OB slice with red dye injected at the site of recording (scale bar = 500 µm). C) Reduction in the spontaneous activity of cells in the

OB at various recorded depths and light intensity. D) (Top) Similar to A but with odor port and sniff sensor placed next to the left and right nostrils, respectively. E) Example traces showing unitary spikes in the control trials (left) and with light (right). Scale bars = 0.5 V and 0.5 s. Dotted vertical line indicates the inhalation onset immediately after the odor onset (indicated in D). Light presentation was 100 ms (blue shaded region). Spike raster for trials without light (left) and with light stimulation (right; blue = light onset). F) Changes in the evoked firing rate relative to light onset. G) Changes in firing rate for light onset occurring at different time points relative to inhalation onset. Mean +- SEM shown.

Light presentations led to reproducible reduction of spontaneous activity in anesthetized mice at different depths of recording and light intensity (Figure 4.1). Light stimulation led to reduction in the spontaneous activity at different depths, although silencing at deeper depths in the OB (900-1200 µm from surface) required higher light intensity. Odor-evoked firing rate and changes to it upon light stimulation were also recorded in these mice.

Inhibition of OB output by optogenetics in behaving mice

After validating the optogenetic approach, I proceeded with behavioral experimentation. The first aim was to determine the general behavioral effect of inhibiting the OB output during the entire odor stimulation period. In this initial experiment, I explored the parameter of light stimulus intensity and its effect on task performances.

For this preliminary behavioral experiment, I intended to use mice with a bilateral cannula implanted on the dorsal OB. There were two variables that I explored here, the first one was light intensity. I used four different intensities of light: 9-, 50, 92- and 172- mW. A separate LED driver sending current to a light source was used for each cannula. Thus, prior to the experiment, I calibrated and confirmed even light stimulation from the two separate light sources beforehand using a light meter (Figure 4.2).

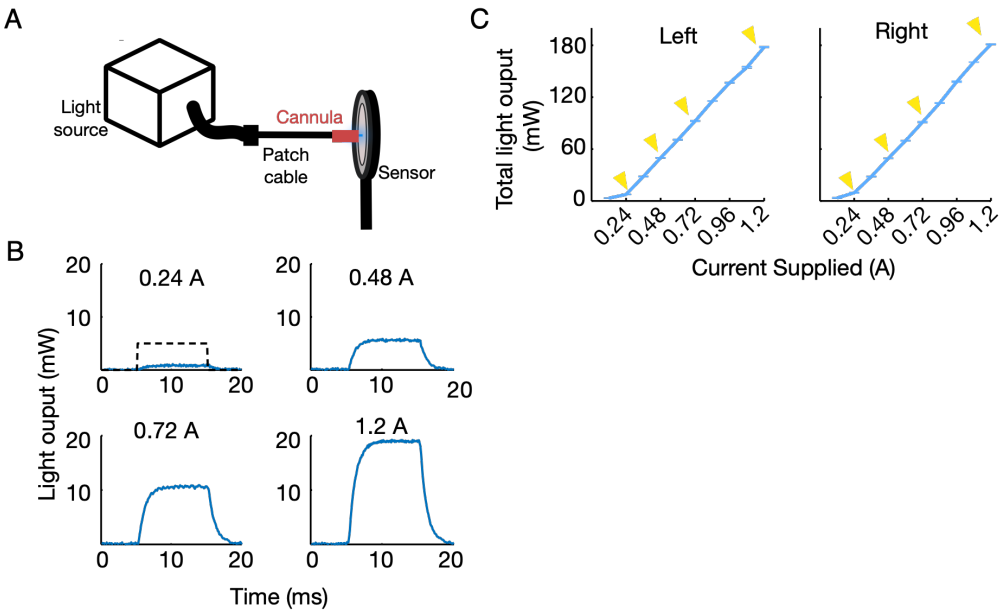

Figure 4. 2 Light stimuli used in the test phase of behavioral experiment
A) Schematic diagram of light recording configuration. An LED driver sends current to a light source that is connected to a fiber patch cable on one end. The other end connects to a fiber optic cannula held by a mating sleeve or an interconnect. A light meter is placed at the tip of the cannula fiber to measure light output. B)

Example optical power waveforms (blue) measured for different currents supplied. Black trace indicates duration of trigger used for testing (100 ms). C) Total light output of the left and right fiber optic canula where modified with increasing current supplied. The chosen light intensities are shown with the yellow arrows.

For the behavioral experiment of trained Vgat-cre::Ai32 mice, odor was applied for 1 second. Light stimulation randomly occurred on 40% of the trials in each session. Light onset occurred simultaneously with the final odor valve opening and also lasted for a second. Only one light intensity level was used throughout one experimental session or day. Thus, no mice underwent consecutive days of behavioral experiment with optogenetics (Figure 4.3 A-D).

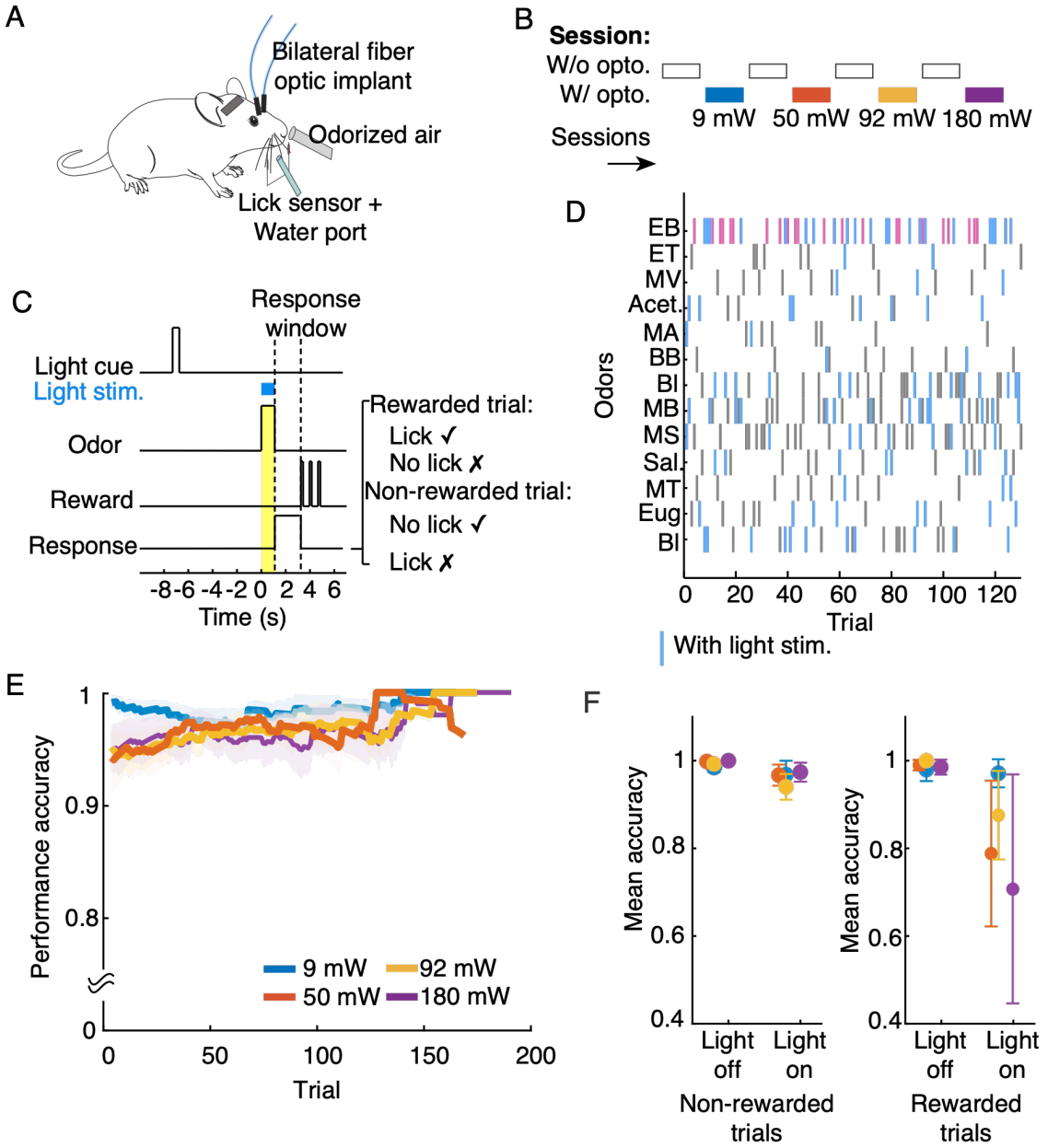

Figure 4. 3 Overall performance accuracies of Vgat-cre::Ai32 mice presented with four different intensities of light

A) Schematic diagram showing head-fixed Vgat-cre::Ai32 mouse with bilateral fiber optic implant on its OB, an odor port, lick sensor and water port for the behavioral experiment with optogenetics. B) Schedule of behavioral experiment. Mice performed figure-ground segregation for one session to prior performing the experiment with optogenetics. Four light intensities (9mW – 180mW) were consecutively used for the optogenetics sessions. Blue = 9mW, orange = 50mW, yellow = 92mW, and purple = 180mW. C) Trial structure of the experiment. (Blue = light stimulation period; yellow = odor period). A correct response is indicated as either licking (at least three times) on rewarded (S+) trials or not licking during non-rewarded trials, regardless whether trial had light on or

off. D) Example session of figure-ground segregation showing trial raster. Light was presented 40% of the time, regardless whether the trial was rewarded or not. (Pink = EB trials; grey = other odors in grey; blue = with light stimulation). E) Overall performance accuracy of mice grouped by light stimulus intensity. Data shown as moving average of 50 trials. Different light intensities are color coded. F) Mean accuracies on non-rewarded (left) and rewarded (right). Data are shown as mean±SEM. (n=3 mice per group).

Given the OB's role in gating the olfactory information, I hypothesized that perturbing the function of the OB during the final odor valve period would prevent mice from accurately performing figure-ground segregation. I expected mice to perform the figure-ground segregation task poorly, especially with increasing light intensities. Overall, mice performed with high accuracy (above 80%) across all light intensities chosen (Figure 4.3 E,F). Looking at the behavioral performance by trial type, I found that all mice performed accurately on non-rewarded trials (with and without light stimulation) and rewarded trials without light stimulation. Variability in response was only evident on the rewarded trials with light stimulation but overall mean accuracy still remained high. This meant that even with the light stimulation, mice were largely still correctly reporting the presence of the target odor (Figure 4.3 E-F). Notably, the lowest light intensity presented (9 mW) seemed to not have any effect; but using the highest light intensity (180mW) caused the worst response (mean accuracy on rewarded trials (light off vs. light on): .98 ± .01 vs. 0.71 ±0.26 (Figure 4.3F).

Given that the behavioral accuracy is calculated with a single threshold and may not have enough resolution to reveal more subtle effects of optogenetic perturbations, I analyzed various aspects of licking behavior, including lick vigor and response/lick onset (Figure 4.4).

Figure 4.4A shows the lick responses of one example Vgat-cre::Ai32 mouse across increasing light intensities. Despite licking and meeting the criterion for a correct trial (at least three licks on rewarded trials), there was a difference in the lick patterns during light stimulation trials. Compared with rewarded trials without light, mice licked less on rewarded trials with light stimulation (from 50-mW onwards). Furthermore, this difference increased with increasing light intensity (Figure 4.4 B and C).

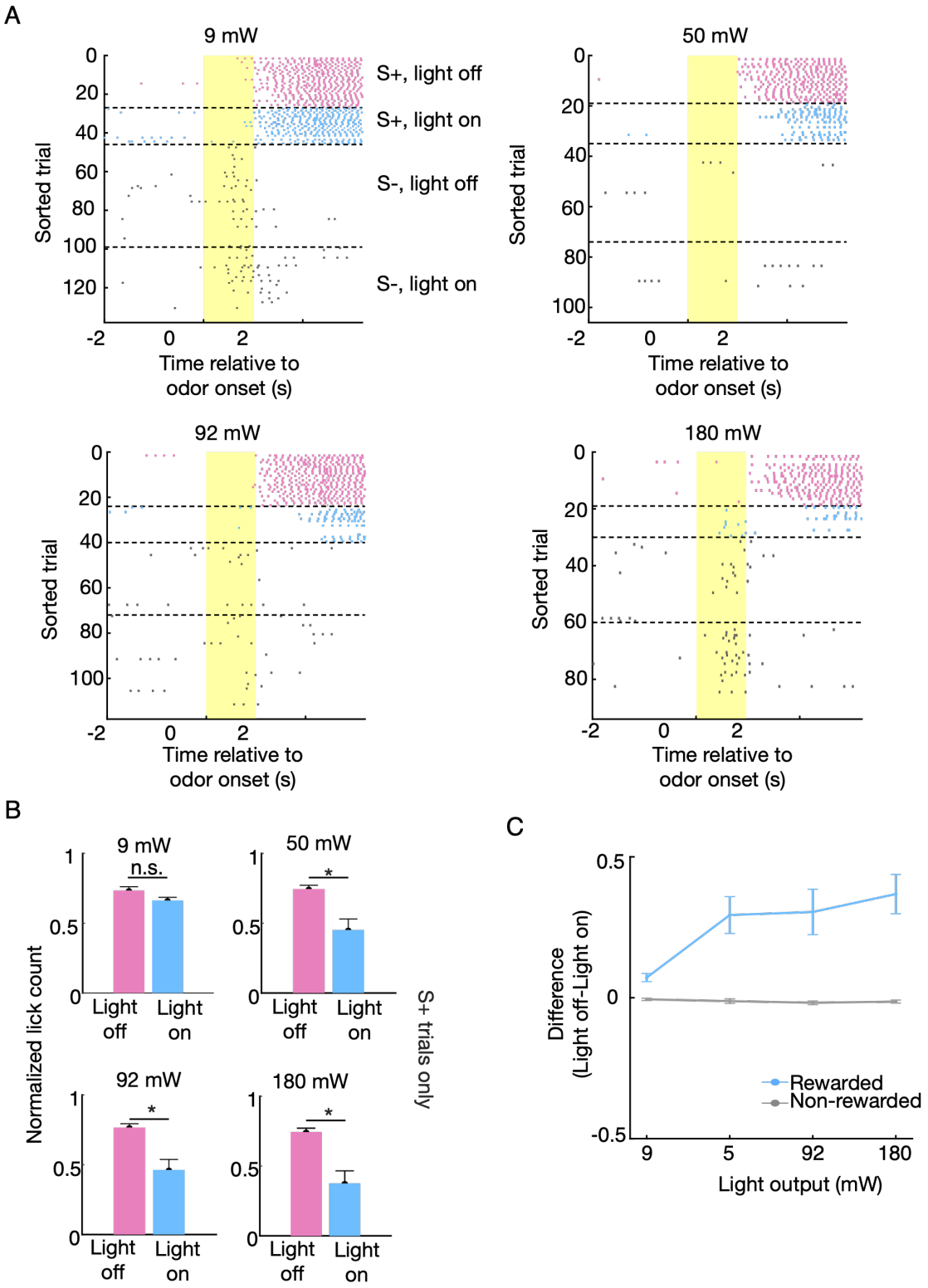
A
9 mW
50 mW
92 mW
180 mW
Sorted trial
Time relative to odor onset (s)
S+, light off
S+, light on
S-, light off
S-, light on
B
Normalized lick count
n.s.
*
Light off
Light on
S+ trials only
C
Difference (Light off-Light on)
Rewarded
Non-rewarded
Light output (mW)

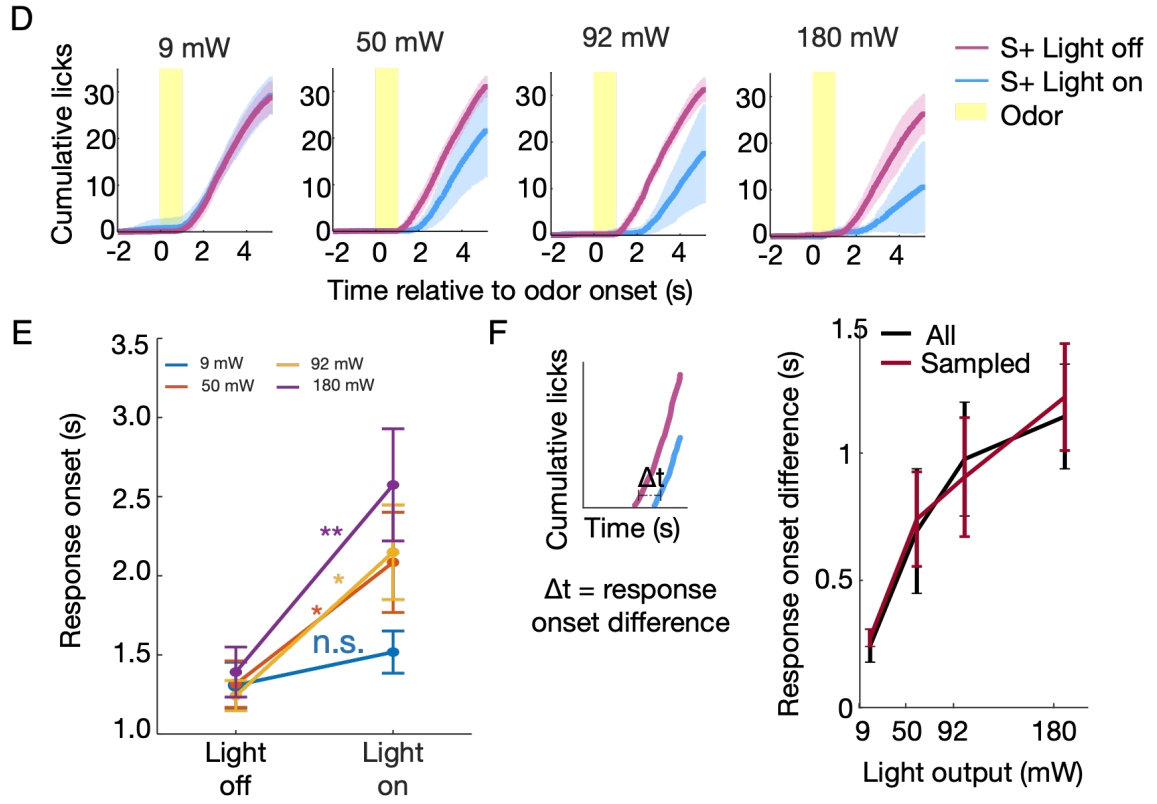

Figure 4. 4 Increasing light intensity to inhibit OB output reduced the lick vigor and delayed response onset of mice during rewarded trials.
A) Lick raster plots of an example animal for all light intensities used. Trials are sorted by type. Yellow = odor duration, pink = licks on rewarded trials without light stimulation, blue = licks on rewarded trials with light stimulation, grey = licks on non-rewarded trials. B) Normalized lick count for rewarded trials. Here, licks were counted and normalized to the maximum number of lick on a rewarded trial for each mouse for each session. Lick counts on non-rewarded trials is no longer shown. Paired t-test, * denotes $p < 0.05$, n.s. not significant. C) Relationship between light output and reduction of lick vigor. D) Cumulative anticipatory licks of the same example mouse in response to rewarded (S+) trials during optogenetic stimulation (on, blue) and non-stimulation (off, pink). E) Overall comparison of response onsets across different intensities of light for light on and off trials. Paired t-test, * denotes $p < 0.05$, n.s. not significant. F) (Left) Response onset difference was calculated by subtracting the mean reaction time (3rd lick onset) during light stimulation trials (blue) from the mean reaction time during non-light stimulation trials (blue). (Right) Delays in start of anticipatory licks upon optogenetic stimulation over different light intensities for all background odors. Black line represents all data, red line represents randomly sampled data from each session. Data are shown as mean±sem (n=3 mice).

Additionally, I looked at the lick resposne onset of the mice. The response onset was defined as the timing of the third instance of anticipatory lick relative to the onset of odor (final odor valve opening). For instances wherein there was no anticipatory lick during the alotted 3.2 second response window, I assigned an arbitrary value of 4 seconds as response onset – regardless whether the rewarded trial had light stimulation or not. This was to account for trials in which light stimulation effectively inhibited the behavioral response. Similar to results in the lick vigor, there was a significant delay in the lick onset of mice during light stimulation especially for the higher light intensities (Figure 4.4 D-F).

Overall, the results so far show that, even though the behavioral response was not completely abolished, it was indeed perturbed by the light stimulation. And, as expected, the more intense the light stimulation, which based on the electrophysiological validation

accessed more inhibitory cells, the bigger the impact on the behavioral response. Optogenetics stimulation, did not affect the responses of non-rewarded trials or even the rewarded, non-stimulus trials in any way.

Effect of odor concentration and optogenetic perturbation

Given that methyl butyrate is a difficult background odor when ethyl butyrate is the target, I briefly explored whether OB output inhibition on increasing concentrations of methyl butyrate. Three different concentrations of MB were used (Figure 4.5A). These concentrations were calibrated so that the photoionization signal amplitude was half ("low"), equal ("mid") or twice ("high") relative to the ethyl butyrate signal.

I measured the change in the response onset with increasing concentration of MB on the same group of mice. I found that increasing the concentration of methyl butyrate in the background did not drastically affect the response onset change during light (Figure 4.5B). As such, for the succeeding behavioral experiment, I used only one concentration (low) of methyl butyrate, similar to what was used in the previous chapters.

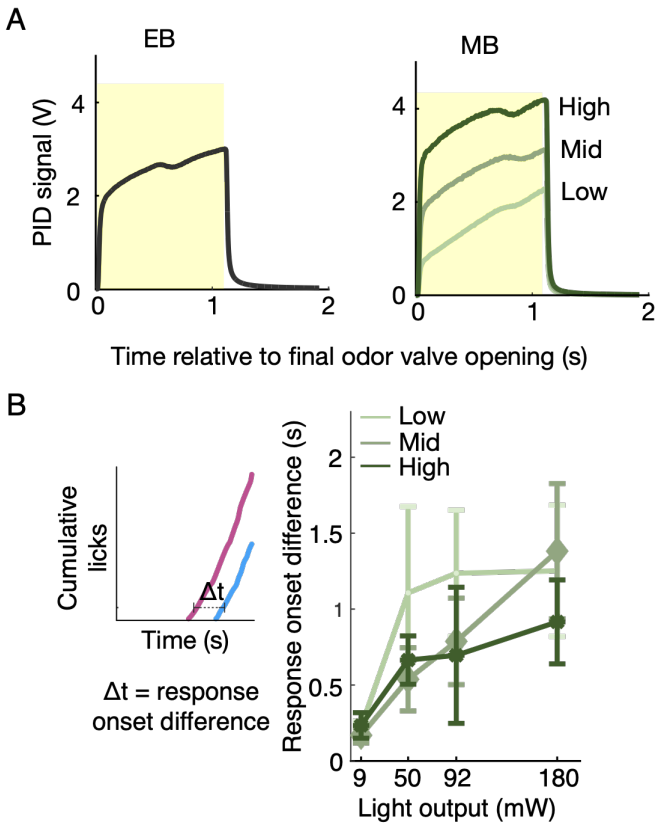

Figure 4. 5 Effect of optogenetic inhibition of OB output on increasing concentration of methyl butyrate background odor during
A) Photoionization detector (PID) traces of EB (left, black trace) and different relative concentrations of MB (right, green). Yellow shading = odor stimulus duration B) left: Schematic of Calculation; pink= without light stimulation blue = with light stimulation. Right: Response onset changes for different concentration of MB, using different light intensities. Data are represented as mean ± SEM, N = 3 mice.

Probing the relevant temporal window in the OB using a one-sniff behavior

To explore the relevant temporal window for the OB perturbation, I aimed to inhibit the olfactory bulb at brief and specific time points during the sampling period. To make this perturbation interpretable, I aimed to allow only one sniff during the stimulus period. This was first done by reducing stimulus period from 1 s, to 115-147 ms (Figure 4.6 A & B). This led to majority (92.53 ± 0.01 %) of the trials containing only one inhalation onset during the stimulus period (Figure 4.6C). In the subsequent experiment, trials with more than one inhalation onset were disregarded.

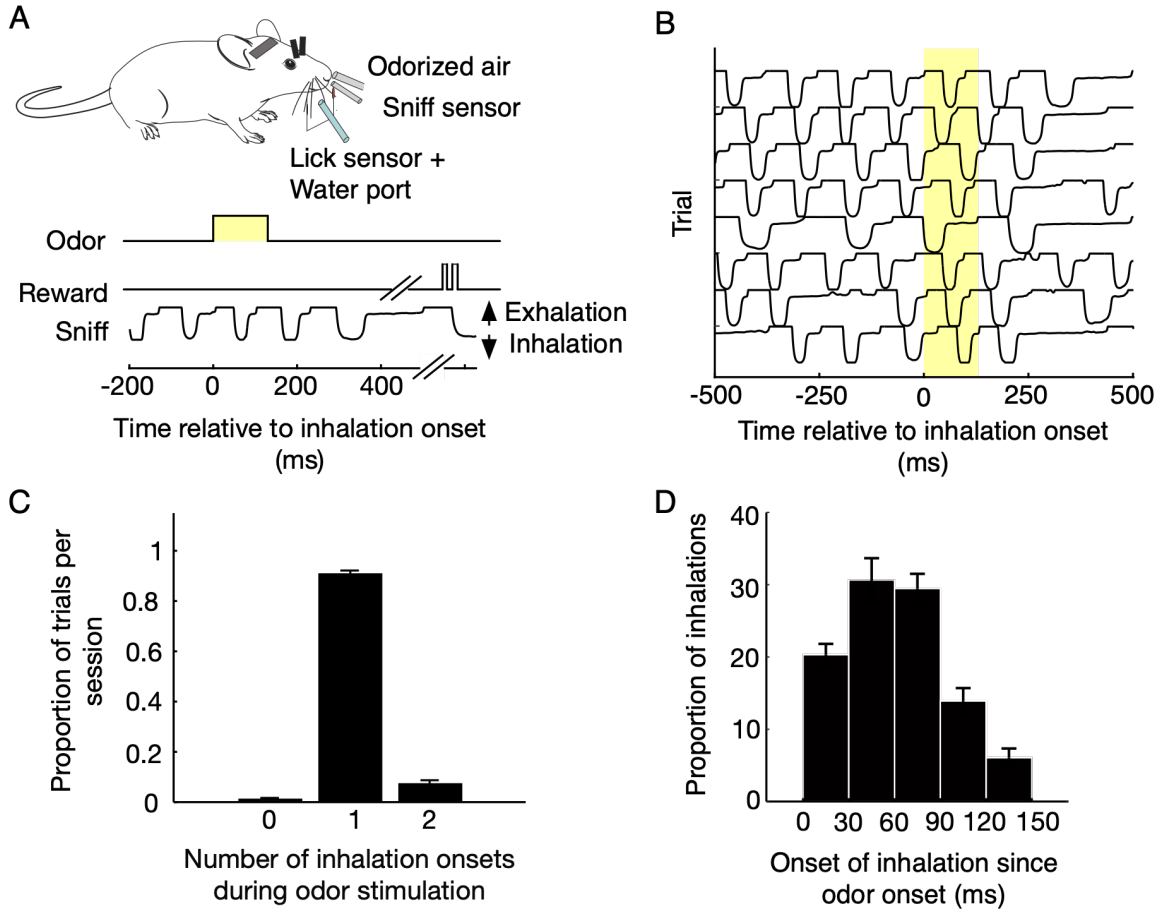

Figure 4. 6 One-sniff behavior with shortened odor pulse duration
A) (Top) Schematic diagram showing head-fixed mouse. A sniff sensor and odor port are located in either nostril. (Bottom) Trial structure of the experiment. Odor duration (yellow) was reduced from 1s to 115-147 ms. B) Example traces of sniff from one animal. Yellow shade indicates the odor stimulation period. Inhalation onsets during this odor period were counted. C) Proportion of trials with zero to three instances on inhalation onsets during the odor period. D) Histogram showing the proportion of one inhalation onset across the odor period. Bin size = 30 ms. Data are represented as mean ± SEM, n = 9 mice.

For the refined optogenetics experiment, a short light pulse (50 ms) was randomly presented in about 50% of the trials. The onset of the light stimulation was varied depending on the sniff cycle but ranged from zero to 400 ms after the opening of the final odor valve.

To determine the effect of the brief light stimulation, I measured the change in reaction time (difference between the response time on the S+ trial with light and the average response

time of S+ trials without light). I expected that if there is a relevant temporal window for the OB, there would be a significant change in the reaction time when the OB output was inhibited during this time point. I looked at the changes in the reaction time across different light onset, grouping together data points per 20 ms light onset.

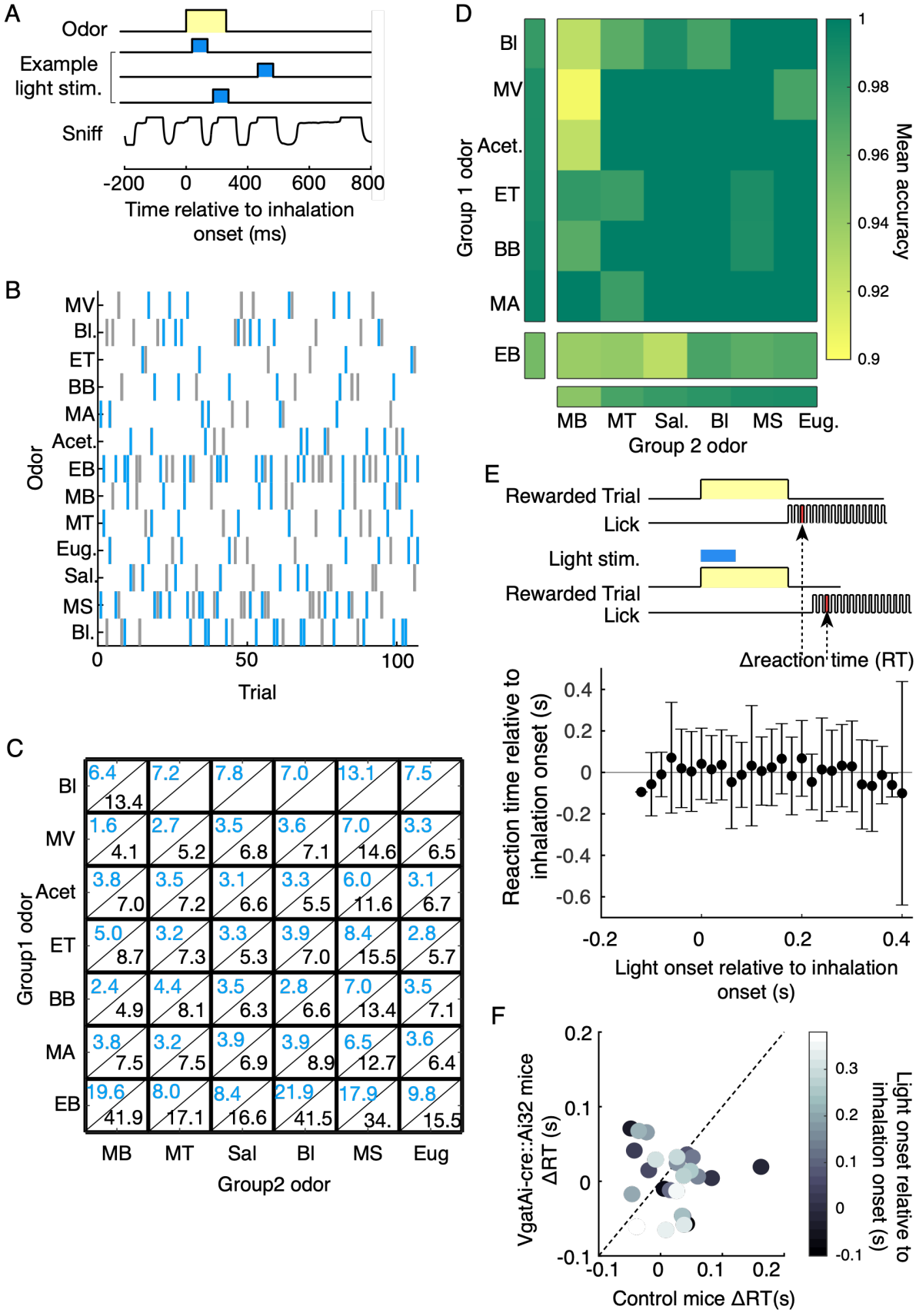

Figure 4. 7 Probing the relevant OB window with random light presentation
A) Trial structure of the experiment. During light stimulation trials, light onset can occur from 0-400 ms after the onset of the final odor valve. B) Example session of figure-ground segregation showing the instances of light

stimulation (blue raster). C) Average number trials (black) and average number of trials with light stimulation (blue) for each odor combination per mouse. D) Odor-specific performance of Vgat-cre::Ai32 mice. E) (Top) Reaction time was calculated by subtracting the difference between each lick onset during rewarded light stimulation trials from the average lick onset of rewarded non-light stimulation trials. (Bottom) Pooled data showing changes in reaction time across different light onsets relative to inhalation onsets of Vgat-cre::Ai32 mice. The average reaction time during rewarded trials without light stimulation was 0.6882± 0.2131 s (bin size = 20 ms). Data are represented as mean ± SD; N = 9 mice. F) Comparison of reaction time differences between Vgat-cre::Ai32 mice (as in C, n=9) and control (N = 2 mice).

I found that the changes in reaction times for the light stimulation trials (maximum change in reaction time was 0.07 ± 0.27 s) were not significantly different from the average reaction time without light stimulation (0.68 ± 0.21) for the Vgat-cre::Ai32 mice (Figure 4.7E). Additionally, I compared the changes in reaction time of this mice with control (non-Chr2-expressing) mice (Figure 4.7F). This indicated that inhibition of OB output in the Vgat-cre::Ai32 mice at any of the specific time onsets relative to inhalation did not lead to any detrimental changes in the behavioral response of the mice during rewarded trials.

Even though the current experiment were inconclusive, I was able to demonstrate that my new behavioral paradigm can be used potentially to reveal insights on neural mechanisms underlying olfactory figure-ground segregation.

Discussion

In this chapter, I demonstrate two use cases of the simple experimental paradigm in probing olfactory mechanisms. First, I discussed a recent paper from the laboratory that applied the experimental paradigm to explore how binary mixture representations are summed in the OB. Pairing the experimental paradigm with imaging revealed that overlapping binary mixture representations (of EB and MB) tend to sum linearly in awake state, in contrast to previous reports in anesthetized animals. The simplicity of the experimental paradigm was advantageous, enabling efficient training and to easily compare observed mixture responses against linear sums of component responses.

On the second part, I demonstrated that, when paired with optogenetics, it may be possible to reveal when OB is critically engaged in the olfactory figure-ground task. The results of my optogenetic experiment was inconclusive. Potential improvements that could help address this is as follows. A previous study have shown that in order to achieve complete anosmia, massive lesions (resulting to only roughly about 15% of the OB intact, or less) must be induced (Erskine et al., 2019). Smaller lesions may affect response to familiar odors, but only to some degree. Additionally, downstream regions like the piriform cortex may recover degraded input from the OB (Bolding et al., 2020). The brief (50 ms light pulse) inhibition of the OB when probing the relevant time window may have only partially degraded the relevant input to downstream cortical areas. Sufficient information may still have remained, which could lead to mice still being able to respond correctly and timely during the light stimulation trials; in contrast to what was observed on the preliminary experiment using (using 1s light stimulation period on a 1s odor pulse period). These factors may explain, the lack of drastic effect observed during OB output inhibition. Thus, in order to potentially probe the relevant temporal window for the OB during figure-ground segregation, it may be imperative to ensure maximizing the volume of the OB that could be inhibited.

Additionally, odor and light onset during the experiment occurred was not triggered by inhalation onset, so the distribution of light onset ranged randomly. Given that primacy coding has suggested that relevant information about odor identity is relayed as early as 100 ms in the OSNs (Wilson et al., 2017), it may be of interest to further put more focus within the early window. Possibly focusing on this period, while at the same time gradually increasing light stimulus period may be a more efficient way to optimize the experiment.

Overall, in this chapter, I demonstrated use cases of the tractable experimental paradigm. Despite the simplicity, the experimental paradigm may be used to probe different neural mechanisms. A simple and tractable experimental model can provide opportunities to explore neural mechanisms in a practical and time-sensitive manner.

General discussion

Summary of the thesis

Gaining insights on neural activities and the interactions between different brain circuits, and their causal relationship to behavior is one of the core pursuits of neuroscience. Doing so involves probing neural activities in animals under carefully controlled and standardized experimental conditions that engage the right cognitive processes and accessing the brain regions of interest.

Practically, the ease of training mice in a task such as figure-ground segregation and being able to acquire relevant data in a short amount of time is an important consideration when establishing an experimental paradigm. In my thesis, I presented the design and use of a simple behavioral paradigm using binary mixtures to study olfactory figure-ground segregation. Despite the task simplicity and familiarity of mice to all individual odor components, a degree of difficulty was still imposed by choosing closely related odors as background. By comparing two training protocols, I found that prior knowledge of odor components enabled animals to generalize task contingencies more readily when presented with a binary mixture containing a novel odor. This is in marked/stark contrast to animals that had not been trained on single odors first, which suggests that their decisions may have involved demixing odors. Lastly, I presented two use cases of this experimental paradigm, and that despite its relative simplicity, it has the capacity to probe mechanisms of olfactory figure-ground segregation (Adefuin et al., 2022).

Limitations of the current study: experimental conditions in relation to "natural" conditions

In designing behavioral paradigms, an important factor to consider is how natural or ethologically relevant behavioral assays are, and to what extent the paradigm captures the cognitive task of interest. As noted previously, the goal is to represent stimulus features mimicking these environments without sacrificing repeatability (Bucci-Mansilla et al., 2021). A balance between these aspects – having carefully-controlled experimental conditions and approximate naturalistic settings – may be crucial in limiting extraneous variable while exploring brain-behavior relationships.

Here, I will discuss some aspects of naturalistic behavioral experimentation that were beyond the scope of my thesis. Specifically, I will be discussing below odor mixture complexity and constraining animal navigation by head-fixation.

Some limitations related to mechanisms that may be specific to complex odor mixtures

Odors typically encountered by animals are highly complex (i.e. comprised of several odorant molecules) rather than binary mixtures. For example, (human) food items may contain up to 40 different key volatile odorants (Dunkel et al., 2014). On the other hand, a single species of flower that can be sensed and pollinated by honeybees can have 15 different odorants in them (Rachersberger et al., 2019).

My thesis deliberately simplified the behavioral paradigm to two odors in mixtures and I did not probe any aspect of figure-ground segregation beyond this mixture size. Notably, some seminal technical olfactory figure-ground segregation studies have used binary and more complex odor mixtures to probe the limits of odor perception (Rokni et al., 2014; Mathis et al

2016; Penker et al., 2020). One might question that given some have pursued studying the task using more complex mixtures on animals, is using binary odor mixtures a significant limitation?

Whether or not experiments using binary mixtures fail to capture behavior or neural processing involved in more complex mixtures is not fully explored. On the behavioral level, odor mixture complexity is associated with how difficult it is to spontaneously perceive its component scents – i.e. whether odors are perceived elementally or configurally (Thomas-Danguin et al., 2014). Studies probing olfactory figure-ground segregation using more complex odor mixtures have been previously explored (Rokni et al., 2014; Mathis et al., 2016; Penker et al., 2020). Binary mixtures tend to be easier for animals compared with more complex ones – with animals performing the task with higher accuracy and shorter training period (Rokni et al., 2014). However, even a binary mixture of the same two components can be perceived either configurally or elementally – depending on the relative concentration ratios (Wilson et al., 2020). Thus, it is worth noting that task difficulty and potential differences in neural mechanisms involved for decision making is not necessarily about the sheer number of odor components *per se*, but rather the identity and properties of the component odors.

Another aspect that may be affected by mixture complexity is the strategy used by the nervous system to solve the figure-ground task. As shown recently, mice trained on monomolecular odorants were able to generalize task contingency when presented with mixtures spanning a range (3, 8, and 14) of components (Mathis et al., 2016). Mice were poorer generalizers on more complex mixtures but could do so when robustly when trained beforehand – suggesting that dealing with significant noise and successfully accomplishing the task with more complex odors requires adjusting decision boundaries (Rokni et al., 2014; Mathis et al., 2016). It should be noted that decision boundaries exhibit flexibility and may depend on numerous factors including sensory evidence itself, task demand, learning, and internal controls by the organism (Zhang, 2012).

Features common with more complex forms of olfactory figure-ground segregation paradigms

Perceptual learning and improvement, overall, require changes in the tuning and specificity of cells (Gilbert et al., 2001). While decision boundaries in an olfactory figure-ground task may differ between simple vs. more complex odor mixtures, this may merely indicate that different neuronal populations undergo plastic changes or modulation, rather than involving entirely different mechanisms or rules to solve the task.

Additionally, binary and complex mixtures evoke responses with some common physiological features. For example, non-linear interactions in mixture responses of olfactory sensory neurons (OSN) input to the OB in anesthetized animals is evident in both binary and more complex mixtures, but they differ in the extent or severity (Cruz and Lowe, 2013; Zak et al., 2020). Secondly, response pattern changes typically associated with improvement in behavioral tasks have been reported in both types of mixtures. Pattern decorrelation, for example, has been reported upon presentation of binary (Gschwend et al., 2015) and more complex mixtures (Barnes et al., 2008). Thus, there is evidence of similar neural processes occurring in mixtures of different sizes, making the use of binary odor mixtures still a plausible choice when investigating figure-ground segregation.

Overall, there are similarities and differences in behavior and physiology when mice are presented with binary and complex mixtures. Further investigation is needed to determine the extent to which mechanisms of figure-ground segregation involving binary and more complex mixtures truly differ. As such, binary mixtures may still capture and mimic, to a degree, similar conditions offered by more complex odors so long as these criteria are met.

Head-fixation of mice

Animals simultaneously perform olfactory figure-ground segregation while roaming around or foraging, which demands the active use of olfactory and non-olfactory functions in response to the high variability and sensory complexity of their natural environments. However, many behavioral paradigms use head fixation of animals. This has an advantage of reducing variability in many factors crucial for the task acquisition and performance, including the duration and concentrations of odor presentation, inter-trial intervals. Further, it gives more mechanical stability crucial for capturing highly accurate sniff measurements, physiological recordings as well as imaging studies. Because head-fixation is restrictive to animal movement and can cause stress, mice are situated on a running wheel, which provides continuous locomotion. This, to an extent, mimics naturalistic conditions for the animal in that it somewhat mitigates stress (Hughes et al., 2020; Juczewski et al., 2020).

Alternatives to head fixation

Another aspect is that my paradigm was a classical conditioning, not instrumental. Because the trials are not initiated by the animals themselves, there may be a whole set of behavioral strategies that our paradigm fails to induce. Some studies have explored more naturalistic settings for mice by applying olfactory search tasks, which require collaboration of different sensorimotor functions (Baker et al., 2018). In this case, a mouse typically performs the task solo in an open field/arena. The behavior they exhibit depends on several factors including how far they are from the stimulus of interest, which relates to the relative concentration of the odor stimulus they sensed (Baker et al., 2018; Liu et al., 2020); and how familiar or predictable the location of the stimulus source is (Gire et al., 2016). One crucial aspect that olfactory search tasks have highlighted is the changes in sniffing pattern of mice (Wesson et al., 2008; Findley et al., 2021). As pointed out recently, the nose movements of freely moving animals to locate the odor source with concentration-variable turbulent plumes is far more dynamic than when mice are exposed to square odor pulses, which is typically used in tasks with head-fixed or nose-poking mice. This is not merely an artifact of the sniffing behavior but rather a behavioral strategy that mice employ. More importantly, sniffing rate was typically faster here upon trial initiation compared to reports of active sampling when mice are head-fixed (Shusterman et al., 2011; Bolding and Franks, 2017) This would have consequences on neurophysiological responses (Findley et al., 2021), which may mean some differences in mechanisms of figure-ground segregation in freely moving compared with head-fixed animals.

Another option for freely moving mice is by using automated home cages. The setups involve an operant conditioning task, typically presenting odor pulses upon nose poking, and have the advantage of recording behavior from tagged animals that are housed together with minimal experimenter interaction. This allows for long-term and high throughput behavioral data

collection without much human intervention, especially when obtaining neurophysiological data is not necessary (Erskine et al., 2019; Reinert et al., 2019; Voikar and Gaburro, 2020).

These setups enable observation of other parameters such as social interactions among animals and circadian rhythm. For example, mice are known to be active during dark cycles (in a 12h/12h light/dark cycle) such that behavioral experiments are typically conducted during this period. The use of automated home cages may be useful when intending to study the behavioral response of animals to a larger set of highly similar binary mixtures, which may require a relatively long experiment period compared with what was used here.

Overall, enabling more naturalistic settings for conducting animal behavioral experiments may be important if the goal is to understand ethological processes of animals. Nonetheless, the behavioral paradigm I presented here offers significant advantages due to its simplicity and may be improved to provide more complex or ethologically relevant features, for example, presenting turbulent plumes to head-fixed mice (Ackels et al., 2021), despite its limitations.

Outlook: potential applications to study unresolved questions on the olfactory figure-ground segregation

The rodent olfactory bulb, an experimentally accessible primary sensory area, is a recipient of various top-down inputs – despite being the first locus of synaptic processing of olfactory signal in the brain. Thus, the mouse olfactory system offers unique advantages for studying figure-ground segregation and its mechanisms. Centrifugal input to the OB can be classified into two: those that come from areas that the OB directly project to, and those that do not directly receive input from the OB. The former includes the piriform cortex, anterior olfactory nucleus (AON), and tenia tacta; while the latter includes areas such as the locus coeruleus (LC) and raphe nuclei, which project neuromodulatory fibers to the bulb (Matsutani and Yamamoto, 2008).

OB granule cells and short axon cells are targets of the piriform cortex – overall promoting odor-evoked inhibition (Shipley and Adamek, 1984; Boyd et al., 2012). Disrupting PCx feedback affect spatial patterning, by increasing odor responsiveness of mitral cells (Otazu et al., 2015). The AON also targets the granule cell layer (GCL) and the glomerular layer (GL) – leading to mitral and tufted cell (MTC) inhibition (Markopoulos et al., 2012). Functional studies show that part of the principal region of the AON affects sensitivity to odors. Inhibition of this AON sub-region improved detection of weak odorants (Aqrabawi et al., 2016), which could have a functional role during figure-ground segregation. Additionally, neuromodulatory centrifugal fibers release neurotransmitters that diffuse throughout the OB, which can have broad effects on neurotransmission of OB output to other regions (Matsutani and Yamamoto, 2008).

As we know that evoked spatial patterns in the OB relate to figure-ground segregation difficulty (Rokni et al., 2014), it would be interesting to explore how these top-down inputs refine odor information in the OB to implement improvement in the figure-ground task. Binary mixtures, as I have presented in this thesis, may be paired with optogenetic or genetic perturbations and two-photon calcium imaging, to provide us an idea which among and how these top-down inputs provide the most task-relevant role in figure-ground segregation. Furthermore, as I have

stated in the third chapter of my results, while I have attempted to resolve the behavioral window in which the OB is most relevant, this question remains to be answered.

Conclusion

The field of olfaction is still full of unknowns including on the mechanisms of olfactory-figure-ground segregation. Behavioral models involving animal experimentation remain to be indispensable in this endeavor. Many factors have to be considered to design behavioral experiments including whether or not they probe the right function, reproducibility and practicality – on top of careful consideration of the use and welfare of animals. In this study, I presented a simple and tractable experimental paradigm for probing olfactory figure-ground segregation using binary mixture that capture some key properties of the olfactory task. Combining the experimental paradigm with neurophysiological techniques offers potential in contributing to our understanding of olfactory processes.

References

Ackels T, Erskine A, Dasgupta D, Marin AC, Warner TPA, Tootoonian S, Fukunaga I, Harris JJ, Schaefer AT (2021) Fast odour dynamics are encoded in the olfactory system and guide behaviour. *Nat 2021 5937860* 593:558–563.

Ackels T, Jordan R, Schaefer AT, Fukunaga I (2020) Respiration-Locking of Olfactory Receptor and Projection Neurons in the Mouse Olfactory Bulb and Its Modulation by Brain State. *Front Cell Neurosci*.

Adefuin AM, Lindeman S, Reinert JK, Fukunaga I (2022) State-dependent representations of mixtures by the olfactory bulb. *Elife* 11.

Aqrabawi AJ, Browne CJ, Dargaei Z, Garand D, Khademullah CS, Woodin MA, Kim JC (2016) Top-down modulation of olfactory-guided behaviours by the anterior olfactory nucleus pars medialis and ventral hippocampus. *Nat Commun* 7:1–9.

Aqrabawi AJ, Kim JC (2020) Olfactory memory representations are stored in the anterior olfactory nucleus. *Nat Commun 2020 111* 11:1–8.

Araneda RC, Kini AD, Firestein S (2000) The molecular receptive range of an odorant receptor. *Nat Neurosci* 3:1248–1255.

Backman TWH, Cao Y, Girke T (2011) ChemMine tools: An online service for analyzing and clustering small molecules. *Nucleic Acids Res* 39.

Baker KL, Dickinson M, Findley TM, Gire DH, Louis M, Suver MP, Verhagen J V., Nagel KI, Smear MC (2018) Algorithms for Olfactory Search across Species. *J Neurosci* 38:9383–9389.

Barnes DDC, Hofacer RRD, Zaman ARA, Rennaker RRL, Wilson DDA (2008) Olfactory perceptual stability and discrimination. *Nat Neurosci* 11:1378–1380.

Bee MA (2015) Treefrogs as animal models for research on auditory scene analysis and the cocktail party problem. *Int J Psychophysiol* 95:216–237.

Blauvelt DG, Sato TF, Wienisch M, Murthy VN (2013) Distinct spatiotemporal activity in principal neurons of the mouse olfactory bulb in anesthetized and awake states. *Front Neural Circuits* 7:1–15.

Blazing RM, Franks KM (2020) Odor coding in piriform cortex: mechanistic insights into distributed coding. *Curr Opin Neurobiol* 64:96–102.

Bolding KA, Franks KM (2017) Complementary codes for odor identity and intensity in olfactory cortex. *Elife* 6:1–26.

Bolding KA, Nagappan S, Han BX, Wang F, Franks KM (2020) Recurrent circuitry is required to stabilize piriform cortex odor representations across brain states. *Elife* 9:1–23.

Boyd AM, Sturgill JF, Poo C, Isaacson JS (2012) Cortical feedback control of olfactory bulb circuits. *Neuron* 76:1161–1174.

Brann DH, Datta SR (2020) Finding the Brain in the Nose. *Annu Rev Neurosci* 43:277–295.

Bucci-Mansilla G, Vicencio-Jimenez S, Concha-Miranda M, Loyola-Navarro R (2021) Challenging Paradigms Through Ecological Neuroscience: Lessons From Visual Models. *Front Neurosci* 15:1499.

Buck L, Axel R (1991) A novel multigene family may encode odorant receptors: a molecular basis for odor recognition. *Cell* 65:175–187.

Burton SD (2017) Inhibitory circuits of the mammalian main olfactory bulb. *J Neurophysiol* 84112:jn.00109.2017.

Cao Y, Jiang T, Girke T (2008) A maximum common substructure-based algorithm for searching and predicting drug-like compounds. *Bioinformatics* 24:i366–i374.

Carandini M, Churchland AK (2013) Probing perceptual decisions in rodents. *Nat Neurosci* 16:824–831.

Chae H, Banerjee A, Albeanu DF (2020) A non-canonical feedforward pathway for computing odor identity. *bioRxiv*:2020.09.28.317248.

Cherry EC (1953) Some Experiments on the Recognition of Speech, with One and with Two Ears. *J Acoust Soc Am* 25:975–979.

Chess A, Simon I, Cedar H, Axel R (1994) Allelic inactivation regulates olfactory receptor gene expression. *Cell* 78:823–834.

Cooke M, Garcia Lecumberri ML, Barker J (2008) The foreign language cocktail party problem: Energetic and informational masking effects in non-native speech perception. *J Acoust Soc Am* 123:414–427.

Courtiol E, Wilson DA (2015) The olfactory thalamus: Unanswered questions about the role of the mediodorsal thalamic nucleus in olfaction. *Front Neural Circuits* 9:49.

Cruz G, Lowe G (2013) Neural coding of binary mixtures in a structurally related odorant pair. *Sci Rep* 3.

Duchamp-Viret P, Duchamp A, Chaput MA (2003) Single olfactory sensory neurons simultaneously integrate the components of an odour mixture. *Eur J Neurosci* 18:2690–2696.

Dunkel A, Steinhaus M, Kotthoff M, Nowak B, Krautwurst D, Schieberle P, Hofmann T (2014) Nature's Chemical Signatures in Human Olfaction: A Foodborne Perspective for Future Biotechnology. *Angew*

Chemie Int Ed 53:7124–7143.
Erskine A, Bus T, Herb JT, Schaefer AT (2019) Autonomouse: High throughput operant conditioning reveals progressive impairment with graded olfactory bulb lesions. *PLoS One* 14:23–28.
Fang F, Boyaci H, Kersten D (2009) Border Ownership Selectivity in Human Early Visual Cortex and its Modulation by Attention. *J Neurosci* 29:460–465.
Findley TM, Wyrick DG, Cramer JL, Brown MA, Holcomb B, Attey R, Yeh D, Monasevitch E, Nouboussi N, Cullen I, Songco JO, King JF, Ahmadian Y, Smear MC (2021) Sniff-synchronized, gradient-guided olfactory search by freely moving mice. *Elife* 10.
Fletcher ML, Chen WR (2010) Neural correlates of olfactory learning: Critical role of centrifugal neuromodulation. *Learn Mem* 17:561–570.
Friedrich RW, Wiechert MT (2014) Neuronal circuits and computations: Pattern decorrelation in the olfactory bulb. *FEBS Lett* 588:2504–2513.
Fukunaga I, Berning M, Kollo M, Schmaltz A, Schaefer AT (2012) Two Distinct Channels of Olfactory Bulb Output. *Neuron* 75:320–329.
Fukunaga I, Herb JT, Kollo M, Boyden ES, Schaefer AT (2014) Independent control of gamma and theta activity by distinct interneuron networks in the olfactory bulb. *Nat Neurosci* 17:1208–1216.
Gilbert CD, Sigman M, Crist RE (2001) The neural basis of perceptual learning. *Neuron* 31:681–697.
Gire DH, Kapoor V, Arrighi-Allisan A, Seminara A, Murthy VN (2016) Mice Develop Efficient Strategies for Foraging and Navigation Using Complex Natural Stimuli In Brief Article Mice Develop Efficient Strategies for Foraging and Navigation Using Complex Natural Stimuli. *Curr Biol* 26:1261–1273.
Grabska-Barwińska A, Barthelmé S, Beck J, Mainen ZF, Pouget A, Latham PE (2017) A probabilistic approach to demixing odors. *Nat Neurosci* 20:98–106.
Groen IIA, Jahfari S, Seijdel N, Ghebreab S, Lamme VAF, Scholte HS (2018) Scene complexity modulates degree of feedback activity during object detection in natural scenes. *PLOS Comput Biol* 14:e1006690.
Gschwend O, Abraham NM, Lagier S, Begnaud F, Rodriguez I, Carleton A (2015) Neuronal pattern separation in the olfactory bulb improves odor discrimination learning. *Nat Neurosci* 18:1474–1482.
Howard JD, Gottfried JA (2014) Configural and Elemental Coding of Natural Odor Mixture Components in the Human Brain. *Neuron* 84:857–869.
Hughes RN, Bakhurin KI, Barter JW, Zhang J, Yin HH (2020) A Head-Fixation System for Continuous Monitoring of Force Generated During Behavior. *Front Integr Neurosci* 14:11.
Igarashi KM, Ieki N, An M, Yamaguchi Y, Nagayama S, Kobayakawa K, Kobayakawa R, Tanifuji M, Sakano H, Chen WR, Mori K (2012) Parallel Mitral and Tufted Cell Pathways Route Distinct Odor Information to Different Targets in the Olfactory Cortex. *J Neurosci* 32:7970–7985.
Inagaki S, Iwata R, Iwamoto M, Imai T (2020) Widespread Inhibition, Antagonism, and Synergy in Mouse Olfactory Sensory Neurons In Vivo. *Cell Rep* 31.
Jinks A, Laing DG (2001) The analysis of odor mixtures by humans: Evidence for a configurational process. *Physiol Behav*.
Johnson BA, Leon M (2008) Chemotopic Odorant Coding in a Mammalian Olfactory System. *J Comp Neurol* 503:1–34.
Johnsrude IS, Mackey A, Hakyemez H, Alexander E, Trang HP, Carlyon RP (2013) Swinging at a Cocktail Party: Voice Familiarity Aids Speech Perception in the Presence of a Competing Voice. *Psychol Sci* 24:1995–2004.
Juczewski K, Koussa JA, Kesner AJ, Lee JO, Lovinger DM (2020) Stress and behavioral correlates in the head-fixed method: stress measurements, habituation dynamics, locomotion, and motor-skill learning in mice. *Sci Reports 2020 101* 10:1–19.
Kandel ER (2012) The Age of Insight: The Quest to Understand the Unconscious in Art, Mind and Brain From Vienna 1900 to the Present, First. New York: Random House.
Kandel ER (2016) Reductionism in Art and Brain Science: Bridging the Two Cultures. West Sussex: Columbia University Press.
Kato HK, Chu MW, Isaacson JS, Komiyama T (2012) Dynamic Sensory Representations in the Olfactory Bulb: Modulation by Wakefulness and Experience. *Neuron* 76:962–975.
Kay LM, Lowry CA, Jacobs HA (2003) Receptor contributions to configural and elemental odor mixture perception. *Behav Neurosci* 117:1108–1114.
Kermen F (2011) Molecular complexity determines the number of olfactory notes and the pleasantness of smells. *Sci Rep* 1:206–206.
Koivisto M, Kastrati G, Revonsuo A (2014) Recurrent processing enhances visual awareness but is not necessary for fast categorization of natural scenes. *J Cogn Neurosci* 26:223–231.
Kok P, Mostert P, De Lange FP (2017) Prior expectations induce prestimulus sensory templates. *Proc Natl Acad Sci U S A* 114:10473–10478.
Koletar MM, Dorr A, Brown ME, McLaurin JA, Stefanovic B (2019) Refinement of a chronic cranial window

implant in the rat for longitudinal in vivo two-photon fluorescence microscopy of neurovascular function. *Sci Rep* 9.
Kurahashi T, Lowe G, Gold GH (1994) Suppression of Odorant Responses by Odorants in Olfactory Receptor Cells. *Science (80-)* 265:118–120.
Laing DG, Francis GW (1989) The capacity of humans to identify odors in mixtures. *Physiol Behav* 46:809–814.
Lamme VAF (1995) The Neurophysiology of Figure-Ground Segregation in Primary Visual Cortex. *J Neurosci* 15:1605–1615.
Land LJ, Shepherd GM (1974) Autoradiographic analysis of olfactory receptor projections in the rabbit. *Brain Res* 70:506–510.
Lindqvist A, Höglund A, Berglund B (2012) The role of odour quality in the perception of binary and higher-order mixtures. *Perception* 41:1373–1391.
Linster C, Cleland TA (2004) Configurational and Elemental Odor Mixture Perception Can Arise from Local Inhibition. *J Comput Neurosci 2004 161* 16:39–47.
Liu A, Papale AE, Hengenius J, Patel K, Ermentrout B, Urban NN (2020) Mouse Navigation Strategies for Odor Source Localization. *Front Neurosci* 14:218.
Livermore A, Laing D (1998a) The influence of odor type on the discrimination and identification of odorants in multicomponent odor mixtures. *Physiol Behav* 65:311–320.
Livermore A, Laing DG (1998b) The influence of odor type on the discrimination and identification of odorants in multicomponent odor mixtures. *Physiol Behav* 65:311–320.
Madisen L et al. (2012) A toolbox of Cre-dependent optogenetic transgenic mice for light-induced activation and silencing. *Nat Neurosci* 15:793–802.
Malnic B, Hirono J, Sato T, Buck LLB (1999) Combinatorial receptor codes for odors. *Cell* 96:713–723.
Markopoulos F, Rokni D, Gire DH, Murthy VN (2012) Functional Properties of Cortical Feedback Projections to the Olfactory Bulb. *Neuron* 76:1175–1188.
Mathis A, Rokni D, Kapoor V, Bethge M, Murthy VN (2016) Reading Out Olfactory Receptors: Feedforward Circuits Detect Odors in Mixtures without Demixing. *Neuron* 91:1110–1123.
Matsutani S, Yamamoto N (2008) Centrifugal innervation of the mammalian olfactory bulb. *Anat Sci Int* 83:218–227.
Mazo C, Grimaud J, Shima Y, Murthy VN, Geoffrey Lau C (2017) Distinct projection patterns of different classes of layer 2 principal neurons in the olfactory cortex. *Sci Reports 2017 71* 7:1–10.
Mesgarani N, Chang EF (2012) Selective cortical representation of attended speaker in multi-talker speech perception. *Nature* 485:233–236.
Mombaerts P, Wang F, Dulac C, Chao SSK, Nemes A, Mendelsohn M, Edmondson J, Axel R, Edmonson J, Axel R (1996) Visualizing an olfactory sensory map. *Cell* 87:675–686.
Nagayama S, Homma R, Imamura F (2014) Neuronal organization of olfactory bulb circuits. *Front Neural Circuits* 8:1–19.
Nielsen BL, Jezierski T, Bolhuis JE, Amo L, Rosell F, Oostindjer M, Christensen JW, McKeegan D, Wells DL, Hepper P (2015) Olfaction: An overlooked sensory modality in applied ethology and animal welfare. *Front Vet Sci* 2:69.
Nityananda V, Bee MA (2011) Finding Your Mate at a Cocktail Party: Frequency Separation Promotes Auditory Stream Segregation of Concurrent Voices in Multi-Species Frog Choruses. *PLoS One* 6:e21191.
Oka Y, Omura M, Kataoka H, Touhara K (2004) Olfactory receptor antagonism between odorants. 23.
Otazu GH, Chae H, Davis MB, Albeanu DF (2015) Cortical Feedback Decorrelates Olfactory Bulb Output in Awake Mice. *Neuron* 86:1461–1477.
Penker S, Licht T, Hofer KT, Rokni D (2020) Mixture Coding and Segmentation in the Anterior Piriform Cortex. *Front Syst Neurosci* 14:1–13.
Poort J, Khan AG, Pachitariu M, Nemri A, Orsolic I, Krupic J, Bauza M, Sahani M, Keller GB, Mrsic-Flogel TD, Hofer SB (2015) Learning Enhances Sensory and Multiple Non-sensory Representations in Primary Visual Cortex. *Neuron* 86:1478–1490.
Qiu F, Von Der Heydt R (2005) Figure and ground in the visual cortex: v2 combines stereoscopic cues with gestalt rules. *Neuron* 47:155–166.
Rachersberger M, Cordeiro GD, Schäffler I, Dötterl S (2019) Honeybee Pollinators Use Visual and Floral Scent Cues to Find Apple (Malus domestica) Flowers. *J Agric Food Chem* 67:13221–13227.
Rao RPN, Ballard DH (1999) Predictive coding in the visual cortex: a functional interpretation of some extra-classical receptive-field effects. *Nat Neurosci 1999 21* 2:79–87.
Reddy G, Zak JD, Vergassola M, Murthy VN (2018) Antagonism in olfactory receptor neurons and its implications for the perception of odor mixtures. *Elife* 7.
Reinert JK, Schaefer AT, Kuner T (2019) High-Throughput Automated Olfactory Phenotyping of Group-Housed Mice. *Front Behav Neurosci* 13:267.
Rescorla RA, Holland PC (1982) Behavioral Studies of Associative Learning in Animals. *Annu Rev Psychol*

33:265–308.
Ressler K, Sullivan S, Buck L (1994) Information coding in the olfactory system: evidence for a stereotyped and highly organized epitope map in the olfactory bulb. *Cell* 79:1245–1255.
Rinberg D (2006) Sparse Odor Coding in Awake Behaving Mice. *J Neurosci* 26:8857–8865.
Rinberg D, Koulakov A, Gelperin A (2006) Speed-Accuracy Tradeoff in Olfaction. *Neuron* 51:351–358.
Roelfsema PR, Lamme VAF, Spekreijse H, Bosch H (2002) Figure-ground segregation in a recurrent network architecture. *J Cogn Neurosci* 14:525–537.
Rokni D, Hemmelder V, Kapoor V, Murthy VN (2014) An olfactory cocktail party: Figure-ground segregation of odorants in rodents. *Nat Neurosci* 17:1225–1232.
Rubin E (1915) Synsoplevede Figurer. Studier i psykologisk Analyse /Visuell wahrgenommene Figuren. Studien in psychologischer Analyse [Visually perceived figures. Studies in psychological analysis]. Copenhagen, Denmark: Gyldendalske Boghandel.
Self MW, Jeurissen D, Van Ham AF, Van Vugt B, Poort J, Roelfsema PR (2019) The Segmentation of Proto-Objects in the Monkey Primary Visual Cortex. *Curr Biol* 29:1019-1029.e4.
Serizawa S, Miyamichi K, Sakano H (2004) One neuron–one receptor rule in the mouse olfactory system. *Trends Genet* 20:648–653.
Shipley MT, Adamek GD (1984) the connections of the mouse olfactory bulb: A study using orthograde and retrograde transport of wheat germ agglutinin conjugated to horseradish peroxidase. *Brain Res Bull*.
Shusterman R, Smear MC, Koulakov AA, Rinberg D (2011) Precise olfactory responses tile the sniff cycle. *Nat Neurosci* 14:1039–1044.
Sinding C, Thomas-Danguin T, Crepeaux G, Schaal B, Coureaud G (2011) Experience influences elemental and configural perception of certain binary odour mixtures in newborn rabbits. *J Exp Biol* 214:4171–4178.
Singh V, Murphy NR, Balasubramanian V, Mainland JD (2019) Competitive binding predicts nonlinear responses of olfactory receptors to complex mixtures. *Proc Natl Acad Sci* 116:9598–9603.
Stettler D, Axel R (2009) Representations of odor in the piriform cortex. *Neuron* 63:854–864.
Stevenson R, Wilson D (2007) Odour perception: an object-recognition approach. *Perception* 36:1821–1833.
Thomas-Danguin T, Sinding C, Romagny S, El Mountassir F, Atanasova B, Le Berre E, Le Bon AM, Coureaud G (2014) The perception of odor objects in everyday life: A review on the processing of odor mixtures. *Front Psychol* 5:504.
Uchida N, Mainen ZF (2003) Speed and accuracy of olfactory discrimination in the rat. *Nat Neurosci* 6:1224–1229.
Uchida N, Takahashi YK, Tanifuji M, Mori K (2000) Odor maps in the mammalian olfactory bulb: Domain organization and odorant structural features. *Nat Neurosci* 3:1035–1043.
Vassar R, Chao SK, Sitcheran R, Nuiiez M, Vosshall LB, Axel R (1994) Topographic O rganization of Sensory Projection to the O lfactory Bulb. *Cell* 79:981–991.
Vecera SE, O'reilly RC (1998) Figure-Ground Organization and Object Recognition Processes: An Interactive Account. 24:441–462.
Voikar V, Gaburro S (2020) Three Pillars of Automated Home-Cage Phenotyping of Mice: Novel Findings, Refinement, and Reproducibility Based on Literature and Experience. *Front Behav Neurosci* 14:193.
Vong L, Ye C, Yang Z, Choi B, Chua S, Lowell BB (2011) Leptin Action on GABAergic Neurons Prevents Obesity and Reduces Inhibitory Tone to POMC Neurons. *Neuron* 71:142–154.
Wagemans J, Elder JH, Kubovy M, Palmer SE, Peterson MA, Singh M, von der Heydt R (2012) A Century of Gestalt Psychology in Visual Perception I. Perceptual Grouping and Figure-Ground Organization. *Psychol Bull* 138:1172.
Wang Y, Zhang J, Zou J, Luo H, Ding N (2019) Prior Knowledge Guides Speech Segregation in Human Auditory Cortex. *Cereb Cortex* 29:1561–1571.
Weiss T, Snitz K, Yablonka A, Khan RM, Gafsou D, Schneidman E, Sobel N (2012) Perceptual convergence of multi-component mixtures in olfaction implies an olfactory white. *Proc Natl Acad Sci* 109:19959–19964.
Wesson DW, Donahou TN, Johnson MO, Wachowiak M (2008) Sniffing behavior of mice during performance in odor-guided tasks. *Chem Senses* 33:581–596.
Wiechert MT, Judkewitz B, Riecke H, Friedrich RW (2010) Mechanisms of pattern decorrelation by recurrent neuronal circuits. *Nat Neurosci* 13:1003–1010.
Wilson CD, Serrano GO, Koulakov AA, Rinberg D (2017) A primacy code for odor identity. *Nat Commun* 8.
Wilson DA, Fleming G, Vervoordt SM, Coureaud G (2020) Cortical processing of configurally perceived odor mixtures. *Brain Res* 1729:146617.
Wiltrout C, Dogra S, Linster C (2003) Configurational and nonconfigurational interactions between odorants in binary mixtures. *Behav Neurosci* 117:236–245.
Zak JD, Reddy G, Vergassola M, Murthy VN (2020) Antagonistic odor interactions in olfactory sensory neurons are widespread in freely breathing mice. *Nat Commun 2020 111* 11:1–12.
Zariwala HA, Kepecs A, Uchida N, Hirokawa J, Mainen ZF (2013) The limits of deliberation in a perceptual

decision task. *Neuron* 78:339–351.
Zelano C, Mohanty A, Gottfried JA (2011) Olfactory Predictive Codes and Stimulus Templates in Piriform Cortex. *Neuron* 72:178–187.
Zhang J (2012) The effects of evidence bounds on decision-making: Theoretical and empirical developments. *Front Psychol* 3:1–19.
Zhou H, Friedman HS, Von Der Heydt R (2000) Coding of border ownership in monkey visual cortex. *J Neurosci* 20:6594–6611.
Head-fixed mouse illustrations were modified and adapted from https://scidraw.io/drawing/123.